

T-2609

COMPARISON OF
FREQUENCY DOMAIN MIGRATION APPROACHES
WITH REGARD TO
VERTICAL VELOCITY VARIATIONS

BY

YO KATAHIRA

ProQuest Number: 10782362

All rights reserved

INFORMATION TO ALL USERS

The quality of this reproduction is dependent upon the quality of the copy submitted.

In the unlikely event that the author did not send a complete manuscript and there are missing pages, these will be noted. Also, if material had to be removed, a note will indicate the deletion.



ProQuest 10782362

Published by ProQuest LLC (2018). Copyright of the Dissertation is held by the Author.

All rights reserved.

This work is protected against unauthorized copying under Title 17, United States Code
Microform Edition © ProQuest LLC.


ProQuest LLC.
789 East Eisenhower Parkway
P.O. Box 1346
Ann Arbor, MI 48106 – 1346

A thesis submitted to the Faculty and the Board of Trustees of the Colorado School of Mines in partial fulfillment of the requirements for the degree of Master of Science in Geophysics.

Golden, Colorado

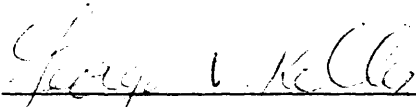
Date: Sept 2, 1952

Signed: 
Yo Katahira

Approved: 
William A. Schneider
Thesis Advisor

Golden, Colorado

Date: Sept 2, 1952


George V. Keller
Head of Department

ABSTRACT

Migration of seismic data is an accepted part of seismic data processing flow today. It is a process which maps stacked seismic section into a section with events properly positioned in x, y, z space.

The incremental method discussed in this paper presents a recursive scheme in the frequency wavenumber domain as opposed to the variable velocity method (Stolt's development). The method projects the wavefield down successively by simple complex multiplications with downward continuation operators, consequently it handles vertical velocity gradients very well. The method is also free from frequency dispersion up to the nyquist frequency.

Synthetic model data are migrated in the presence of vertical velocity gradients and migration results are compared with results obtained by the variable velocity method. Comparisons between the two methods, given the accurate knowledge of velocity, show that the incremental method gives better results than Stolt's variable velocity method.

A simple coordinate transformation extends the applicability of the incremental method to accommodate minor lateral velocity gradients. This transformation maps an

original time section into a section governed by a mean velocity for an entire section. Then migration proceeds as before with the mean velocity. The result is encouraging but more analytical study is suggested in order to establish the scheme for laterally inhomogeneous media.

TABLE OF CONTENTS

	Page
ABSTRACT	iii
LIST OF FIGURES	vii
LIST OF TABLES	xii
ACKNOWLEDGEMENTS	xiii
INTRODUCTION	1
OVERVIEW OF WAVE EQUATION MIGRATION	3
The need for migration	3
Wave equation migration	6
F - K MIGRATION	13
Basic theory for a constant velocity medium	13
Variable velocity method	22
Incremental method	34
COMPARISON OF FREQUENCY DOMAIN MIGRATION METHOD	39
One horizon test model (Model 1)	40
Four horizons with gradual velocity increase with depth (Model 2)	53
Three horizons with large velocity jump (Model 3)	65
POSSIBLE EXTENSION OF THE INCREMENTAL METHOD IN THE PRESENCE OF LATERAL VELOCITY VARIATIONS	78
Dipping layer with diffractor (Model 4)	82
SUMMARY AND CONCLUSIONS	107
BIBLIOGRAPHY	109

	Page
APPENDIX A	111
DESCRIPTION OF THE COMPUTER PROGRAM	111
APPENDIX B	127
LIST OF THE COMPUTER PROGRAM	127

LIST OF FIGURES

<u>Figure</u>		<u>Page</u>
1	True and interpreted positions of a dipping segment.	4
2	A diffraction from a scattering point.	5
3	Migration of seismic section: Downward continuation and Imaging.	8
4	Some of existing downward continuation techniques: Finite difference, Kirchhoff integral, and Frequency wavenumber.	9
5	Simplified picture of downward continuation.	14
6	Migration mapping procedure for a constant velocity case.	19
7	An example of migration mapping for a constant velocity case.	20
8	Simplified flow chart of constant velocity method.	21
9	An example of stretching.	25
10	W plotted as a function of α and t.	30
11	Pseudo - depth converted theoretical diffraction curves for different W.	32
12	Pseudo - depth converted real diffraction curves for different velocity ratio (V_2/V_1).	33
13	Diagram of the incremental model.	34
14	Simplified diagram of the incremental process.	37
15	Simplified flow diagram of the incremental method.	38

<u>Figure</u>		<u>Page</u>
16	Physical parameters of model 1.	41
17	Normal incidence time section of model 1.	43
18	Wave - theory modelling of model 1.	43
19	Real and theoretical diffraction curves in the pseudo - depth domain of model 1 for velocity ratio of 1.2.	44
20	The variable velocity migration of model 1 with $W=1.0$ for velocity ratio of 1.2.	45
21	The incremental migration of model 1 for velocity ratio of 1.2.	46
22	Real and theoretical diffraction curves in the pseudo - depth domain of model 1 for velocity ratio of 2.0.	48
23	The variable velocity migration of model 1 for velocity ratio of 2.0. $W=1.0$ was used here.	50
24	The variable velocity migration of model 1 for velocity ratio of 2.0. $W=0.0$ was used here.	51
25	The incremental migration of model 1 for velocity ratio of 2.0.	52
26	Physical parameters of model 2.	54
27	Normal incidence time section of model 2.	55
28	Wave - theory modelling of model 2.	56
29	The variable velocity migration of model 2 with $W=1.0$, standard F - K migration.	57
30	Velocity distribution of model 2.	58
31	The variable velocity migration of model 2 with $W=0.6$.	60

<u>Figure</u>		<u>Page</u>
32	The incremental migration of model 2.	61
33	Schematic of real and theoretical diffraction curves in the pseudo - depth domain.	62
34	The variable velocity migration of model 2 with $W = 0.0$.	63
35	Physical parameters of model 3.	66
36	Velocity distribution of model 3.	67
37	Normal incidence time section of model 3.	68
38	Wave - theory modelling of model 3.	69
39	The variable velocity migration of model 3 with $W = 1.0$, standard F - K migration.	70
40	A schematic of real and theoretical diffraction curves in the pseudo - depth domain.	71
41	The variable velocity migration of model 3 with $W = 0.6$.	73
42	The incremental migration of model 3.	74
43	The variable velocity migration of model 3 with $W = 0.4$.	75
44	The variable velocity migration of model 3 with $W = 0.5$.	76
45	The variable velocity migration of model 3 with $W = 0.75$.	77
46	The simplified diagram showing how to obtain new time t' .	80
47	Schematic of trace interpolation.	81

<u>Figure</u>		<u>Page</u>
48	Physical parameters of model 4.	83
49	Synthetic time section of model 4.	84
50	Bottom: raypaths from a scatterer below a dipping interface. The interface separates a low-velocity layer above from a high-velocity layer below. Top: resulting diffraction curve on a time section.	85
51	The variable velocity migration of model 4 with $W = 1.0$.	86
52	The variable velocity migration of model 4 with $W = -0.43$.	88
53	The variable velocity migration of model 4 with $W = -0.2$.	89
54	The variable velocity migration of model 4 with $W = 0.2$.	90
55	The variable velocity migration of model 4 with $W = 0.43$.	91
56	The variable velocity migration of model 4 with $W = 0.43$ and velocity increase by 10%.	93
57	The variable velocity migration of model 4 with $W = 0.43$ and velocity increase by 15%.	94
58	The variable velocity migration of model 4 with $W = 0.43$ and velocity increase by 20%.	95
59	The variable velocity migration of model 4 with $W = 0.43$ and velocity increase by 25%.	96
60	The variable velocity migration of model 4 with $W = 0.43$ and velocity increase by 30%.	97
61	The plot of T^2 vs. x^2 of original synthetic section (Fig. 49) for traces 1 through 50.	99
62	The plot of T^2 vs. x^2 of original synthetic section (Fig. 49) for traces 50 through 100.	100

<u>Figure</u>		<u>Page</u>
63	Top: mean velocity used for the incremental migration. Bottom: corresponding depth function.	101
64	The incremental migration of model 4 without interpolation of trace before and after the migration.	102
65	The interpolated section before migration using the mean velocity of Figure 61.	104
66	The incremental migration of model 4 using the mean velocity of Figure 61.	105
67	The incremental migration of model 4 using the mean velocity increased by 10%.	106
A-1	Flow diagram of overlay YOMIG (1,0).	118
A-2	Flow diagram of overlay ZYFKA (1,1).	119
A-3	Flow diagram of subroutine BMUX1 in overlay ZYFKA.	120
A-4	Flow diagram of subroutine RFFT in overlay ZYFKA.	121
A-5	Flow diagram of overlay ZYFKB (1,1).	122
A-6	Flow diagram of subroutine KTRANSl in overlay ZYFKB.	123
A-7	Flow diagram of overlay ZYFKC (1,1).	124
A-8	Flow diagram of subroutine RIFFT in overlay ZYFKC.	125
A-9	Flow diagram of subroutine BDMUX in overlay ZYFKC.	126

LIST OF TABLES

<u>Table</u>		<u>Page</u>
I	Comparison of three different migration methods.	11
II	Theoretical and real diffraction curves in a pseudo - depth domain.	49
III	Table of velocity increases used in the variable velocity migration of model 4.	92

ACKNOWLEDGEMENTS

I wish to thank Drs. W. A. Schneider, F. A. Hadsell, and M. W. Majors for serving as my committee members. Special thanks go to my advisor, Dr. W. A. Schneider, for his dedicated guidance throughout the course of this study. The author is especially grateful to the late Dr. G. R. Pickett who served as a committee member until his death. Also, special thanks go to my fellow students for their encouragements, and to S. L. Faulkner for reviewing the manuscript.

Grateful acknowledgement is extended to the Integrated Geophysics Project for their financial support.

Finally, most sincere gratitude goes to my parents for their constant encouragements and financial and moral support throughout the years.

INTRODUCTION

Migration of seismic data has been important for some time in the field of exploration seismology.

Since the introduction of the finite - difference algorithm by Claerbout (1972), many studies have been published on the subject of wave equation migration.

Schneider (1978) formalized the Kirchhoff Integral technique. This method has historic ties to the conventional diffraction summation approach. He developed the explicit relationships existing between the Kirchhoff and the Frequency - Wavenumber approach discussed below.

Another approach to migration was popularized by Stolt (1978). He discussed the formulation of wave equation migration in the frequency domain (Variable velocity method) taking into account vertical velocity gradients. He showed that migration in the $f-k$ domain is a straight mapping procedure. In his development of a migration scheme, Stolt made modifications to the original wave equation in order to incorporate a vertical velocity gradient. In his final form of the wave equation, he argued that W , a function of velocity, time, depth, etc., is supposed to take care of a vertical velocity gradient. Stolt proposed W be held constant along the entire seismic section (a value usually between 0.5 and 1.0).

Bolondi (1978) and Gazdag (1978) discussed a recursive type of scheme in the $f-k$ domain (incremental method), in which the subsurface is discretized into layers with constant velocities and the wavefield is extrapolated downward layer by layer.

Recently a new approach to migration was introduced by Berkhout (1979, 1980). His method performs migration in the space - frequency domain ($F-X$ migration). In his method, a seismic section is first Fourier transformed in the t - direction only and the data in the $f-x$ domain is convolved with the downward continuation operator along the x - axis for each temporal frequency component.

This thesis work deals with the implementation and the evaluation of the incremental method on synthetic data. Also the two $F-K$ migration schemes; namely, the variable velocity method and the incremental method, will be compared on the basis of their performances in the presence of vertical velocity gradients. Furthermore, the possible extension of the incremental method in the presence of lateral velocity gradient will be discussed.

All the computer work is done on CYBER - 720 at the Colorado School of Mines using CGG and AIMS software packages except for the incremental migration routine which was developed.

OVERVIEW OF WAVE EQUATION MIGRATION

This chapter briefly describes the migration principle and some of the major migration techniques available today; namely, Finite Difference, Kirchhoff Integral, and Frequency-Wavenumber.

The need for migration

All seismic processing today is based on the common assumption which states that the earth can be approximated by layers of rocks and that the layers are flat and horizontal. If this assumption is violated, as we often see in real geology, events are incorrectly positioned either vertically or horizontally, or even both.

Figure 1 illustrates the case where a dipping layer exists in a constant velocity medium. The source - receiver coincidence rays are drawn perpendicular to the reflector. This process is called Normal Incidence Ray Tracing and simulates a CDP stacked imaged section.

As we notice in Figure 1, seismic events (the dipping segment) are plotted directly beneath the source - receiver locations reached by the rays. This leads to an incorrect interpretation of data. A similar example of a diffractor is given in Figure 2. The diffraction curve is hyperbolic in nature, and occurs where any discontinuity exists.

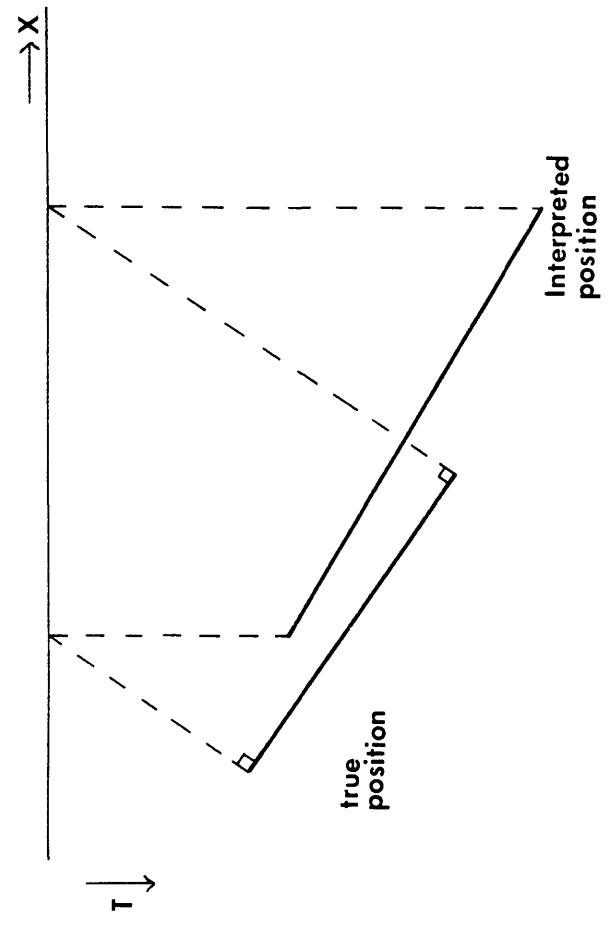


Figure 1: True and interpreted positions of a dipping segment.

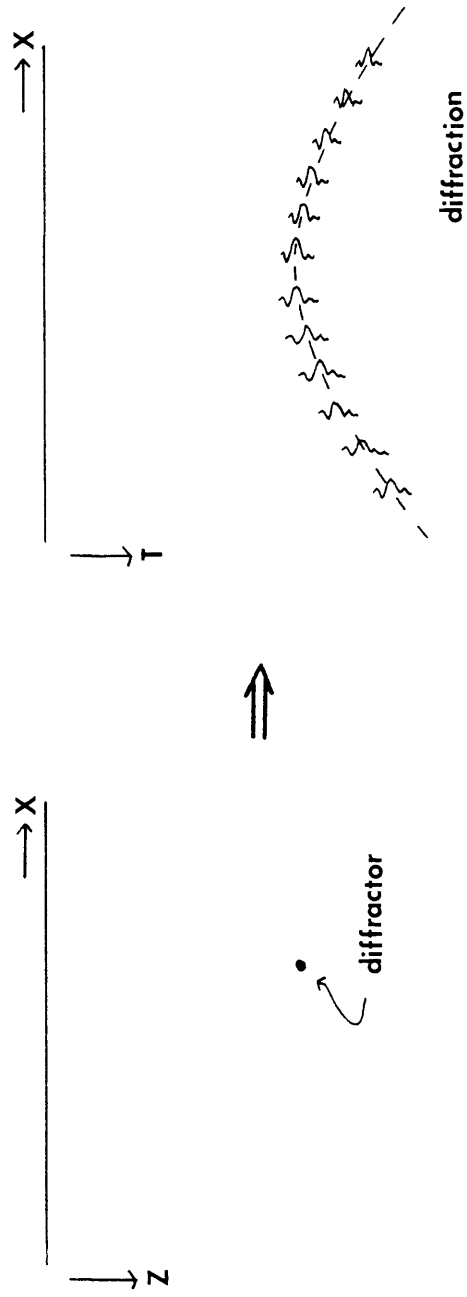


Figure 2: A diffraction from a scattering point.

Wave equation migration

Wave equation migration is the process which maps observed seismic data into either time or depth section at their correct vertical and horizontal position. It is based on numerical solution to the scalar wave equation,

$$\nabla^2 U - \frac{1}{c^2} U_{tt} = 0.$$

In implementation of two dimensional migration schemes today, there are three main assumptions:

- 1) data are primary reflections or diffractions,
- 2) cross - dip can be neglected,
- 3) velocity distribution is known

(Sheriff, 1978).

One of the main concerns is the problem of cross - dip. In two dimensional approach, we assume that there is no energy coming from out-of-plane structures. This is a poor assumption we have made. In real world, reflections come from all directions. Therefore, it should be emphasized that true migration can only be accomplished by processing in 3-D. It might be mentioned that the true three-dimensional migration is not obtained by separately migrating lines in two-dimensional form.

Wave equation migration is carried out in two steps (Figure 3);

1) Downward continuation.

Take the observed upgoing wave field at the surface and project it downward. This operation generates a series of new sections which estimate the recording of the wave field which would have been acquired at lower depth levels. Thus it gives us more detail and resolution.

2) Imaging.

The imaging principle states that the migrated section is composed of the downward continued recorded data for all depths, evaluated at $t = 0$.

There are a number of different migration methods available (Figure 4):

Finite - difference,
Kirchhoff integral,
Frequency - wavenumber,
Space - frequency.

All of these methods are based on the scalar wave equation. The differences in results are in the approximation made in their application rather than being intrinsic in

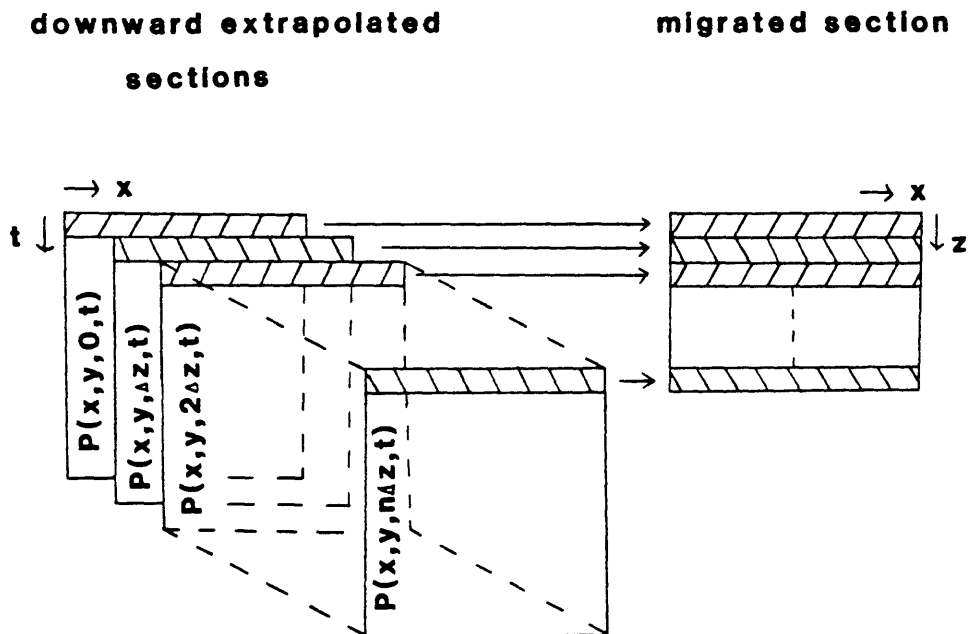


Figure 3: Migration of seismic section:
Downward continuation and Imaging.
(After Berkhout, 1980).

EXISTING DOWNWARD-EXTRAPOLATION
TECHNIQUES

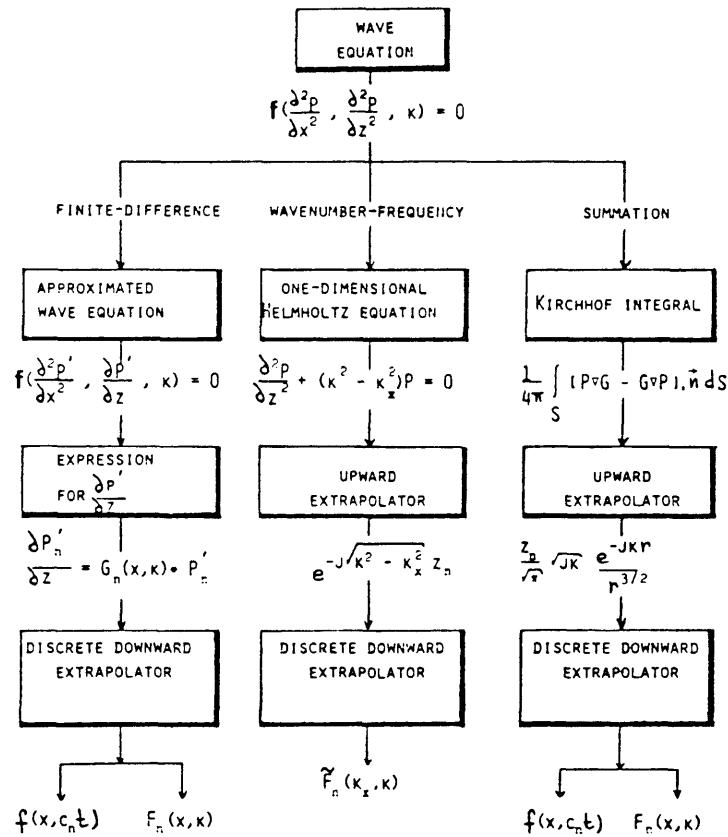


Figure 4: Some of existing downward continuation techniques: Finite difference, Kirchhoff integral, and Frequency wavenumber. (After Berkhout, 1979).

either approach (Sheriff, 1978). Table 1 summarizes the comparison of some of the techniques mentioned above.

The Finite difference method, introduced by Claerbout, transforms the scalar wave equation into difference equation. In his original development, performance was limited to about 15° dip. Refinement of his theory enables one to migrate up to 45° dip. The Finite difference algorithm handles a vertical velocity variation better than any other method. The major disadvantage is the dip limitation and large computer run time.

The Kirchhoff integral approach was introduced by French (1975) and Schneider (1978). This approach clearly shows historic ties to conventional diffraction summation approach, which simply summed trace amplitudes along diffraction curves. The main advantage of the method is good performance with steep dip, but it probably is the slowest of the current migration methods available.

Frequency wavenumber migration, popularized by Stolt (1978), has become a viable alternative to the conventional Finite difference or Kirchhoff integral approach. Unlike the other methods which migrate in the time domain, this method effects migration in the frequency wavenumber domain. With the aid of specially designed FFT hardware, computer run time is far less than any other methods. Stolt's development is a straight mapping process.

TABLE I
SUBJECTIVE SUMMARY

	F-D (t,x,z) (t,K _x ,z)	"F-K" (K _x ,K _z)	KIRCHHOFF (t,x,z)
SPACE			
COST	2	1	3
VELOCITY VARIATION	1	3	2
STEEP DIP	3	2	1
DISPERSION	3	1	2
TREATMENT OF NOISE	1	2	3
COSMETIC APPEARANCE	1	3	2
BEFORE STACK	3	2	1

Table I: Comparison of three different migration methods. "1" means best and "3" means worst. (After Johnson, 1978).

Bolondi (1978) and Gazdag (1978) discussed the idea of a recursive scheme in the $f-k$ domain. Both approaches, the former a straight mapping and the latter a recursive scheme, theoretically migrate any dip up to 90° . Also they do not suffer from frequency dispersion within the Nyquist band.

There still exists difficulties in migration. Such difficulties include noise, rapidly varying velocities, steep dip, and other problems which no current migration techniques handles perfectly (Chun, 1978).

F - K MIGRATION

In this chapter we discuss the theoretical development of migration of the frequency - wavenumber domain.

Basic theory for a constant velocity medium

Let the CDP stacked section be denoted by $\psi (x, z=0, t)$ where x is a spatial midpoint coordinate and t is a travel time coordinate. We assume that ψ is governed by the scalar wave equation with a constant propagation velocity c ,

$$\psi_{xx} + \psi_{zz} = \frac{1}{(c/2)^2} \psi_{tt}. \quad (1)$$

Here subscripts x , z , and t denote differentiation with respect to the corresponding coordinate. The $c/2$ in equation (1) results from the fact that t equals the two way travel time. Now we employ the basic imaging principle; that is, migration is accomplished by transforming the surface wave field $\psi(x,0,t)$ into the wave field at a depth z , evaluated at $t=0$ $\psi(x,z,0)$. This is equivalent to the downward continuation of source - receivers from $z=0$ to a particular depth and evaluating at $t=0$. (Figure 5)

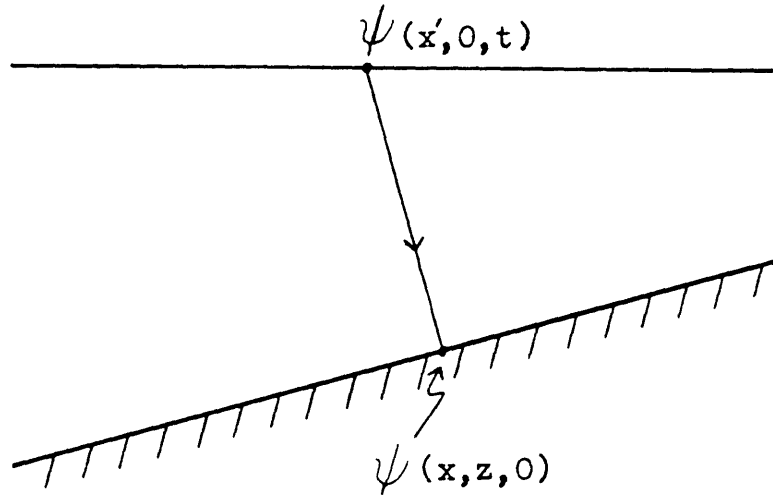


Figure 5: Simplified picture of downward continuation. x' is a surface midpoint coordinate and x is a migrated coordinate.

In order to carry out this scheme in the frequency-wavenumber domain, we have to take a two dimensional Fourier transform of equation (1) with respect to x and t . Let the two dimensional Fourier transform be defined as

$$U(k_x, f, z) = \int_{-\infty}^{\infty} \int_{-\infty}^{\infty} dt \, dx \, \psi(x, t, z) e^{-j2\pi(ft+xk_x)}. \quad (2)$$

The Fourier transform of each term in equation (1) is given as follows by the differentiation property,

$$\psi_{xx} \longleftrightarrow (j2\pi k_x)^2 U, \quad (3-a)$$

$$\psi_{tt} \longleftrightarrow (j2\pi f)^2 U, \quad (3-b)$$

$$\psi_{zz} \longleftrightarrow U_{zz}. \quad (3-c)$$

Here " \longleftrightarrow " denotes Fourier transform pairs. Substituting equations (3-a), (3-b), and (3-c) into the original equation (1), we have

$$-4\pi^2 k_x^2 U + U_{zz} = -\frac{4}{c^2} 4\pi^2 f^2 U.$$

Rearranging the terms, finally we have in the transformed domain,

$$U_{zz} = -4\pi^2 \left(\frac{4f^2}{c^2} - k_x^2 \right) U. \quad (4)$$

The solution to this second order differential equation is

$$U(k_x, f, z) = A e^{j2\pi z \left(\frac{4f^2}{c^2} - k_x^2 \right)^{1/2}}. \quad (5)$$

The coefficient A can be determined from the boundary condition by setting $z=0$ and we have finally,

$$U(k_x, f, z) = U(k_x, f, 0) e^{j2\pi z \left(\frac{4f^2}{c^2} - k_x^2 \right)^{1/2}}. \quad (6)$$

The above equation relates the wave field at depth z to the wave field at $z=0$ (surface data). Qualitatively,

$U(k_x, f, z)$ Two dimensional Fourier transform of $\psi(x, z, t)$.

$U(k_x, f, 0)$ Two dimensional Fourier transform of $\psi(x, 0, t)$, which is the surface data.

and

$e^{j2\pi z (\frac{4f^2}{c^2} - k_x^2)^{1/2}}$ Operator to extrapolate the surface wave field downward by a distance z .

The next step we must take is to transform equation (6) back into the time domain. The two dimensional inverse Fourier transform of equation (6) is

$$\psi(x, z, t) = \int_{-\infty}^{\infty} \int_{-\infty}^{\infty} df dk_x U(k_x, f, z) e^{j2\pi(ft+k_x x)}. \quad (7)$$

Substituting equation (6) for U in equation (7), we have,

$$\psi(x, z, t) = \int_{-\infty}^{\infty} \int_{-\infty}^{\infty} df dk_x U(k_x, f, 0) e^{j2\pi z (\frac{4f^2}{c^2} - k_x^2)^{1/2}} \cdot e^{j2\pi(ft+k_x x)}. \quad (8)$$

Now referring back to the imaging principle, what we want is $\psi(x, z, 0)$ not $\psi(x, z, t)$, therefore we may set $t=0$ in equation (8), giving the migrated section,

$$\psi(x, z, 0) = \int_{-\infty}^{\infty} \int_{-\infty}^{\infty} df dk_x U(k_x, f, 0) e^{j2\pi \left[z \left(\frac{4f^2}{c^2} - k_x^2 \right)^{1/2} + k_x x \right]}. \quad (9)$$

The above equation, as it stands, is not very economical since for each depth z , we must perform a double integral over f and k_x . However by a simple change of variables, we can transform equation (9) into what looks like a two dimensional inverse Fourier transform.

Let

$$k_z = \left(\frac{4f^2}{c^2} - k_x^2 \right)^{1/2} \quad (10)$$

then,

$$f = \frac{c}{2} (k_z^2 + k_x^2)^{1/2}, \quad (11)$$

$$df = \frac{c}{2} \frac{k_z}{(k_z^2 + k_x^2)^{1/2}} dk_z. \quad (12)$$

Substituting equations (11) and (12) into equation (9), we have

$$\psi(x, z, 0) = \frac{c}{2} \int_{-\infty}^{\infty} \int_{-\infty}^{\infty} dk_x dk_z Q(k_x, k_z) e^{j2\pi(k_z z + k_x x)} \quad (13)$$

where

$$Q(k_x, k_z) = \frac{k_z}{(k_z^2 + k_x^2)^{1/2}} U(k_x, \frac{c}{2}(k_z^2 + k_x^2)^{1/2}) \quad (14)$$

Finally, equations (11), (13), and (14) represent the solution to our problem.

The coordinate transformation equations (10) and (14) represent a shift of frequency from f to a lower frequency $f' = (f^2 - \frac{c^2 k_x^2}{4})^{1/2}$ for a constant k_x . This is similar to a moveout correction where f takes the place of time, and k_x of offset. Figure 6 shows the nature of this coordinate transformation. Points in the $f - k_x$ plane move vertically down to points in the $k_z - k_x$ plane. Taking an example in Figure 6, points at a constant frequency f_0 map onto a circle in the $k_z - k_x$ domain such that $2f_0/c = (k_x^2 + k_z^2)^{1/2}$. In the constant velocity medium, no propagation energy exists below the line $f = c \cdot k_x$. All physically realizable energy must lie within the region bounded by $f = \pm c k_x$. After the migration, the wedge shaped region is transformed into a hemisphere governed by equation (11) as shown in Figure 7. Figure 8 summarizes the scheme in a simple block diagram for a constant velocity medium.

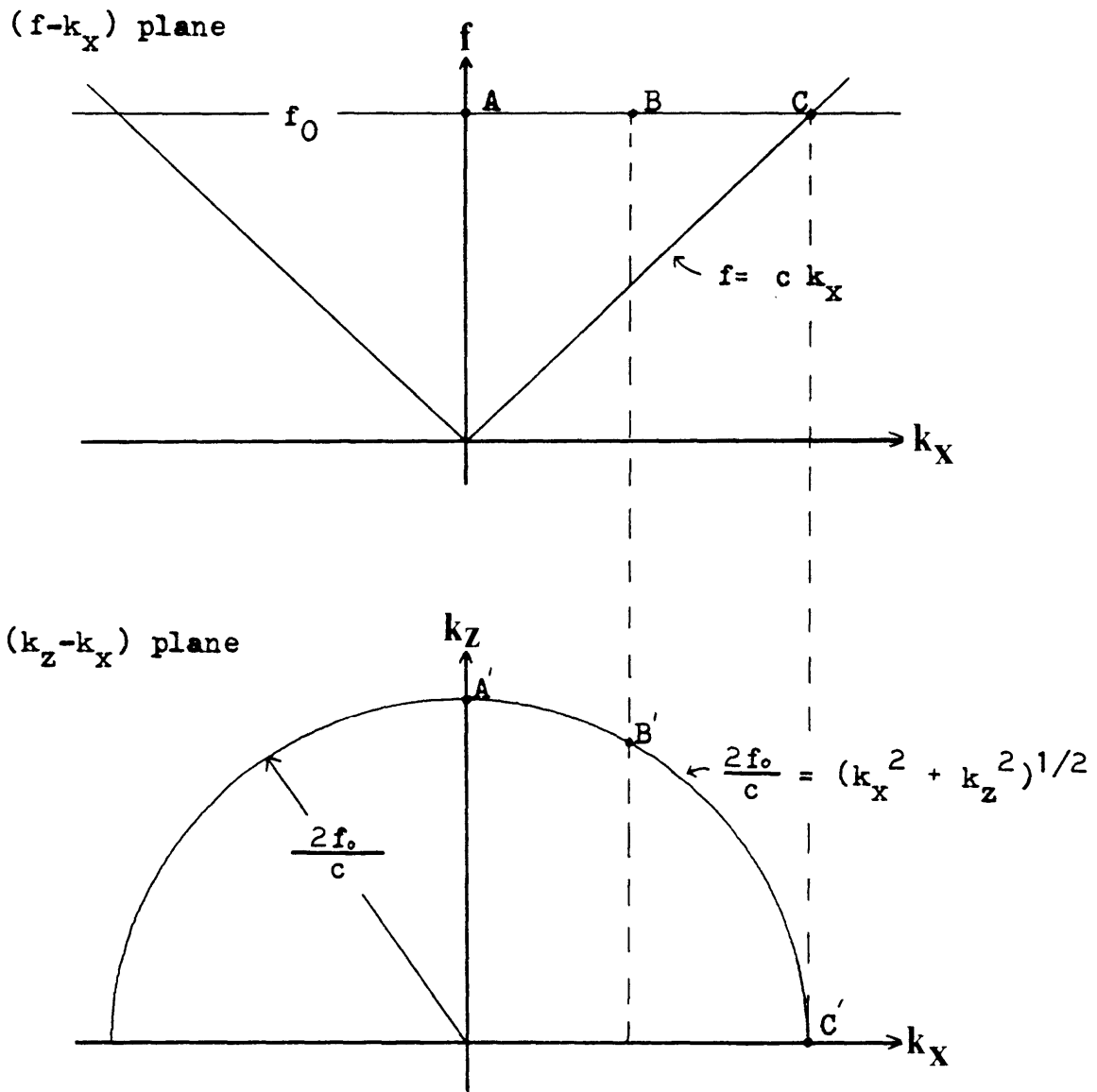


Figure 6: Migration mapping procedure for a constant velocity case.

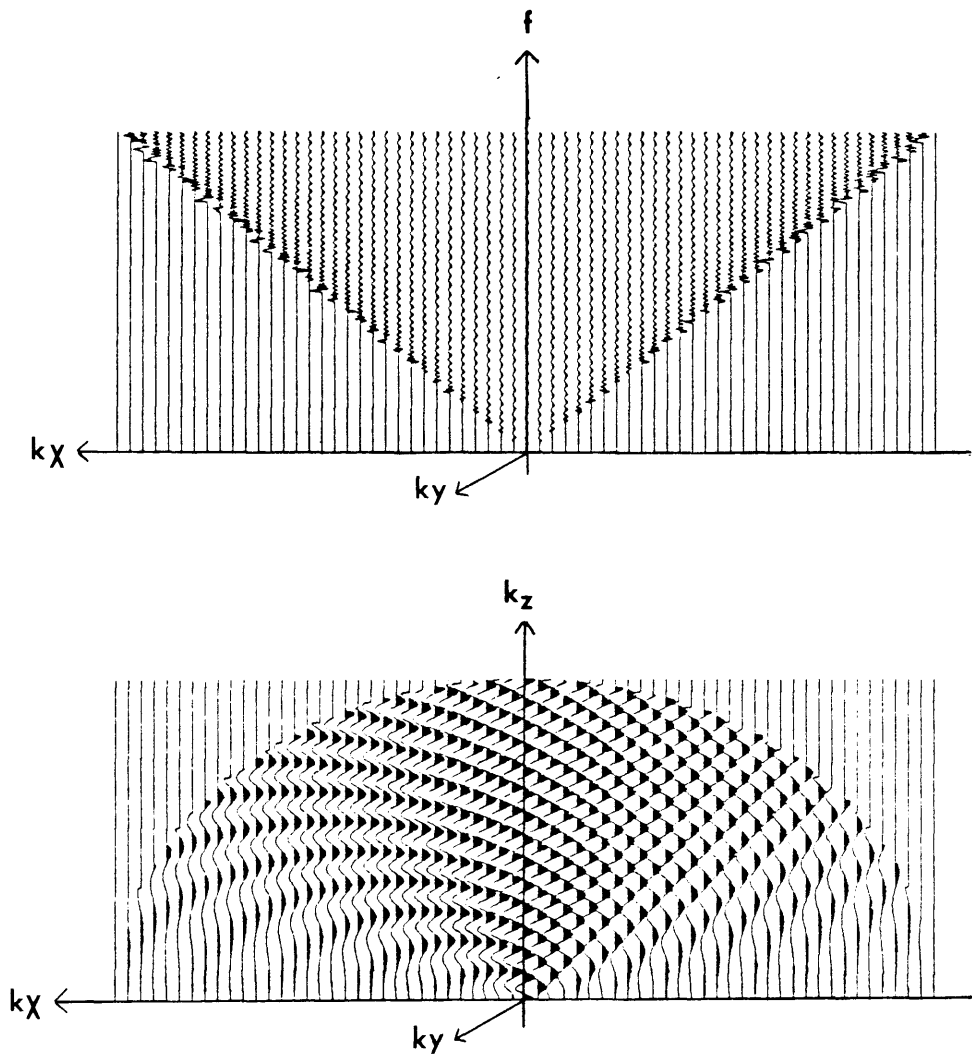


Figure 7: An example of migration mapping for a constant velocity case. f and k_x are not plotted on the same scale. This transformation from top to bottom is governed by equation(10). The wiggles shown in the plots represent moduli of Fourier spectrum.

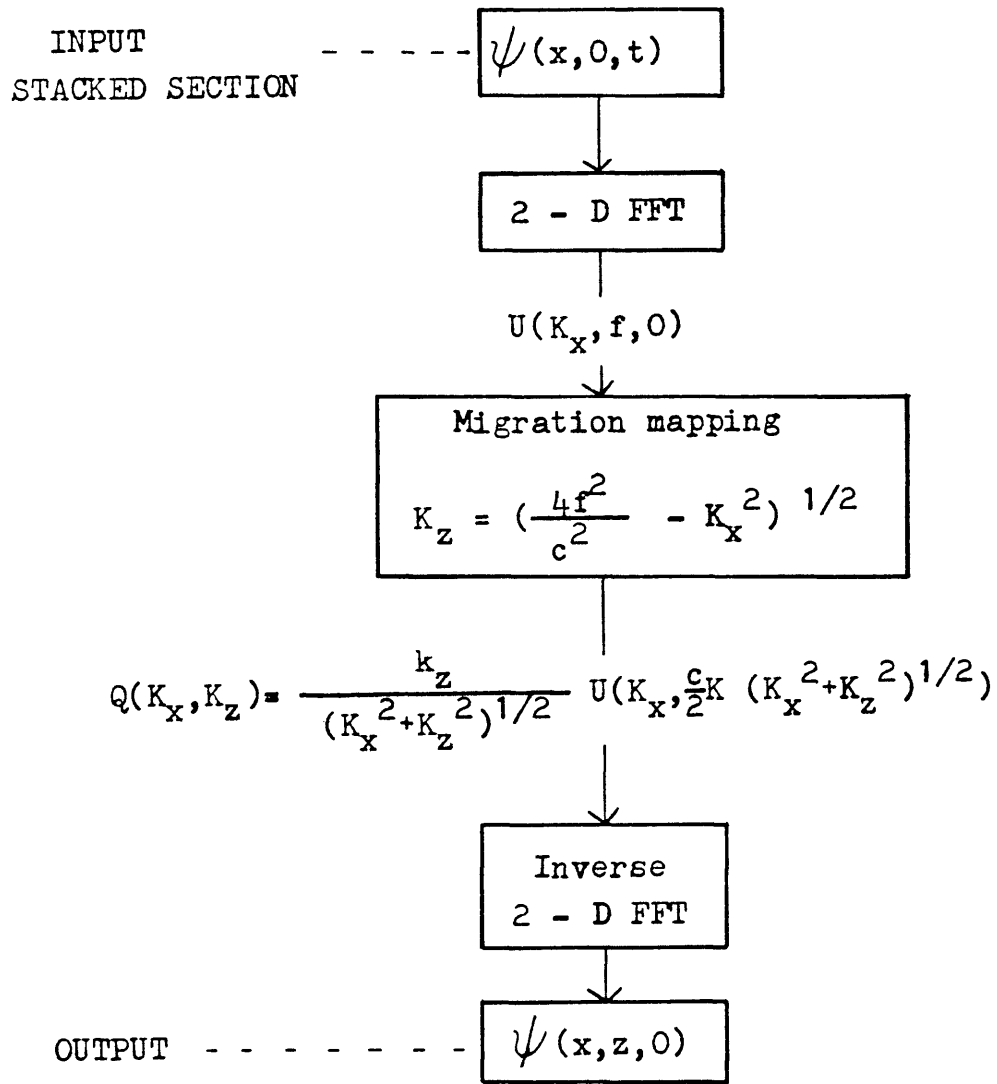


Figure 8: Simplified flow chart of constant velocity method.

Variable velocity method

The foregoing discussion assumes a constant propagation velocity c . Stolt (1978) made modifications to the constant velocity procedure in order to incorporate a vertical velocity gradient. After a series of coordinate transformations and approximations, Stolt obtained the new wave equation which is in an oblique coordinate system. Unlike the constant velocity case which is the exact solution to the scalar wave equation, this refined development of Stolt's approximates the wave equation. However, approximations he made are no worse than the ones made in other migration techniques such as Finite difference or Kirchhoff integral methods.

Starting with equations which govern $\psi(x_s, z_s, x_o, z_o, t)$,

$$\psi_{x_s x_s} + \psi_{z_s z_s} - \psi_{tt}/c(x_s, z_s)^2 = 0 \quad (15)$$

and

$$\psi_{x_o x_o} + \psi_{z_o z_o} - \psi_{tt}/c(x_o, z_o)^2 = 0 \quad (16)$$

where x_s, z_s is a source location and x_o, z_o is a receiver location. If we pretend that "stacked" sections are equivalent to normal incidence sections, that is, $(x_s, z_s) = (x_o, z_o)$. Defining midpoint coordinates,

$$X = (x_s + x_o)/2 \quad \text{and} \quad Z = (z_s + z_o)/2 \quad (17)$$

and offset coordinates,

$$x = (x_o - x_s)/2 \text{ and } z = (z_o - z_s)/2 \quad (18)$$

Setting $\psi(X,x,Z,z,t) = \psi(x_s, z_s, x_o, z_o, t)$, and ignoring first derivatives with respect to x and z (see footnote on pp. 24, Stolt, 1978), equations (15) and (16) becomes

$$\psi_{XX} + \psi_{ZZ} = 4/C(X,Z)^2 \psi_{tt} = 0 \quad (\text{Stolt, 1978}) \quad (19)$$

Performing a series of coordinate transformations, neglecting velocity derivatives, and by setting $\phi(X,d,D) = \psi(X,Z,t)$ Stolt has come up with the equation

$$\phi_{XX} + W(X,d,D) \phi_{dd} + 2 \phi_{dD} = 0 \quad (20)$$

where

$$W = \frac{C(X,Z)^2}{\eta^2} + \frac{2d}{D} \left(1 - \frac{C(X,Z)^2 D^2}{\eta} \right), \quad (21)$$

$$D = \sqrt{2 \int_0^t \tau \cdot V_{rms}^2(\tau) d\tau}, \quad (22)$$

(Stolt, 1978)

η and d are variables defined during Stolt's coordinate transformations.

Now migration proceeds from the half plane,

$$d = 0, D > 0,$$

to the half plane,

$$d = D, D > 0.$$

Here D replaces time and is length dimensioned. We call this a "pseudo - depth" since only if the velocity is constant does D have a physical sense of depth. And d replaces Z which is a real depth variable of the original coordinate system. So all that these coordinate transformations amount to is that a stretching and a de-stretching of the input traces has to be carried out by using equation (22).

Figure 9 depicts an example of a diffraction stretching. The solid line indicates a real diffraction curve and the dashed line indicates a pseudo - depth converted diffraction curve.

Here we see that the pseudo - depth converted diffraction has been stretched down. This converted diffraction will not, therefore, be collapsed completely just by using the velocity of the upper medium, even though this velocity is the only parameter responsible for the diffraction. This is the reason we have to be very careful about the selection of W . We will discuss this point later in this section.

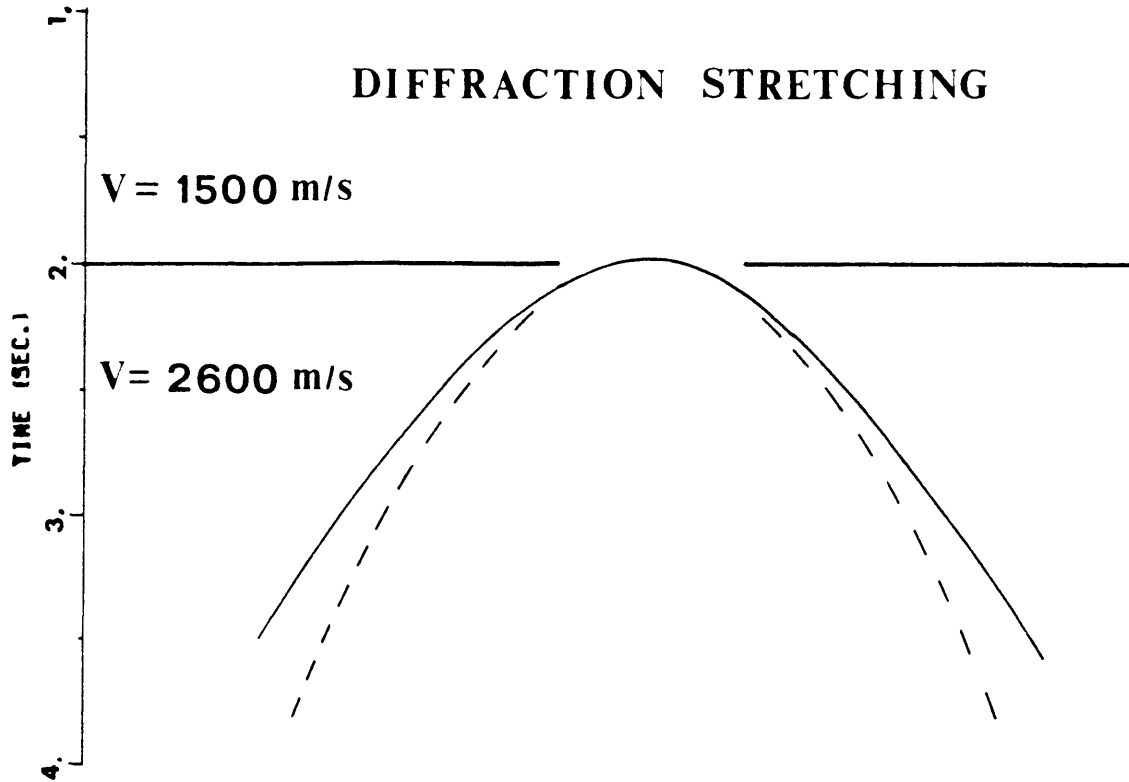


Figure 9: An example of stretching. The solid line indicates the real diffraction curve, the dashed line indicates the pseudo - depth converted diffraction curve.

Now let us proceed to obtain mapping equations from equation (20), we have

$$\phi_{XX} + W\phi_{dd} + 2\phi_{dD} = 0. \quad (\text{Stolt, 1978}) \quad (20)$$

By taking a two dimensional Fourier transform with respect to X and D, we have in the transformed domain

$$W U_{dd} + 4\pi j k_D U_z = 4\pi^2 k_x^2 U. \quad (23)$$

The solution to this differential equation is

$$U(k_x, k_D, d) = U(k_x, k_D, 0) e^{j2\pi d} - \left[\frac{k_D}{W} + \sqrt{\frac{k_D^2}{W^2} - \frac{k_x^2}{W}} \right]. \quad (24)$$

By taking the inverse two dimensional Fourier transform of equation (24), we have

$$\phi(X, d, D) = \int_{-\infty}^{\infty} \int_{-\infty}^{\infty} dk_x dk_D U(k_x, k_D, 0) e^{j2\pi} \left\{ Xk_x + Dk_D + d \left[-\frac{k_D}{W} + \sqrt{\frac{k_D^2}{W^2} - \frac{k_x^2}{W}} \right] \right\}. \quad (25)$$

Now we apply the imaging principle; that is, the migrated section occurs when $d=D$, then equation (25) becomes

$$\phi(X, D, D) = \int_{-\infty}^{\infty} \int_{-\infty}^{\infty} dk_x dk_D U(k_x, k_D, 0) e^{j2\pi} \left\{ Xk_x + D \left[\frac{k_D(W-1)}{W} + \sqrt{\frac{k_D^2}{W^2} - \frac{k_x^2}{W}} \right] \right\}. \quad (26)$$

As it has been shown in the constant velocity case, a change of variables will help us here too.

Let

$$k_z = \frac{k_D (W-1)}{W} + \sqrt{\frac{k_D^2}{W^2} - \frac{k_x^2}{W}}. \quad (27)$$

After some manipulations, we have

$$k_D = \frac{(1-W) k_z + \sqrt{k_z^2 + (2-W) k_x^2}}{(2-W)} \quad (28)$$

and

$$dk_D = \frac{k_z + (1-W) \sqrt{k_z^2 + (2-W) k_x^2}}{(2-W) \sqrt{k_z^2 + (2-W) k_x^2}} dk_z. \quad (29)$$

Therefore we have for the migrated section

$$\phi(X, D, D) = \int_{-\infty}^{\infty} \int_{-\infty}^{\infty} dk_x dk_z Q(k_x, k_z) e^{j2\pi(Xk_x + Dk_z)}, \quad (30)$$

where

$$Q(k_x, k_z) = \frac{k_z + (1-W) \sqrt{k_z^2 + (2-W) k_x^2}}{(2-W) \sqrt{k_z^2 + (2-W) k_x^2}} \cdot U\left(k_x, \frac{(1-W)k_z + \sqrt{k_z^2 + (2-W) k_x^2}}{(2-W)}\right). \quad (31)$$

Note in equation (31), in the case of $W=1$,

$$Q(k_x, k_z) = \frac{k_z}{\sqrt{k_z^2 + k_x^2}} U(k_x, \sqrt{k_z^2 + k_x^2})$$

which is equivalent to the constant velocity case.

From this point the migration proceeds as follows

- 1) time to pseudo - depth conversion with equation (22)
- 2) two dimensional Fourier transform
- 3) migration mapping with equation (31)
- 4) two dimensional inverse Fourier transform
- 5) pseudo - depth to time conversion with equation (22).

Now let us turn our attention back to the discussion of W , the shaping parameter. Equation (20) shows that all explicit dependence on X and Z now resides in the coefficient W of ϕ_{dd} . $W \neq 1$ reflects the fact that diffractions are not pure hyperbolas in a layered medium (Stolt, 1978). Stolt also argued that W , a function of all variables, is supposed to take care of a vertical velocity gradient. Stolt proposed W be held constant along the entire seismic section (a value usually between 0.5 and 1.0). Looking back in Figure 9, for greater dips the two curves are significantly diverging from each other.

This means that standard F - K migration of such dips will result in mislocated events. This is a threat to one of the more attractive features of the variable velocity method, which is the ability to migrate any dip up to 90°.

The detailed study done by J. P. Diet (1979) indicated that in the medium where velocity is a linear function of depth, W can be calculated using the following equation

$$W = \frac{e^{-2\alpha t} + 2\alpha t - 1}{e^{2\alpha t} + e^{-2\alpha t} - 2} , \quad (\text{Diet, 1979}) \quad (32)$$

where α is the vertical velocity gradient, and t is the one way travel time. Figure 10 displays W as a function of α and t . The idea he used is to compare the theoretical diffraction curves in a pseudo - depth domain with the real ones we want to collapse and used the parameter W to make them fit each other as well as possible. From theory Diet obtained the following equations in a pseudo - depth domain, for theoretical diffraction curves as a function of W,

$$D(x) = D_0 \frac{W-1}{W} + \frac{D_0}{W} \sqrt{1 + x^2 \frac{W}{D_0^2}} , \quad (\text{Diet, 1979}) \quad (33)$$

and for observed diffraction curves as a function of velocity ration ($V_{\text{lower}}/V_{\text{upper}}$) only for a small offset,

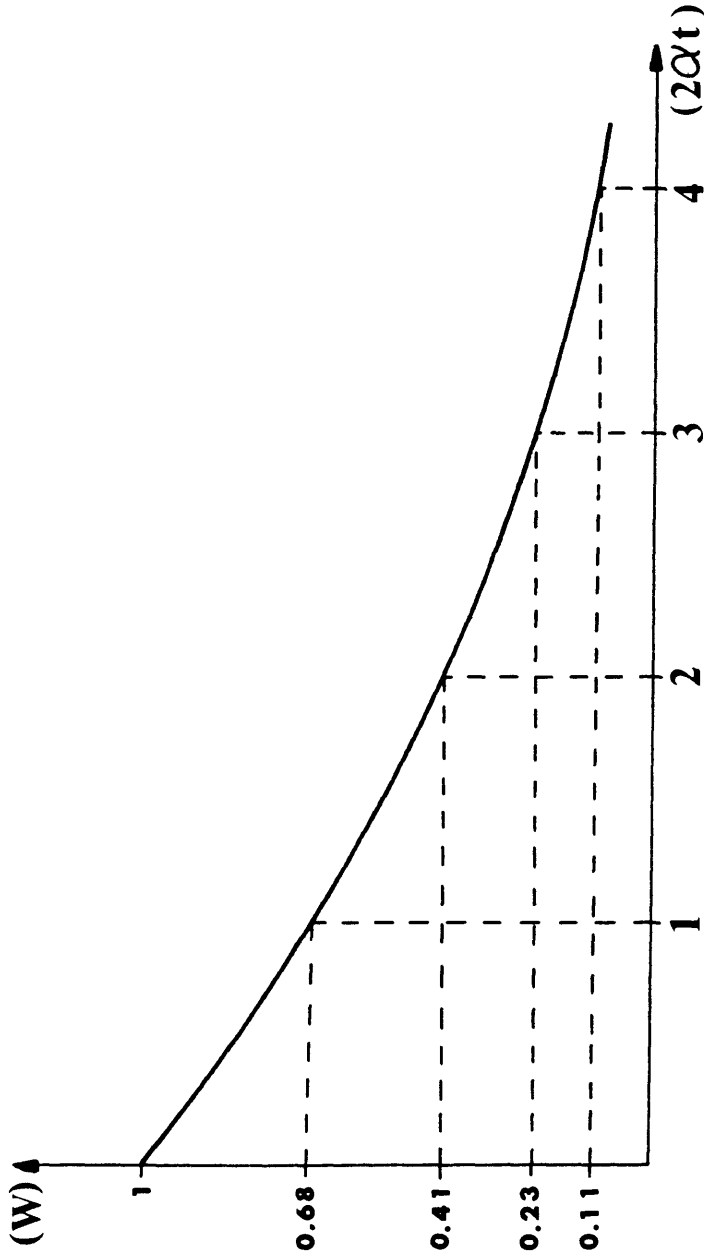


Figure 10: W plotted as a function of Q and t . Q is the velocity gradient and t is a one way travel time. (Replotted after Diet, 1979).

$$D(x) \approx D_0 + \frac{x^2}{2D_0} - \frac{x^4}{8D_0^3} \left(2 - \frac{v_u^2}{v_l^2} \right), \quad (34)$$

(Diet, 1979)

where in both equations, x is the offset distance and D_0 is the pseudo - depth of the diffracting point. An example of a simple two layer model is shown in Figure 11 and 12. Figure 11 shows theoretical diffraction curves in a pseudo - depth domain calculated as a function of W , and Figure 12 shows diffraction curves calculated as a function of velocity ratio ($v_{\text{lower}}/v_{\text{upper}}$). D_0 in both figures is the pseudo - depth of the diffracting point. Notice that the curve for $W=1$ in Figure 11 and the one for velocity ratio = 1 are the same because they both reflect the constant velocity case.

For a given seismic section, the value of W may be chosen in order to focus the region of interest even though the value may not be the best choice for other parts of the section.

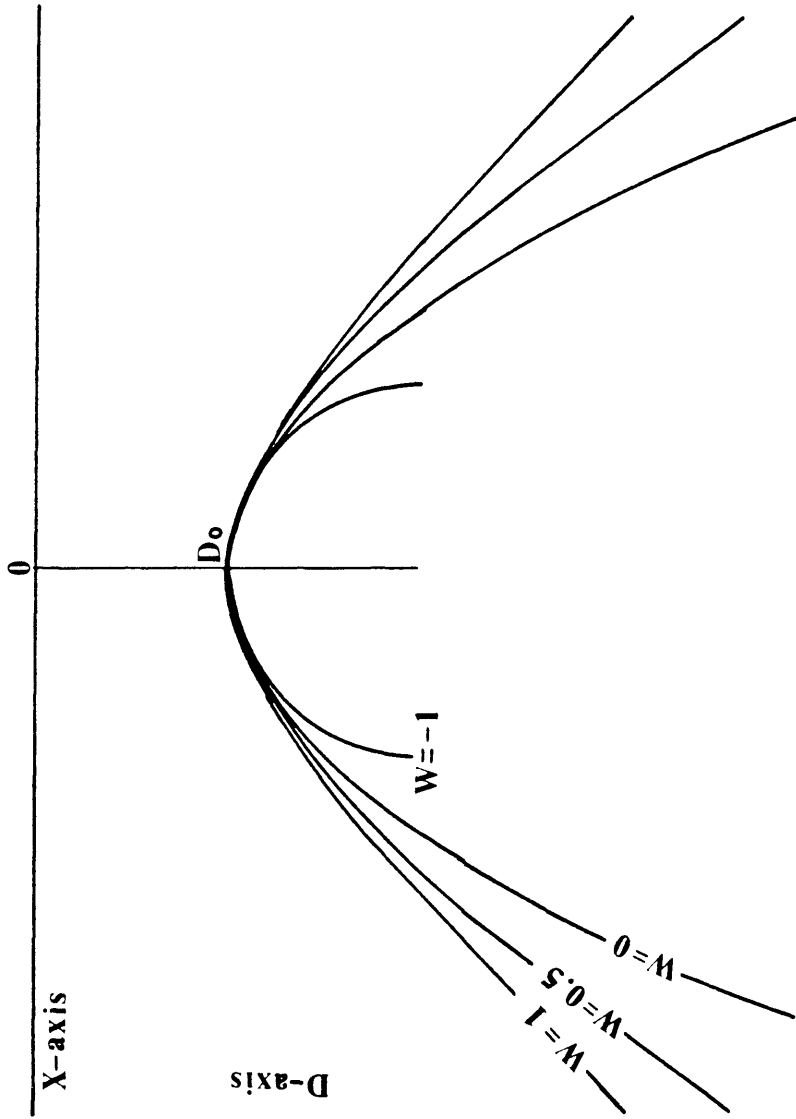


Figure 11: Pseudo - depth converted theoretical diffraction curves for different W . (Replotted after Diet, 1979).

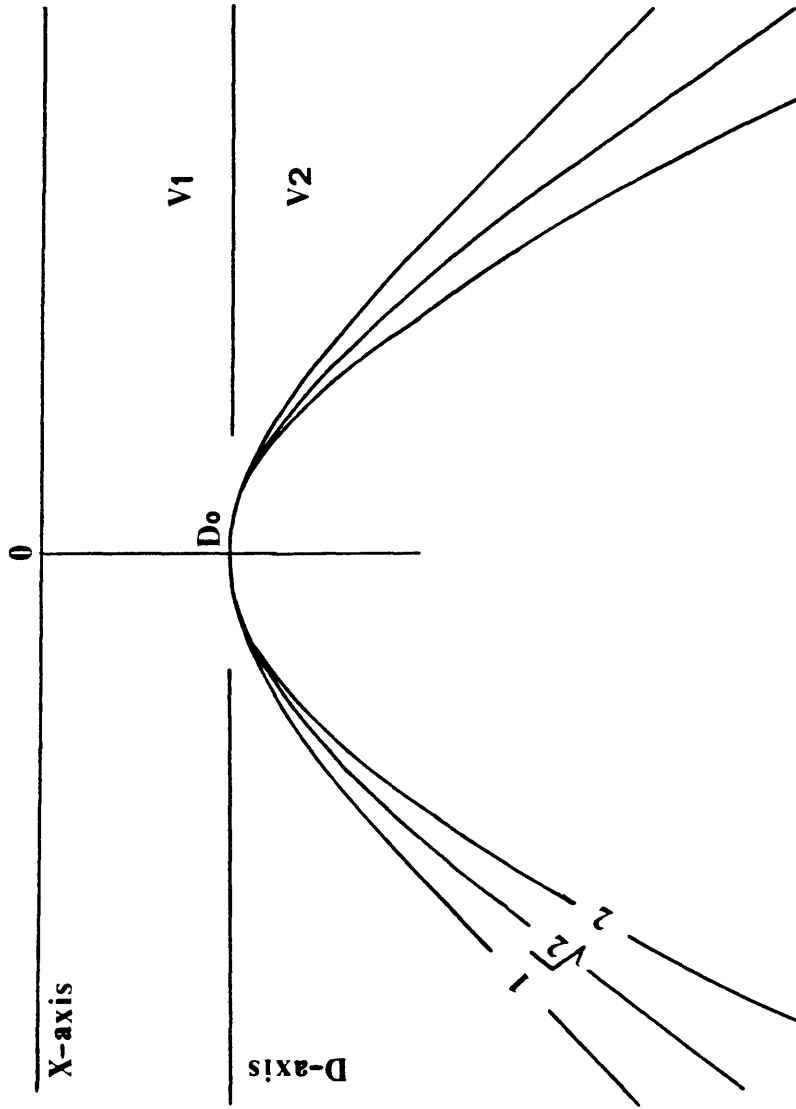


Figure 12: Pseudo - depth converted real diffraction curves for different velocity ratio (V_2 / V_1). (Replotted after Diet, 1979).

Incremental method

The incremental method also performs migration in the frequency wavenumber domain. This is a recursive type of scheme, in which the subsurface is discretized into layers with constant velocities and the wave field is extrapolated layer by layer (Figure 13).

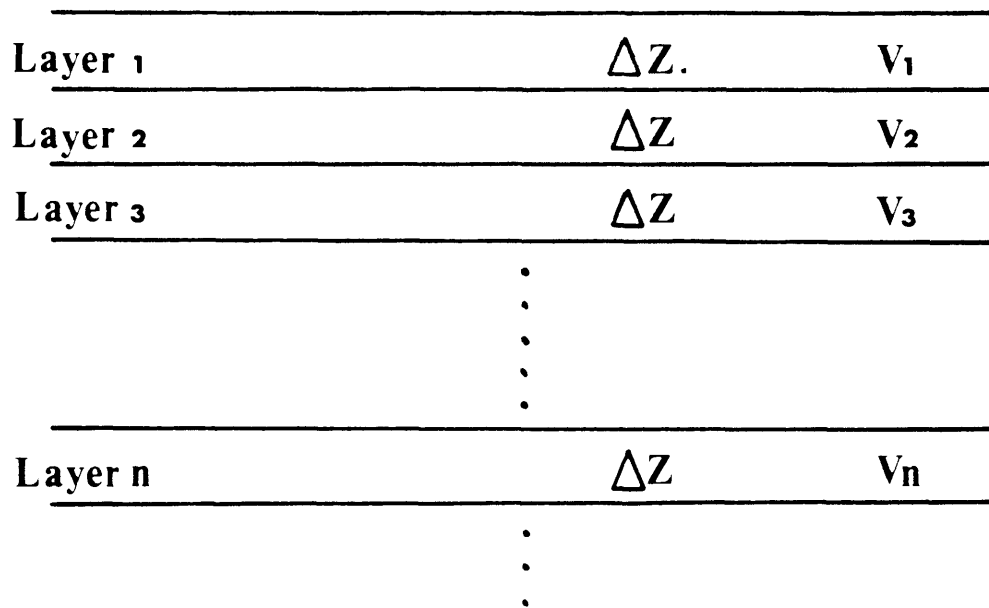


Figure 13: Diagram of the incremental model.

Naturally, one might then suspect that computation time is increased. However a big advantage of the incremental method over the variable velocity method is that the wave extrapolation is exact, since the subsurface is subdivided into constant velocity layers. Consequently, it gives us more accurate imaging of the section in the presence of a vertical velocity gradient. If one desires, the subdivision can be broken down to each sampling interval.

Let $U(k_x, f, 0)$ be a two dimensional Fourier transform of the stacked section. Then we know from equation (6) in the basic theory section, the downward continued wave field across layer 1 is given by

$$U(k_x, f, \Delta z) = U(k_x, f, 0) e^{j2\pi\Delta z \left(\frac{4f^2}{c_1^2} - k_x^2\right)^{1/2}}. \quad (35)$$

The extrapolation across layer 2 is given by

$$\begin{aligned} U(k_x, f, 2\Delta z) &= U(k_x, f, \Delta z) e^{j2\pi\Delta z \left(\frac{4f^2}{c_2^2} - k_x^2\right)^{1/2}} \\ &= U(k_x, f, 0) e^{j2\pi\Delta z \sum_{i=1}^2 \left(\frac{4f^2}{c_i^2} - k_x^2\right)^{1/2}}. \end{aligned} \quad (36)$$

By successive extrapolations of the wave field we have

$$U(k_x, f, z_n) = U(k_x, f, 0) e^{j2\pi\Delta z \sum_{i=1}^N \left(\frac{4f^2}{c_i^2} - k_x^2\right)^{1/2}}. \quad (37)$$

Now we have to take the two dimensional inverse Fourier transform; that is,

$$\phi(x, z_n, t) = \int_{-\infty}^{\infty} \int_{-\infty}^{\infty} U(k_x, f, z_n) e^{j2\pi(xk_x + tf)} dk_x df, \quad (38)$$

Referring back to the imaging principle, what we really want is the wave field at $t=0$ at some particular depth z_n . Then by setting $t=0$ in equation (38), we have

$$\phi(x, z_n, 0) = \int_{-\infty}^{\infty} \int_{-\infty}^{\infty} U(k_x, f, z_n) e^{j2\pi xk_x} df dk_x, \quad (39)$$

Equation (39) indicates that we have to integrate over frequency then take the inverse Fourier transform along the spatial axis (Figure 14). Then the migration proceeds as follows:

- 1) two dimensional Fourier transform of the stacked section.
- 2) at each desired depth
 - multiply the wave field by the extrapolation operator
 - sum frequency at common k_x 's
 - inverse one dimensional Fourier transform along the k_x axis.

Figure 15 shows a simplified flow diagram of the process.

MATHEMATICAL DEVELOPMENT

Incremental F,K Migration

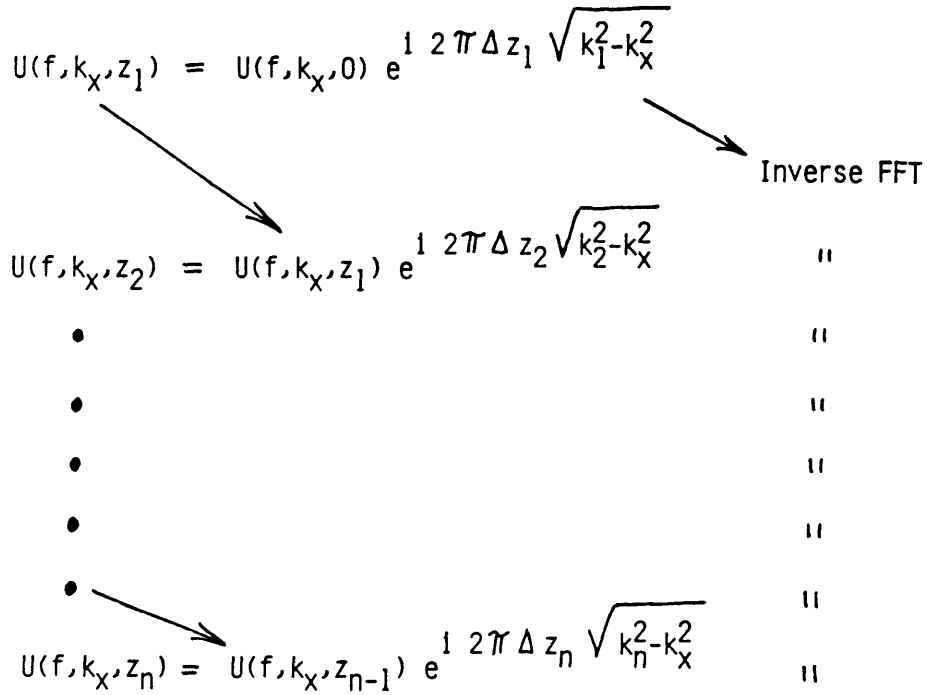


Figure 14: Simplified diagram of the incremental process.

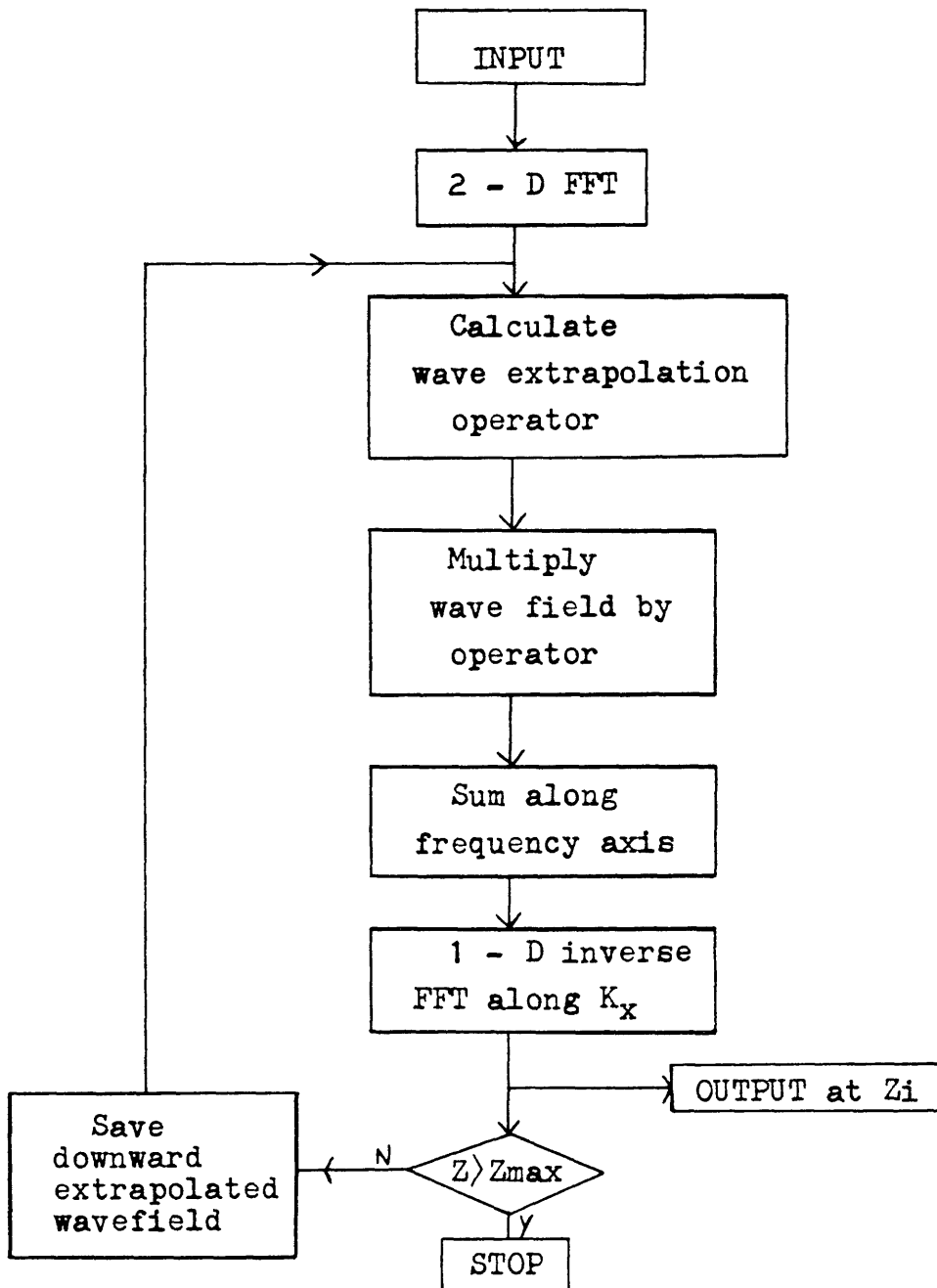


Figure 15: Simplified flow diagram of the incremental method.

COMPARISON OF FREQUENCY DOMAIN MIGRATION METHODS

In order to carry out the comparison of the two migration schemes, several examples are presented here. For forward synthetic modelling, the CGG wave equation modelling package was used. The sampling interval, the CDP spacing, and the wavelet used for synthetic time sections are 1 msec., 50 feet, and a bandpass wavelet with corner frequencies at (10,30,80,100) hz, respectively. Synthetic time sections were migrated by FKMIG (CGG) for the variable velocity method and YOMIG (written by the author) for the incremental method in order to establish a basis for comparison of the two methods.

One horizon test model (Model 1)

Model 1 was intended primarily for the testing of the incremental method and for the reconfirmation of Diet's study (1979). Figures 16, 17, and 18 show the physical parameters, normal incidence time section and wave - theory modelling of model 1, respectively. There is no geological significance to this model, densities are varied to give diffractions. Figure 19 illustrates a pseudo - depth converted real diffraction and a pseudo - depth converted theoretical diffraction curve with $W=1.0$. Since the velocity ratio, 1.2, is very small, two diffraction curves in the pseudo - depth domain are very close, in fact indistinguishable in this figure. Consequently, we expect migration to be very close to perfect. And indeed, the migrated result of this synthetic model is very good. Figures 20 and 21 show migrations of model 1 by the variable velocity method, and by the incremental method, respectively. Here we observed that the variable velocity method gives us acceptable results when the velocity ratio is close to 1.0.

Next, the velocity ratio is increased to 2.0. Synthetic time section of this model is the same as the one illustrated in Figure 18. The velocity of the upper medium is the only factor responsible for the diffraction

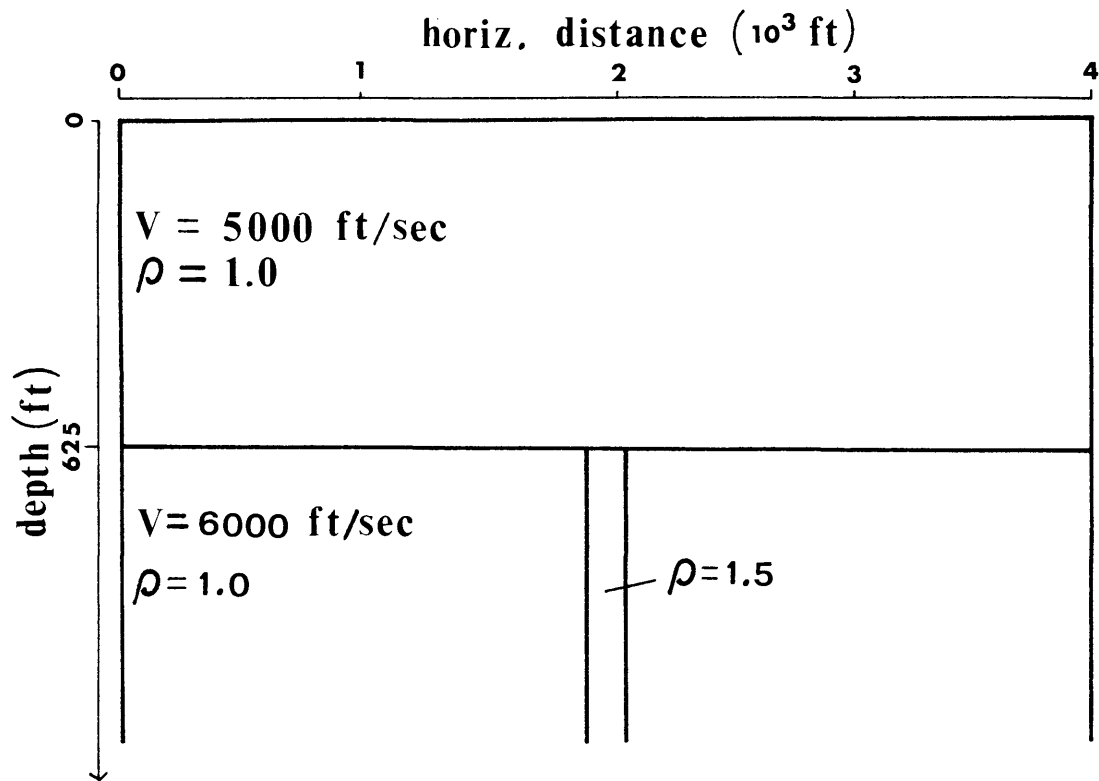


Figure 16: Physical parameters of model 1.

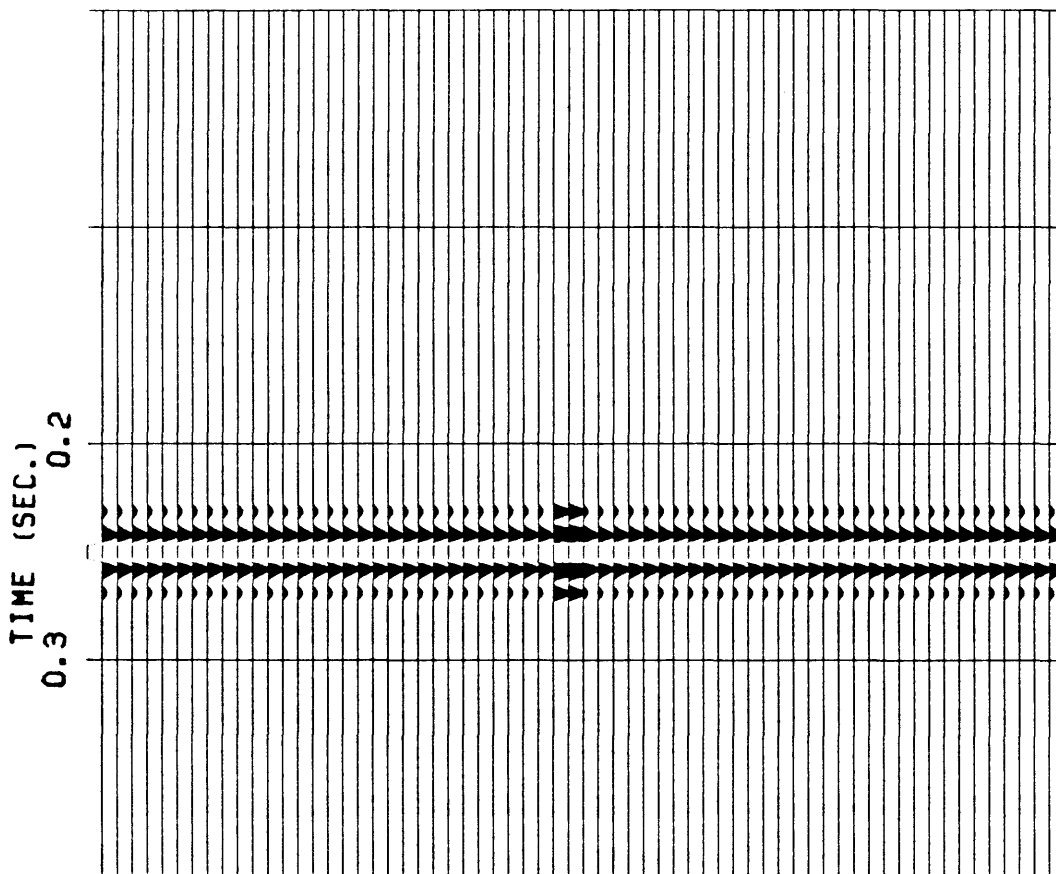


Figure 17: Normal incidence time section of model 1.

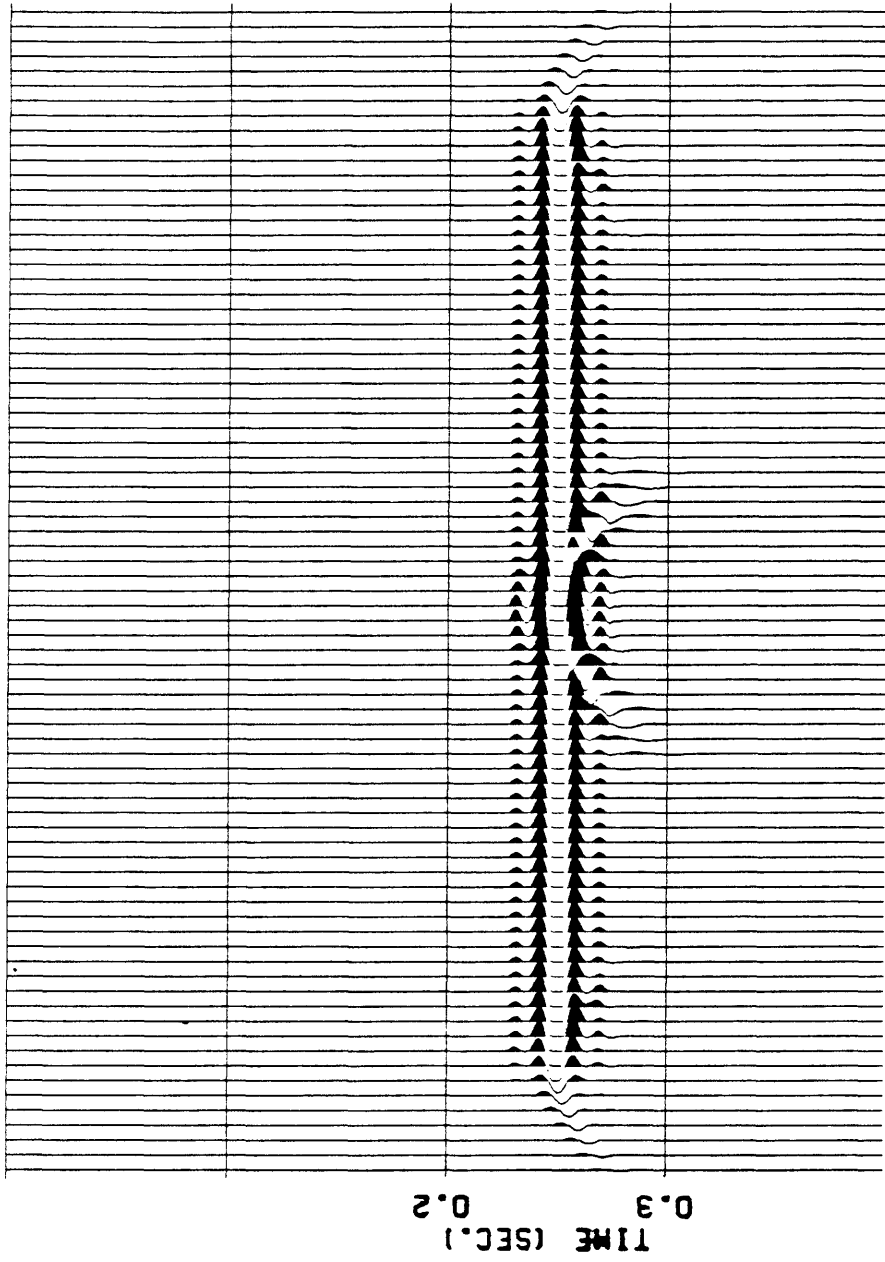


Figure 18: Wave - theory modelling of model 1.

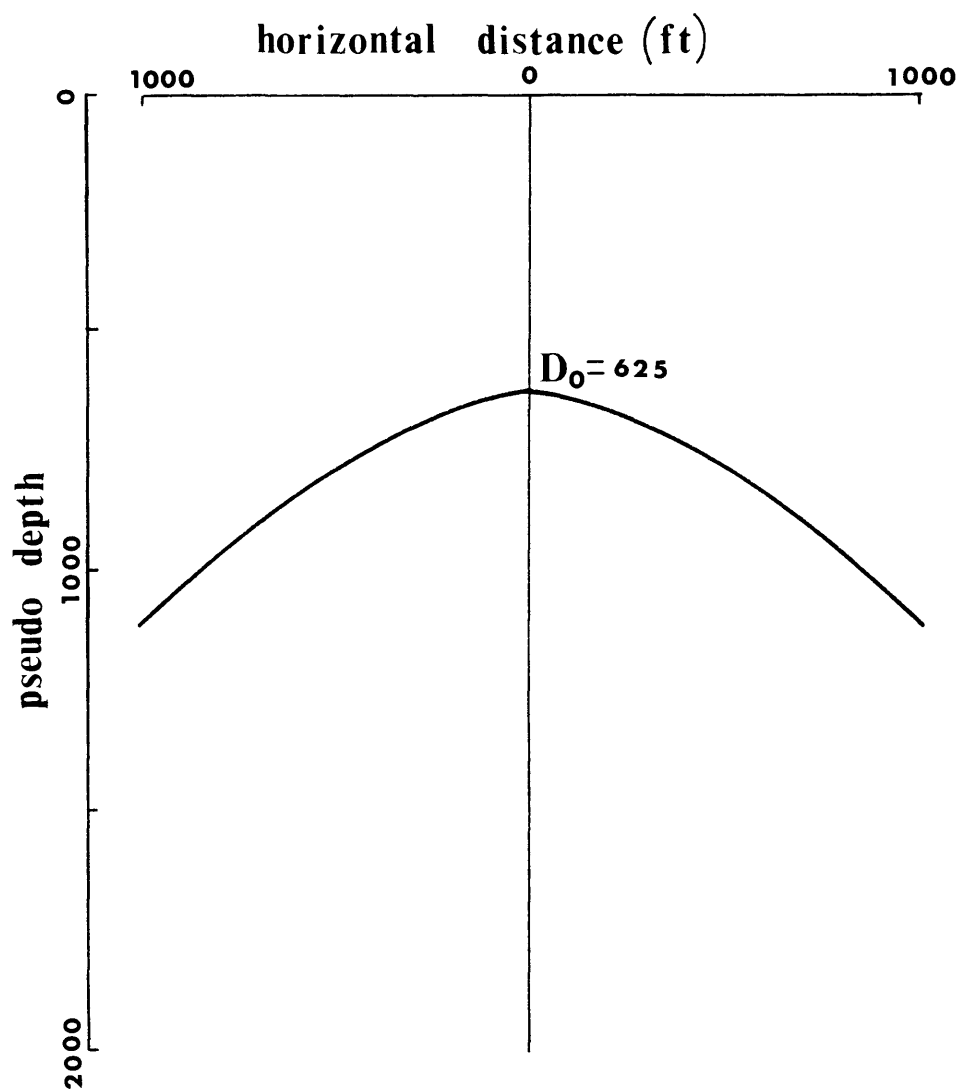


Figure 19: Real and theoretical diffraction curves in the pseudo - depth domain of model 1 for velocity ratio of 1.2 .
 D_0 is pseudo - depth of the diffracting point.

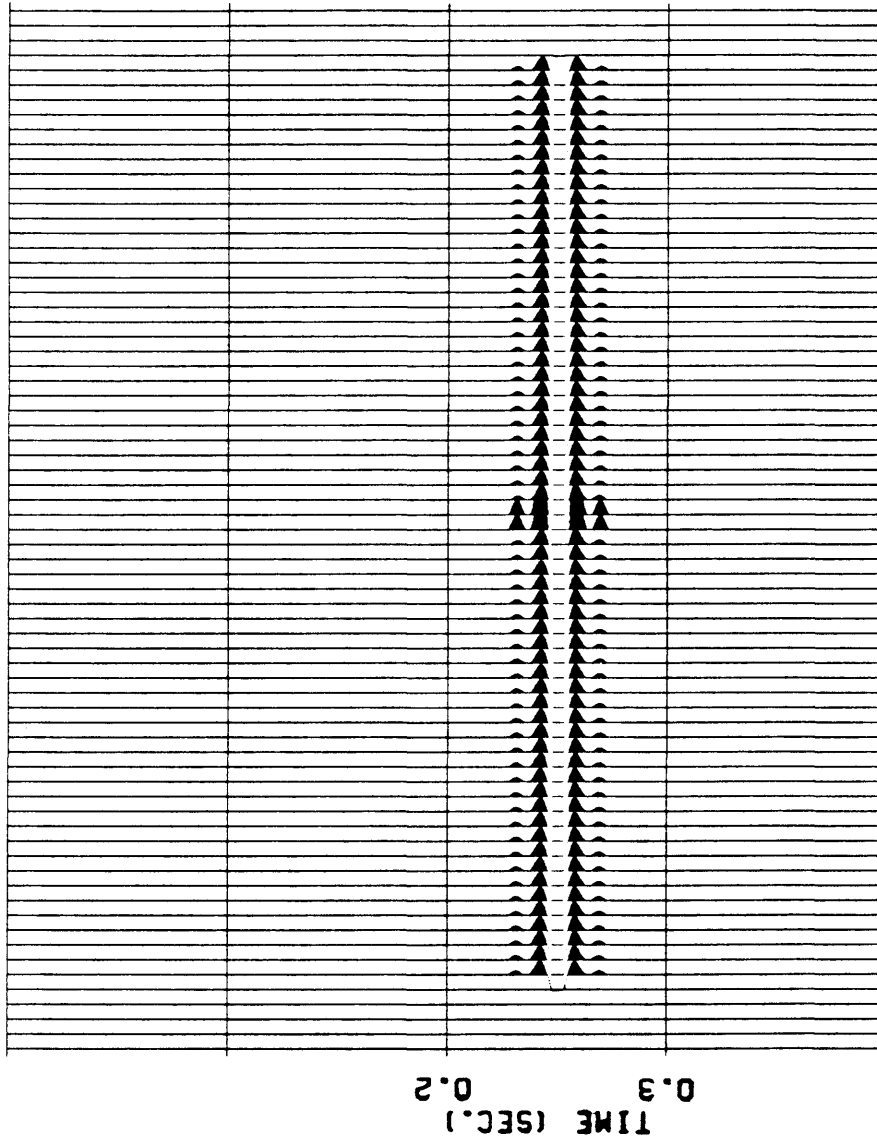


Figure 20: The variable velocity migration of model 1 with $W = 1.0$ for velocity ratio of 1.2 .

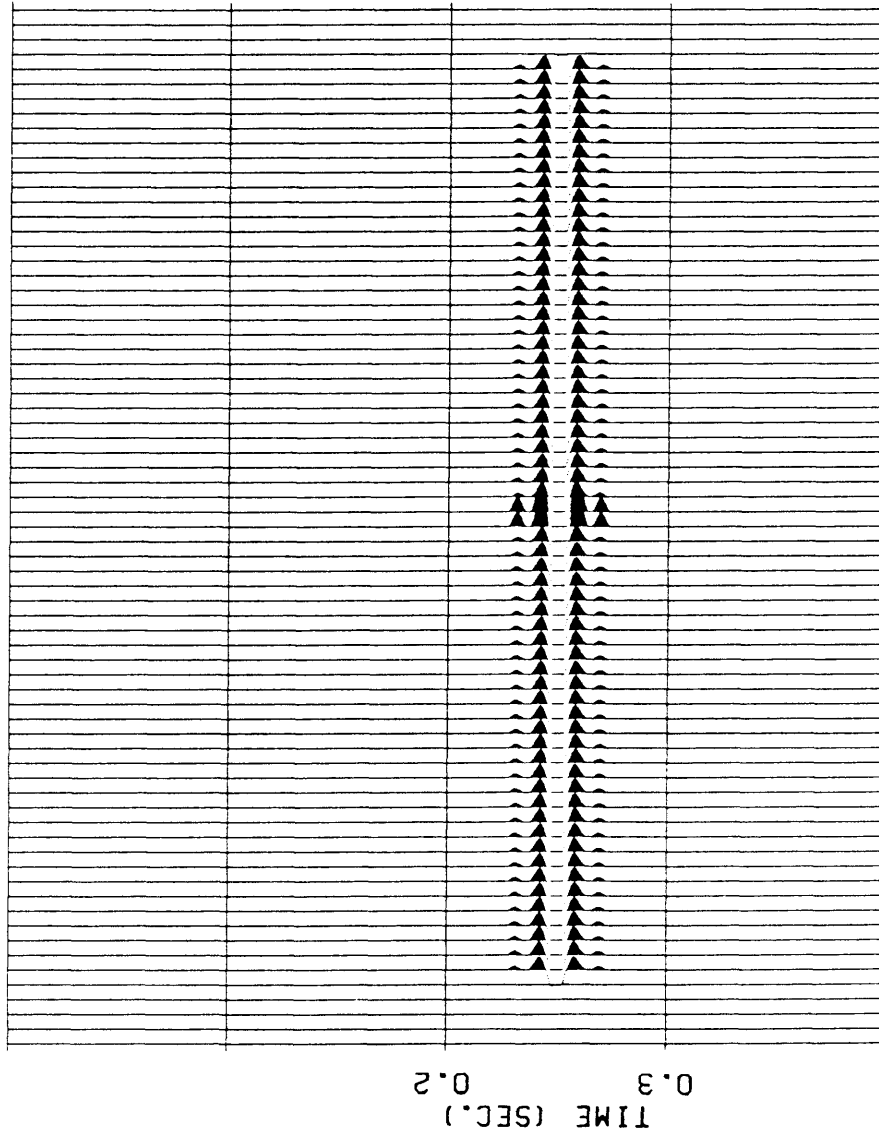


Figure 21: The incremental migration of model 1 for velocity ratio of 1.2 .

except the reflection coefficient. Figure 22 shows the theoretical and the real diffraction curves in the pseudo-depth domain. Here, the solid line indicates a pseudo-depth converted real diffraction curve and the dashed line indicates a pseudo-depth converted theoretical diffraction curve with $W = 1.0$. The difference between two curves is more than the one with the velocity ratio of 1.2. We expect that the migration with $W = 1.0$ would result in overmigration since the real diffraction curve is more open than the theoretical curve with $W = 1.0$. And the result shows a small amount of overmigration as is seen in Figure 23. The next step which we have to take is to change the value of W so that the two diffraction curves in the pseudo-depth domain fit closer. Looking back in Figure 12 of the variable velocity section, the value of W comes out to be about 0.0. Figure 24 shows the result of this migration with $W = 0.0$. The diffraction has been collapsed very well. The incremental method, as we expect, results in perfect migration (Figure 25), since this method does not suffer from stretching of data.

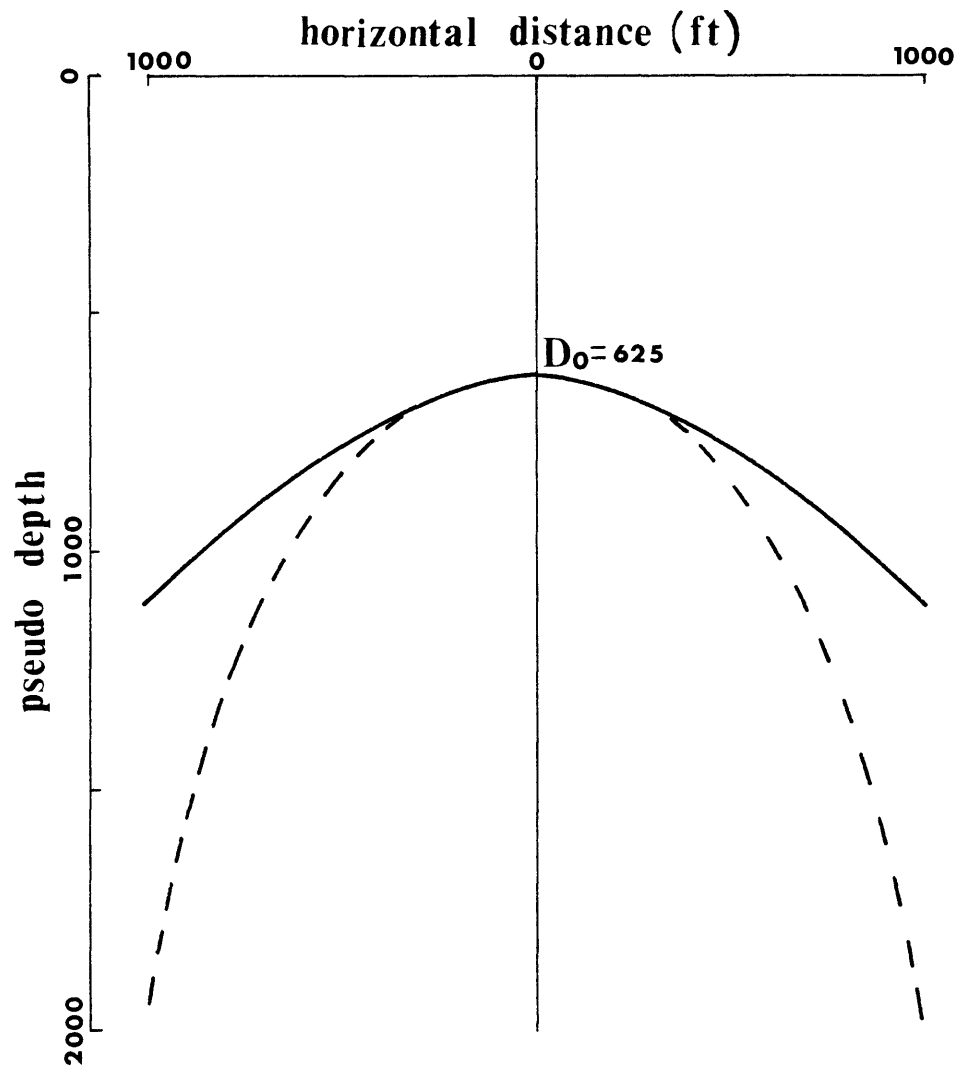


Figure 22: Real and theoretical diffraction curves in the pseudo - depth domain of model 1 for velocity ratio of 2.0 . D_0 is pseudo - depth of the diffracting point.

TABLE II

Offset	Theoretical (W=1.0)	Real (V.R.=1.2)	Real (V.R.= 2.0)
0.0	625.0	625.0	625.0
50.0	627.0	627.0	627.01
100.0	632.95	632.97	633.10
150.0	642.75	642.85	643.52
200.0	656.22	656.54	658.64
250.0	673.15	673.88	679.0
300.0	693.27	694.68	705.29
350.0	716.33	718.70	738.37
400.0	742.04	745.66	779.21
450.0	770.15	775.24	828.99
500.0	800.39	807.08	889.0
550.0	832.54	840.76	960.70
600.0	866.39	875.84	1045.71

Table II: Theoretical and real diffraction curves in a pseudo - depth domain. Numbers are in feet.

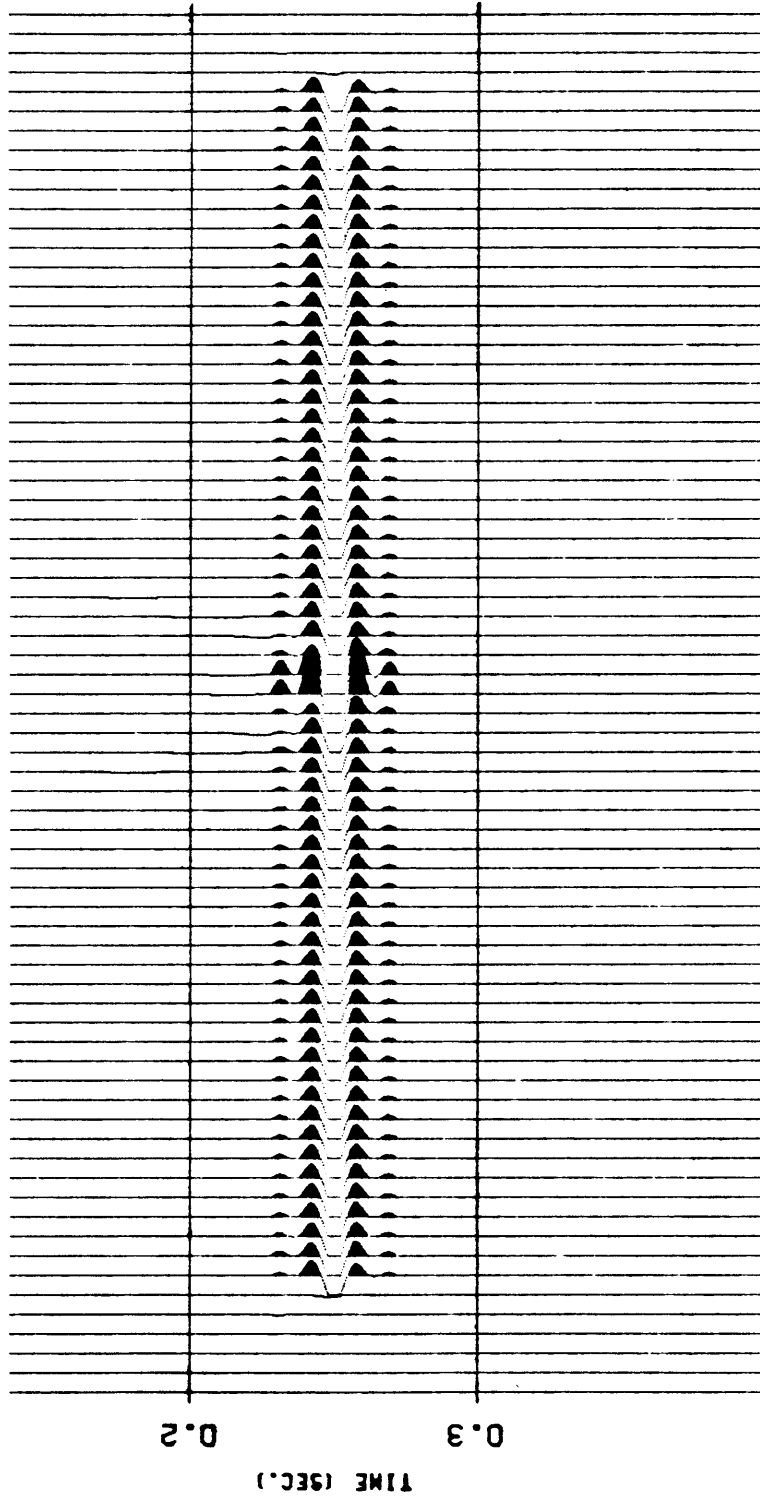


Figure 23: The variable velocity migration of model 1 for velocity ratio of 2.0 . W = 1.0 was used here.

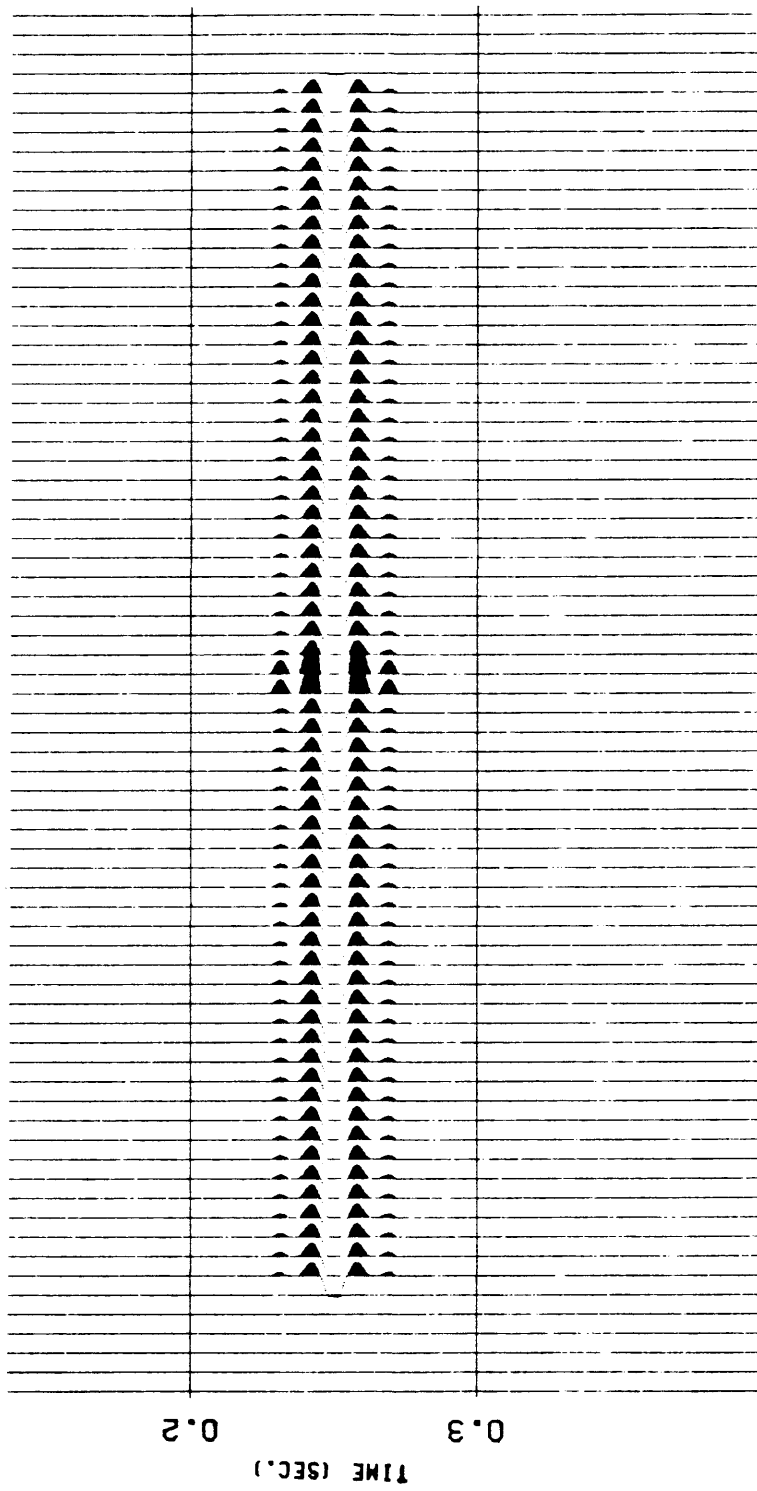


Figure 24: The variable velocity migration of model 1 for velocity ratio of 2.0 . $\bar{W} = 0.0$ was used here.

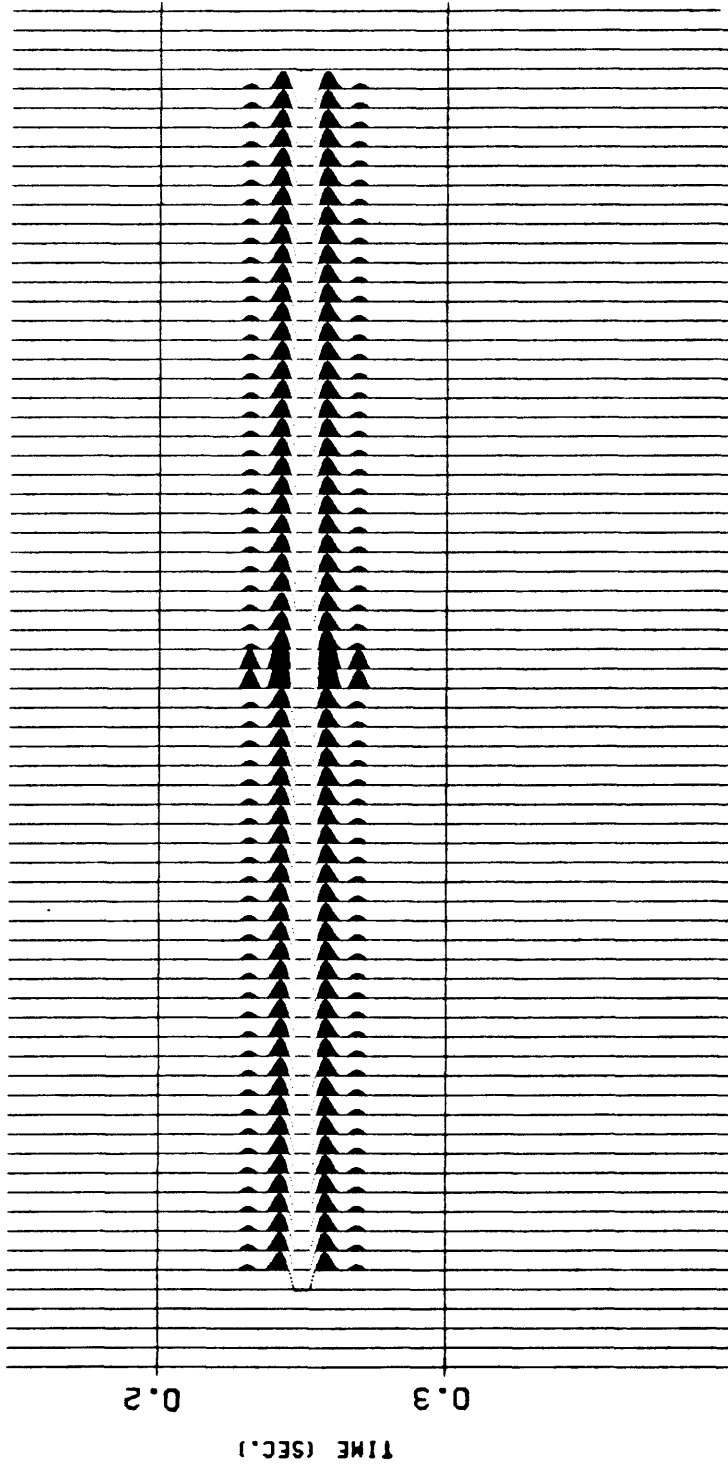


Figure 25: The incremental migration of model 1 for velocity ratio of 2.0.

Four horizons with gradual velocity increase with depth
(Model 2)

This model is more complex in terms of determining the value of W . Figure 26 shows the physical parameters for this model which again do not have any geological significance. Velocity increases with depth at a fairly uniform rate. Figures 27 and 28 shows the corresponding normal incidence and wave - theory modelling sections, respectively. The variable velocity migration was carried out with $W = 1.0$, standard F - K migration, and is shown in Figure 29. This is a very good result, but the deepest diffraction at 0.4 sec. is not collapsed completely. This suggests to us that a change in the value of W might focus the deepest diffraction better. Diet (1979) pointed out that if velocity is a linear function of depth, equation (32) can be used to determine an optimum value of W . Figure 30 shows the velocity distribution of this model. By smoothing this discretized velocity model, an approximate value of α may be found. α is the velocity gradient in the form of $V = V_0 + \alpha z$, where V_0 is the initial velocity and α is the vertical velocity gradient. α obtained by this method came out to be about 2.3. Consequently, W is obtained by using either equation (32) or the chart in Figure 10 and for $\alpha = 2.3$, W is about 0.6.

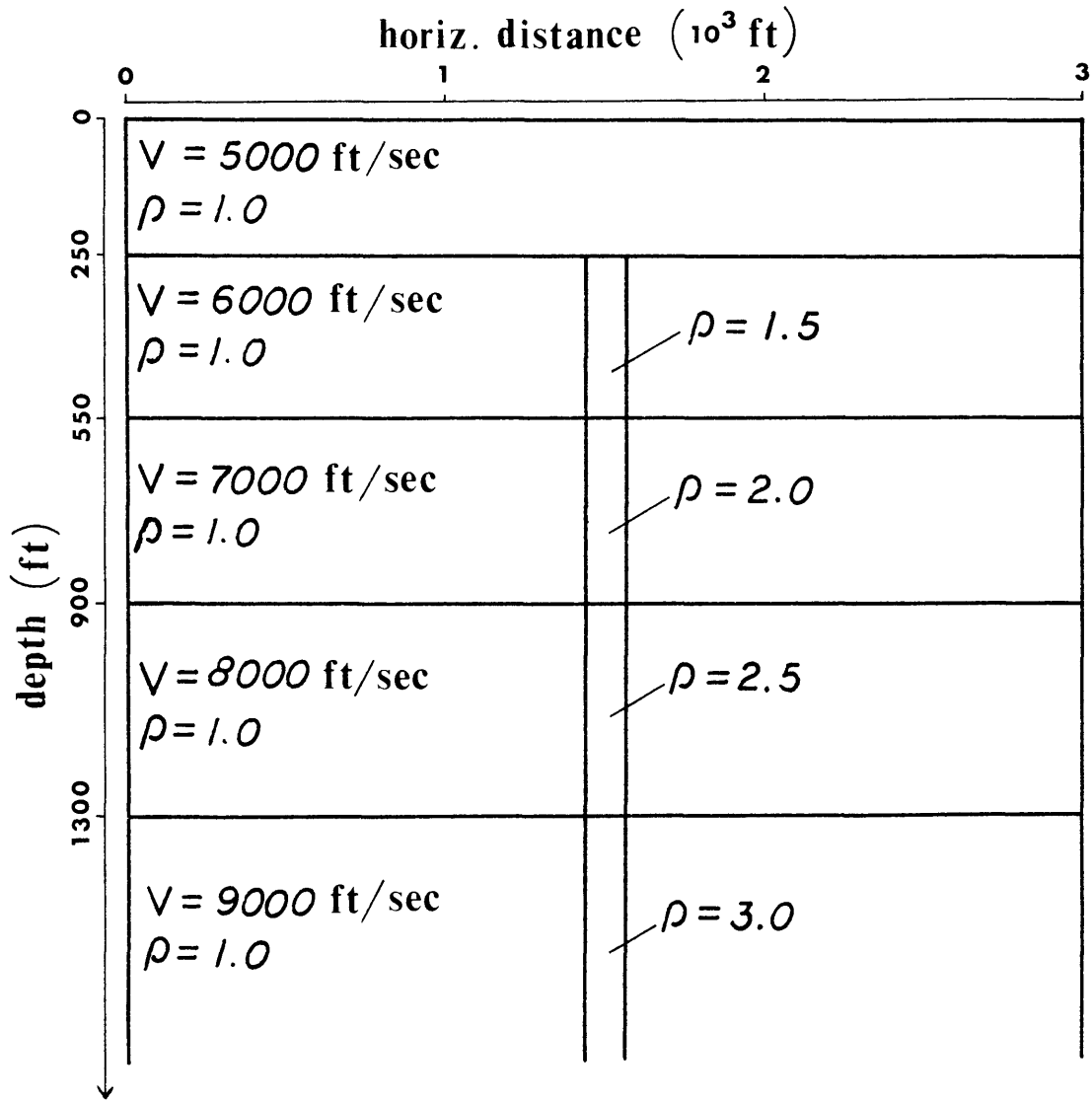


Figure 26: Physical parameters of model 2 .

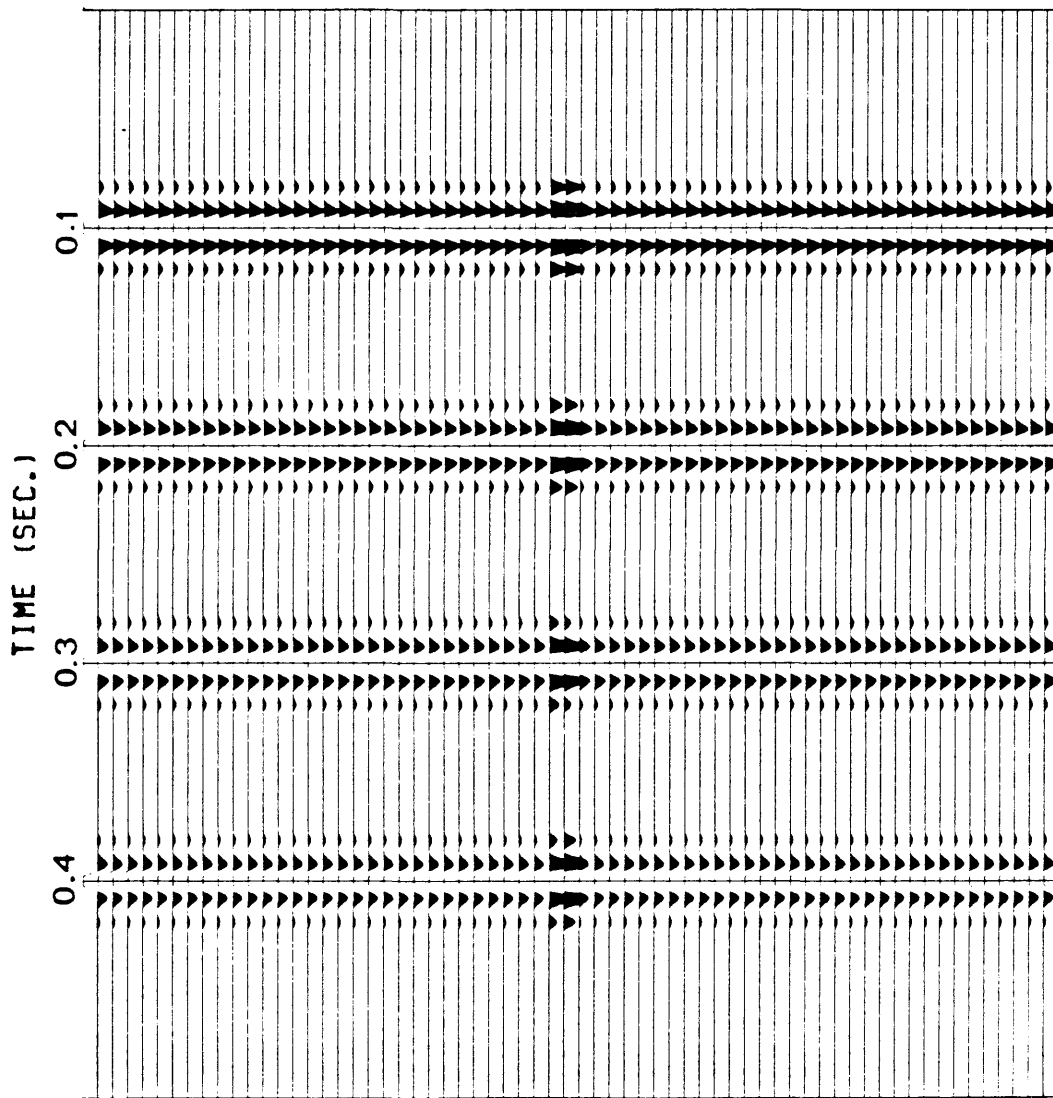


Figure 27: Normal incidence time section of model 2.

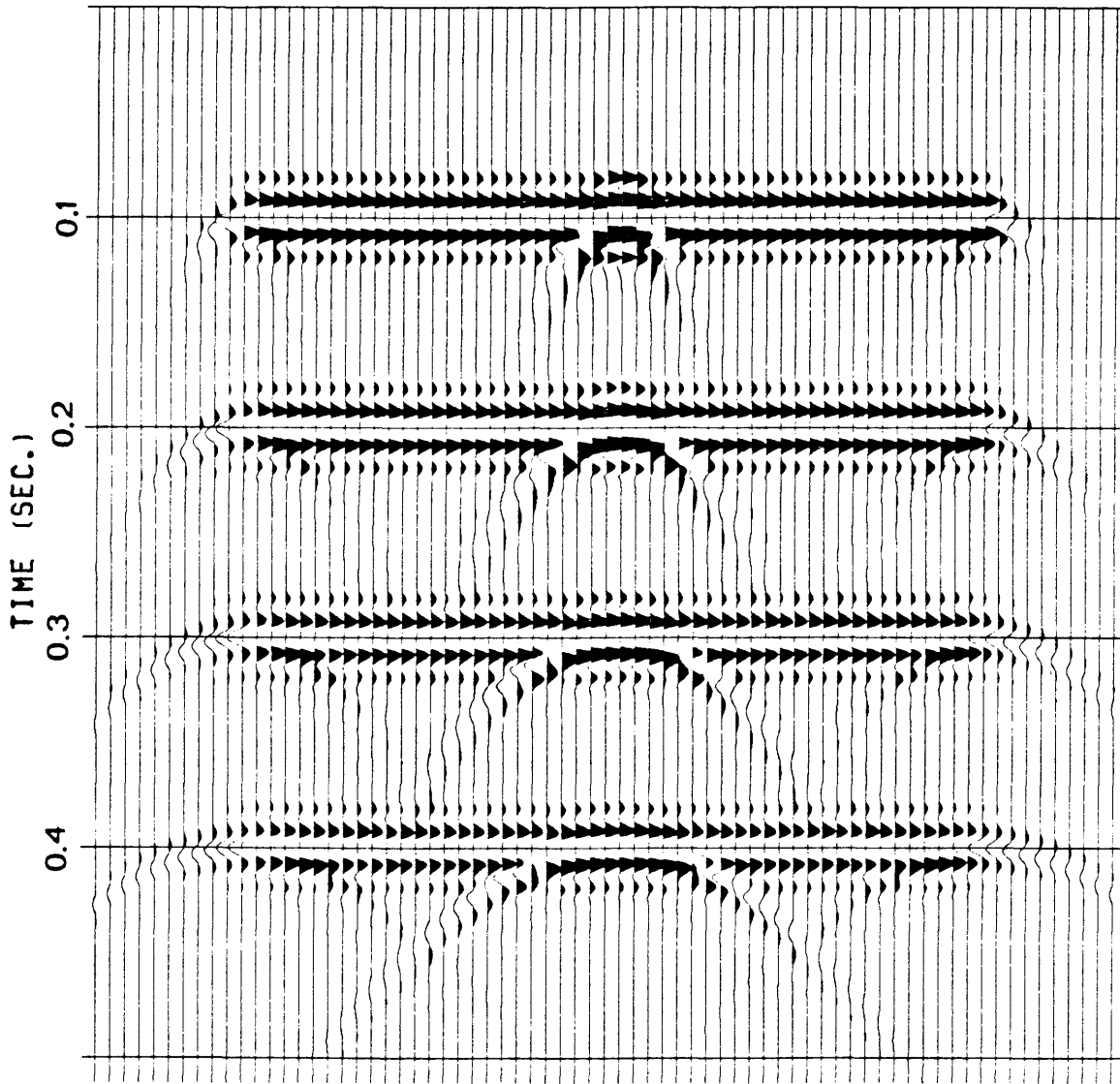


Figure 28: Wave - theory modelling of model 2.

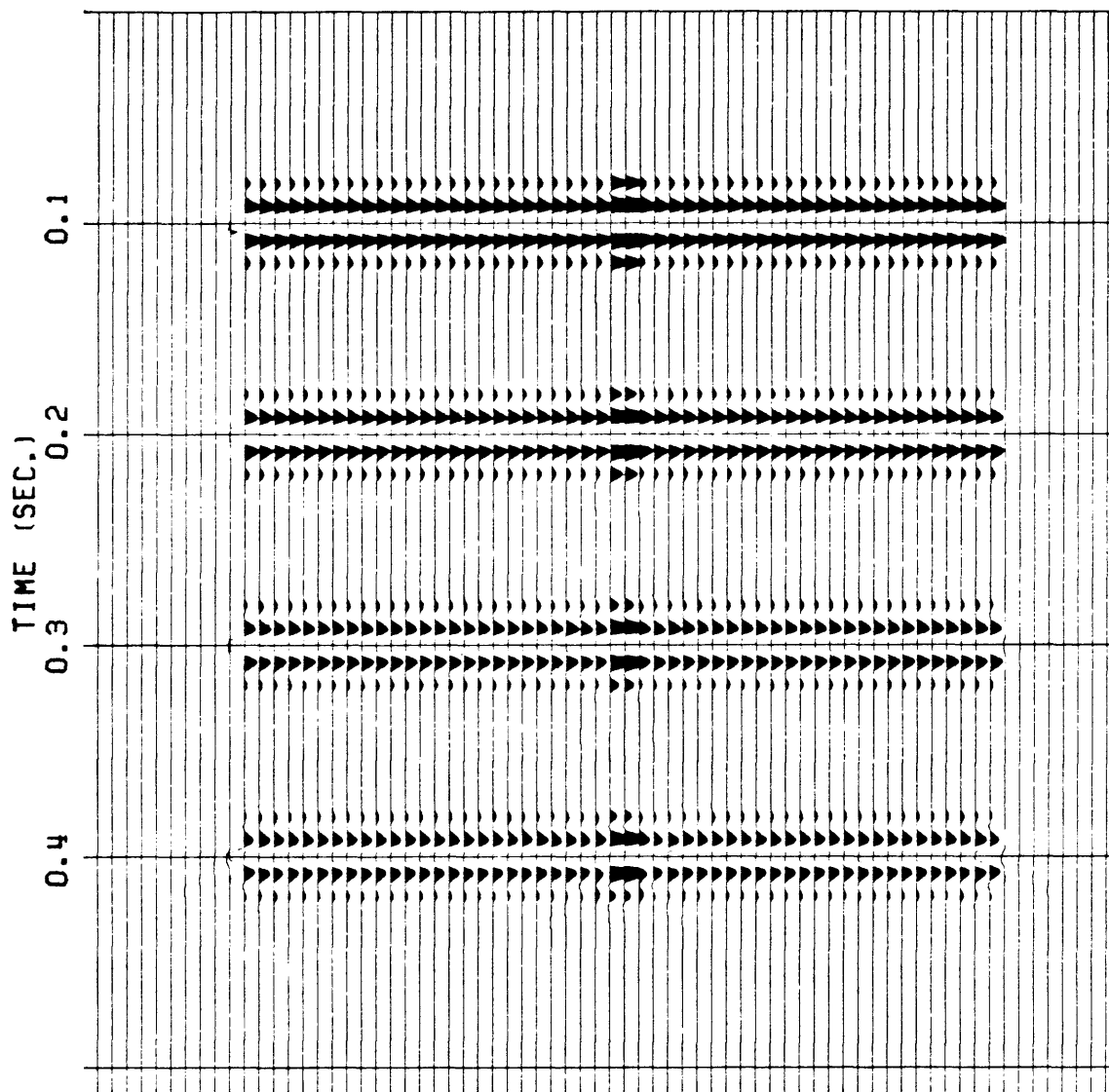


Figure 29: The variable velocity migration of model 2 with $W = 1.0$, standard F - K migration.

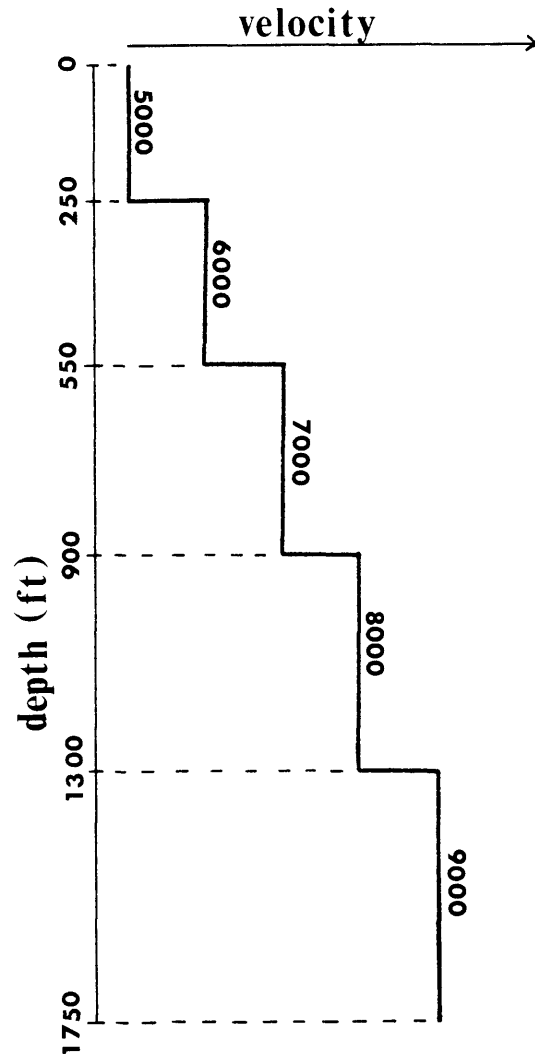


Figure 30: Velocity distribution of model 2, velocities are in feet / sec. .

Figure 31 shows the result of the variable velocity migration with $W = 0.6$. Unfortunately, the result does not look as good as the one with $W = 1.0$, even though 0.6 was calculated to be an optimum value of W . Figure 32 shows the result by the incremental method. Again the migration result is in very good shape even down to the deepest horizon.

The simplified picture in Figure 33 illustrates what we think happened to the diffractions in the pseudo - depth domain. The solid lines indicate the theoretical curves with $W = 1.0$, and the dashed lines indicate the real diffraction curves. The upper three dashed lines are so similar to the solid lines that they are indistinguishable from each other. The top three real diffractions fit very well with the theoretical ones, and this is reflected in the migration result. Notice that for the deepest diffraction the two curves, the theoretical and the real, are not similar enough to give us the correct result with this value of W . Since 1.0 is the maximum value we could assign to W , this should give us the best result. In order to confirm this observation, the synthetic section was migrated with $W = 0.0$. Figure 34 is the corresponding migrated section. As we have expected, the result is not as good as the one with $W = 1.0$. The third horizon is now out of focus as well as the fourth one.

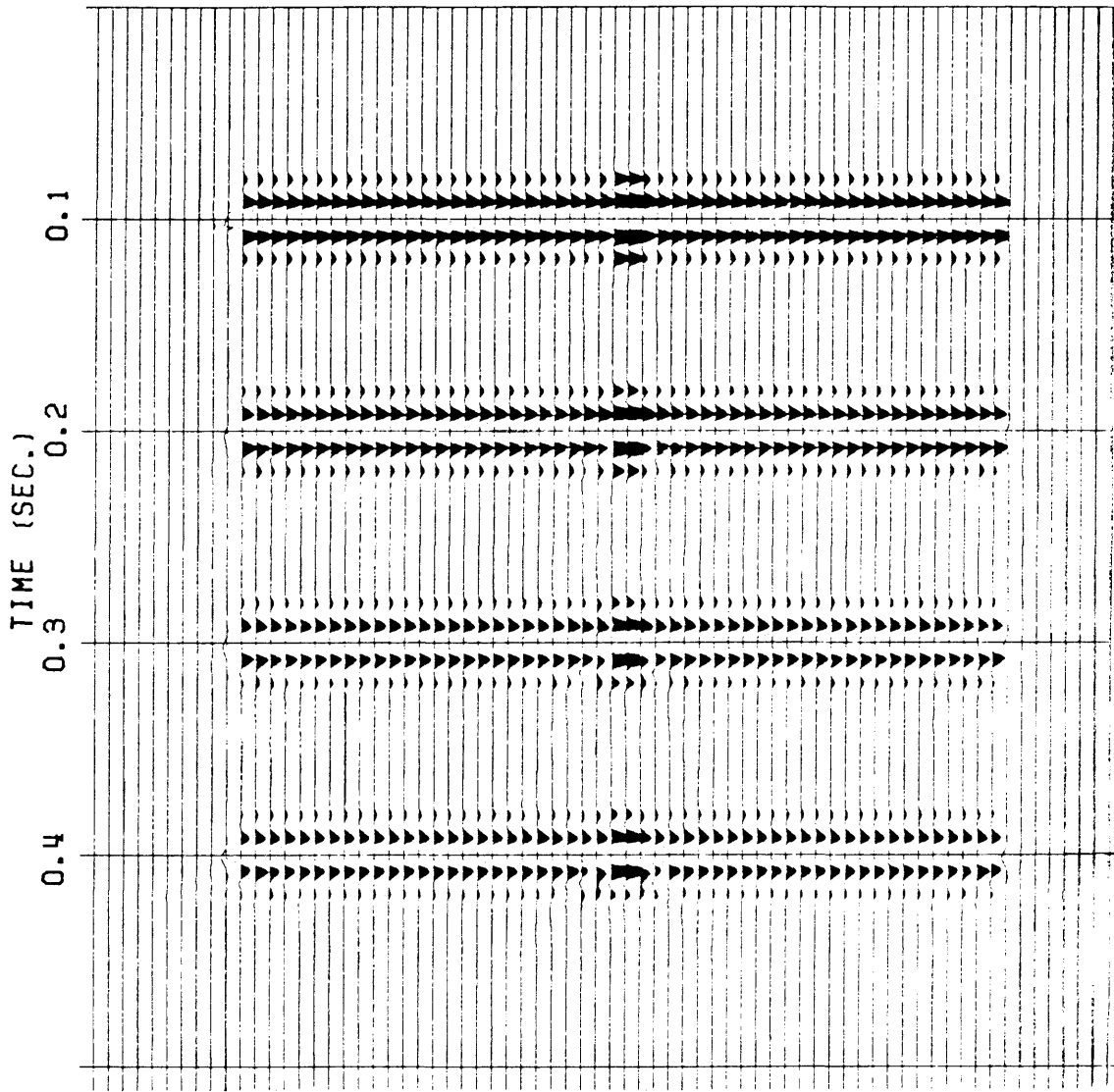


Figure 31: The variable velocity migration of model 2 with $W = 0.6$.

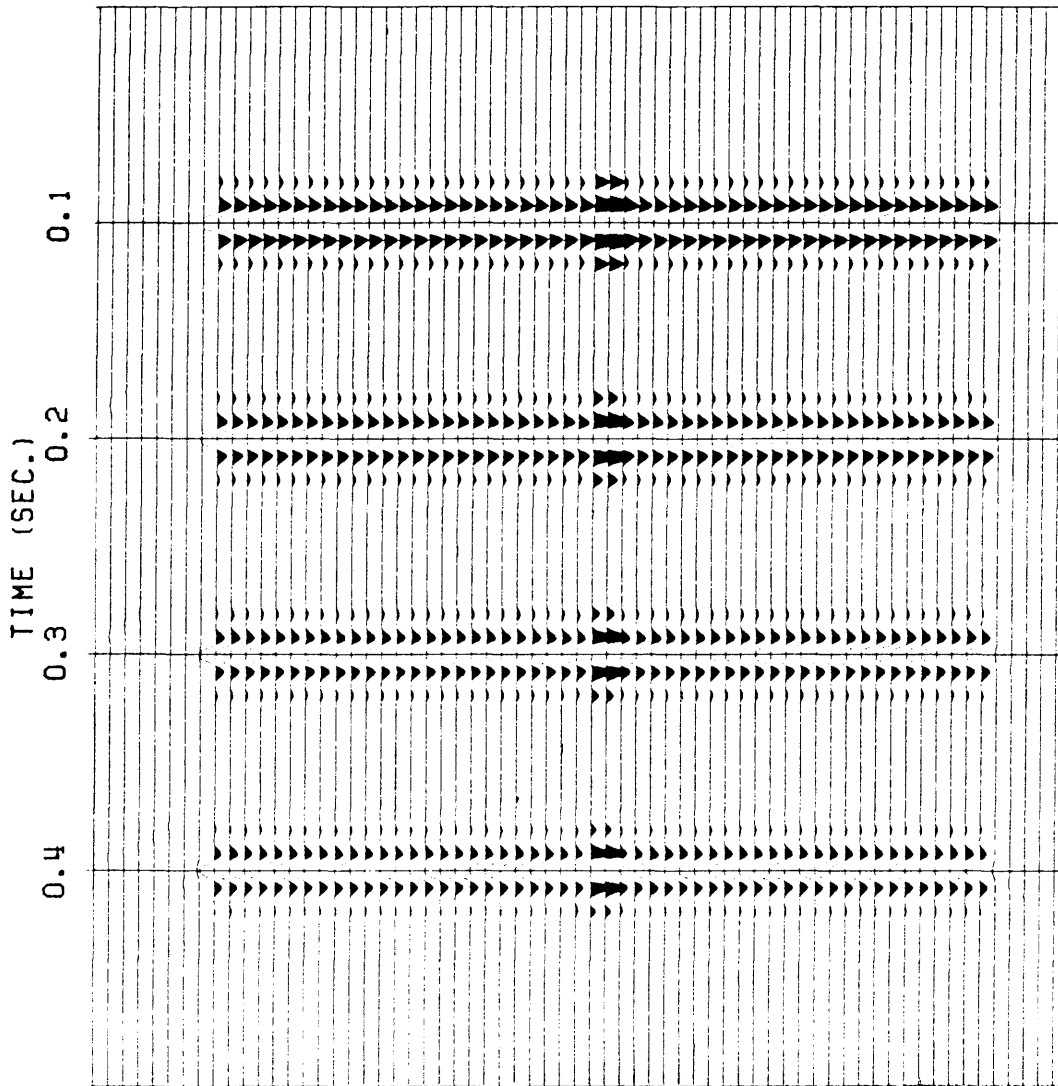


Figure 32: The incremental migration of model 2.

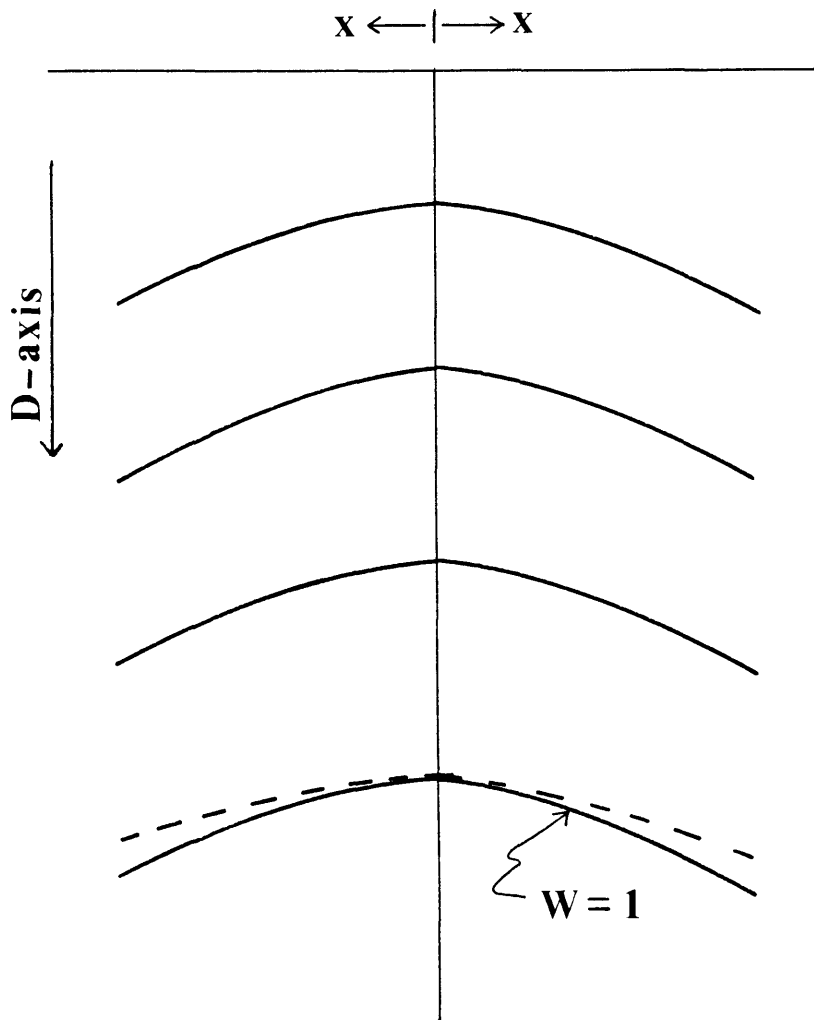


Figure 33: Schematic of real and theoretical diffraction curves in the pseudo - depth domain. Solid lines indicate theoretical curves and dashed lines indicate real curves.

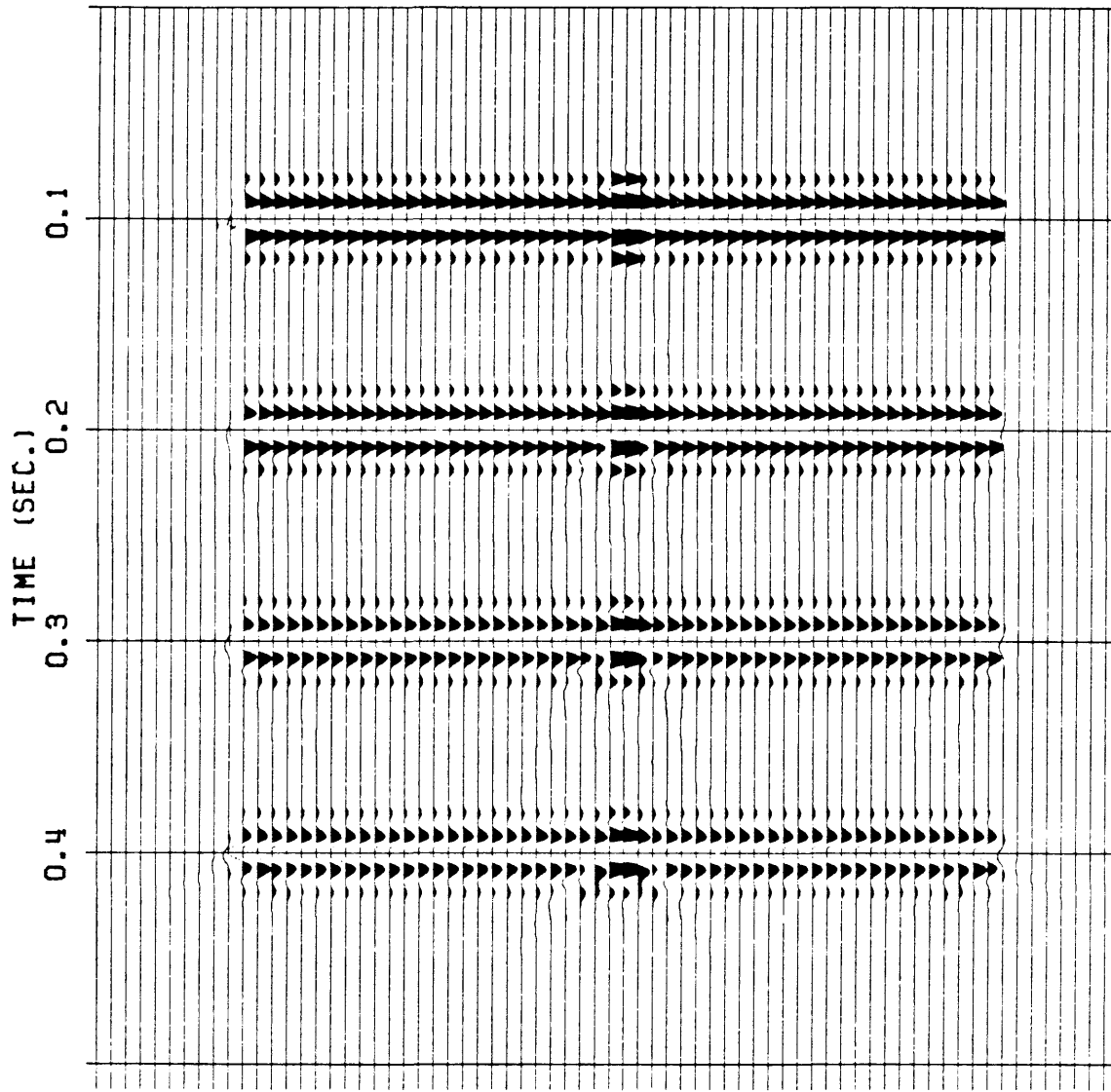


Figure 34: The variable velocity migration of model 2 with $W = 0.0$.

We have investigated performances of the two F - K migration schemes with the model having a fairly uniform rate of velocity increase with depth. Both schemes worked well in this type of model. However for the variable velocity method, the optimum value of W did not give us the best result.

Three horizons with large velocity jump. (Model 3)

Model 3 (Figure 35) is very similar to model 2. The difference is that larger steps in the velocity distribution have been made, as is shown in Figure 36. This way, the determination of an optimum W may be difficult. Figures 37 and 38 show the normal incidence and wave - theory modelling sections of this model, respectively. As we have done in model 2, we could calculate an optimum value of W . However, let us proceed to migrate the synthetic section with $W = 1.0$, standard F - K migration. Figure 39 shows this migration result. Again the deepest horizon is undermigrated, and this time it is worse than the previous example. This fact tells us that the theoretical diffraction curve with $W = 1.0$ is less open than the real diffraction curve in the pseudo - depth domain. This observation is depicted in Figure 40, again the solid lines indicate the theoretical curves and the dashed lines indicate the real curves.

α and the optimum W obtained for this model are about 2.3 and 0.6, respectively. These are almost the same values as those in the previous example. If we are to migrate this data with $W = 0.6$, the result is expected to be less focused. Indeed it is not quite as good of a

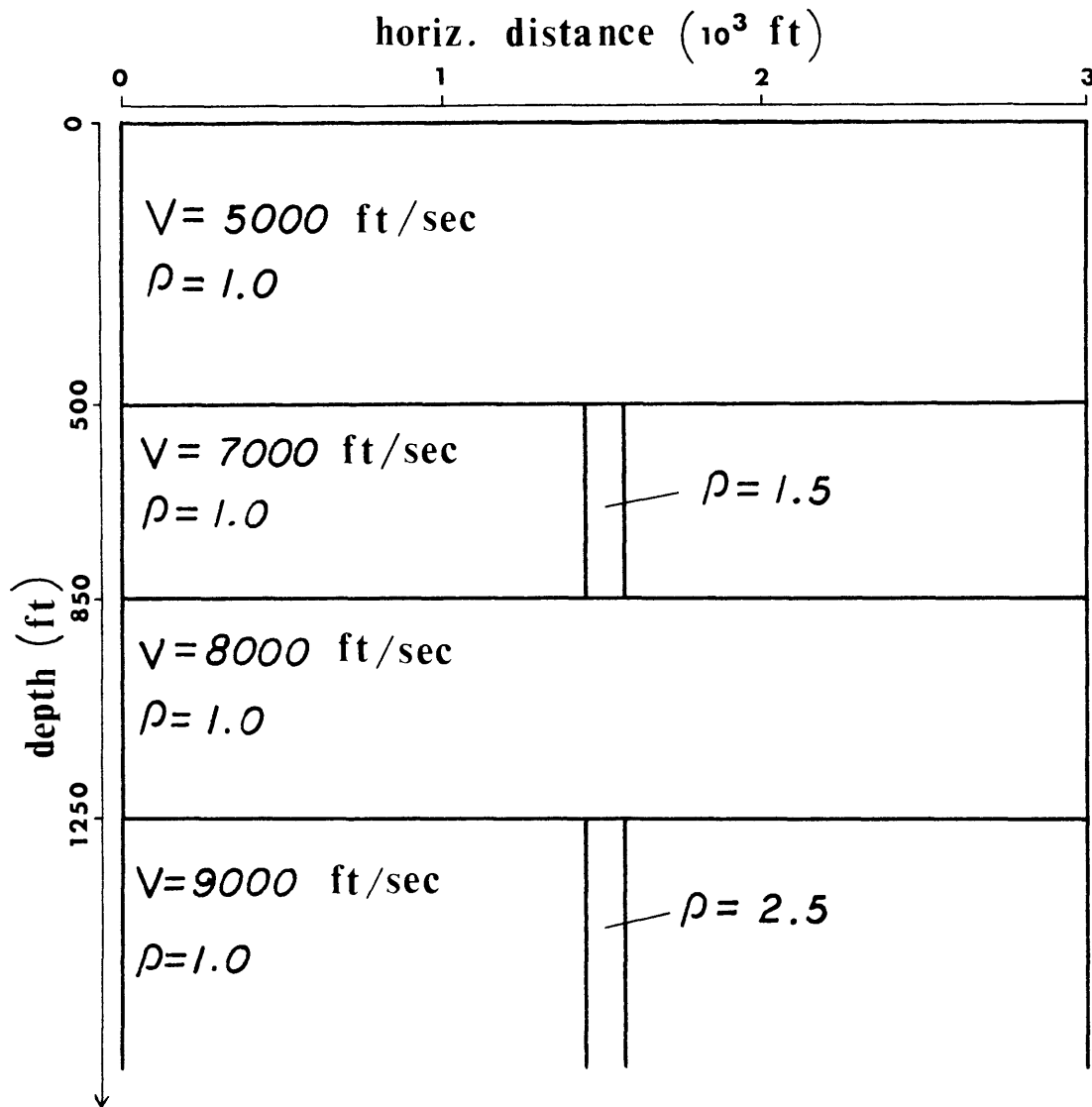


Figure 35: Physical parameters of model 3.

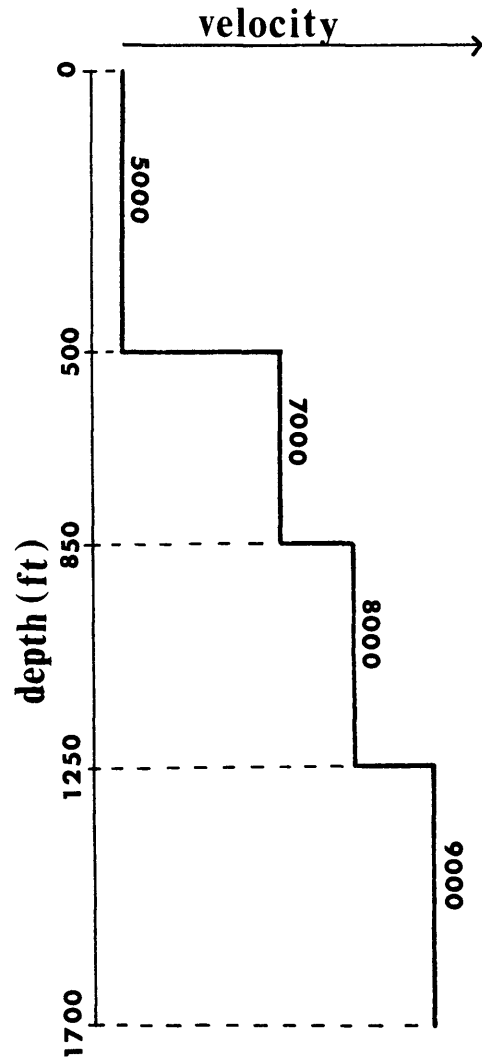


Figure 36: Velocity distribution of model 3, velocities are in feet / sec. .

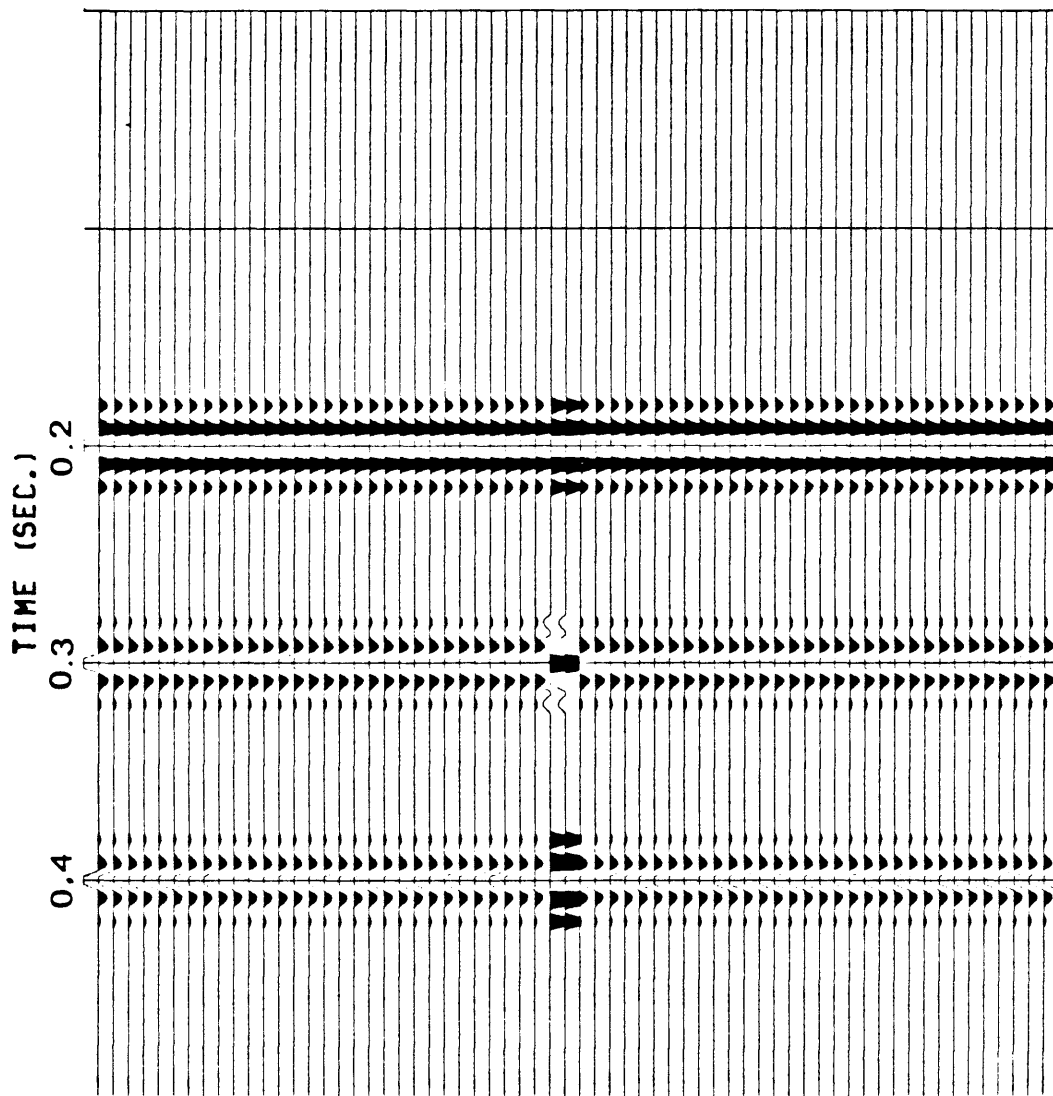


Figure 37: Normal incidence time section of model 3.

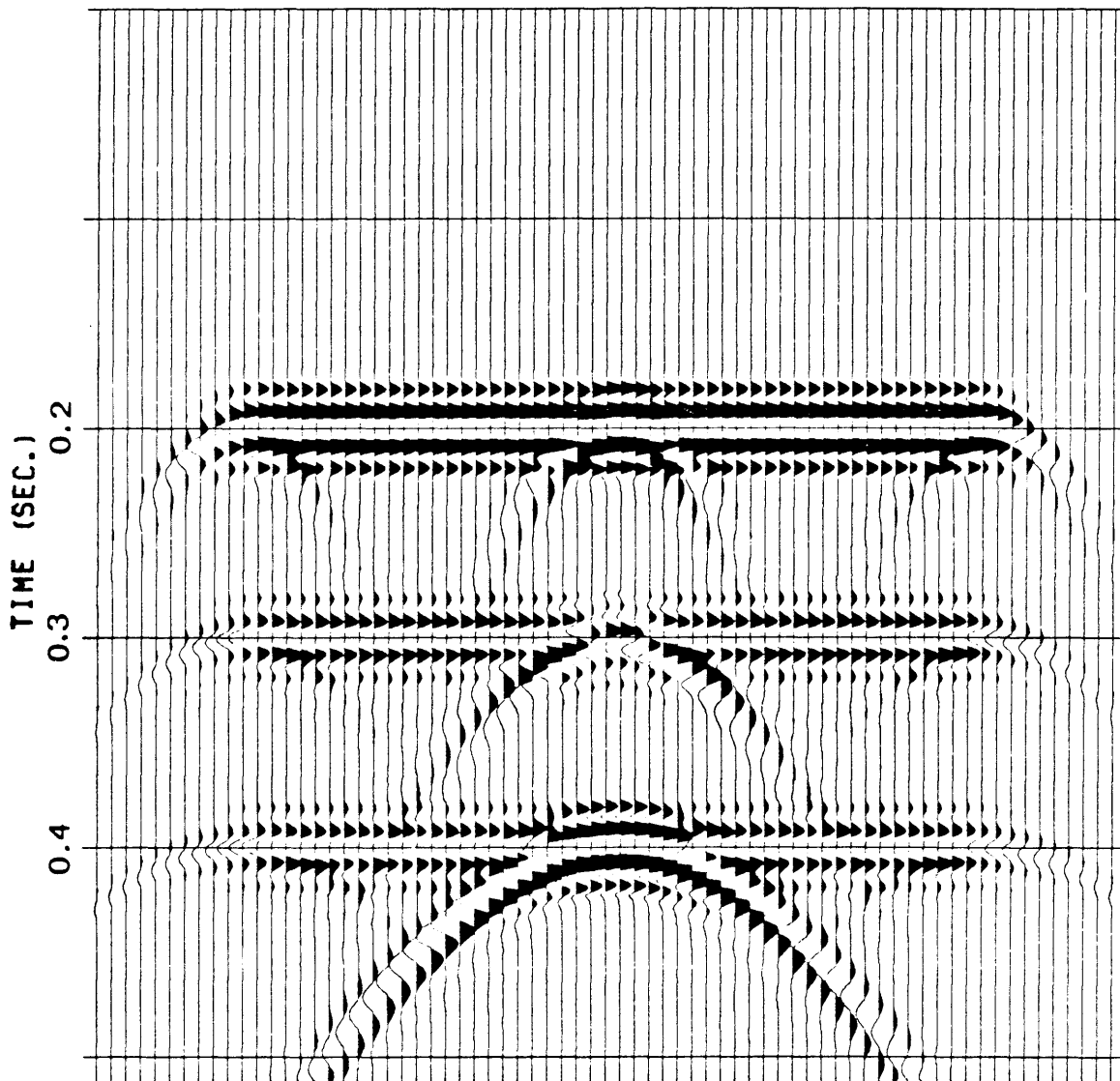


Figure 38: Wave - theory modelling of model 3.

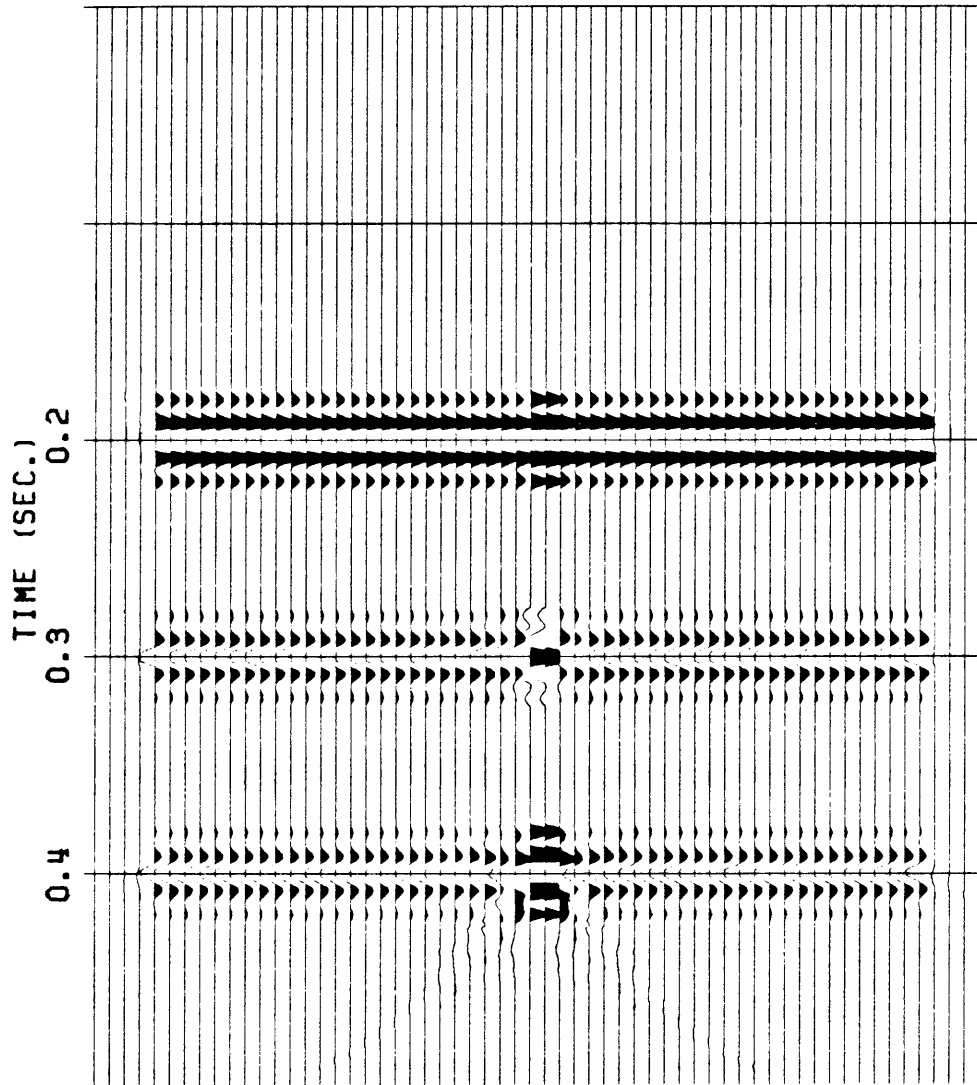


Figure 39: The variable velocity migration of model 3 with $W = 1.0$, standard F - K migration.

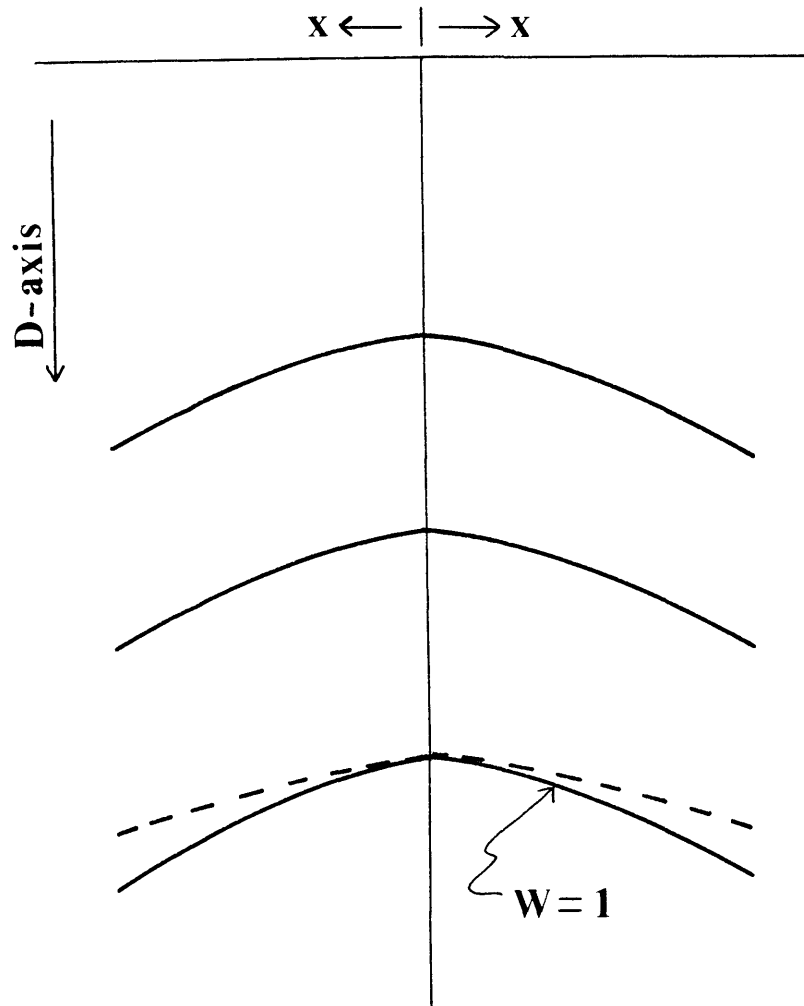


Figure 40: A schematic of real and theoretical diffraction curves in the pseudo - depth domain. Solid lines indicate theoretical curves and dashed lines indicate real curves.

result as the one with $W = 1.0$. Figure 41 shows the corresponding migrated section with $W = 0.6$.

On the other hand, the incremental method gives us a well focused result as is shown in Figure 42. There is some undermigrated energy around the deepest horizon, however this result is superior to the one obtained by the variable velocity method.

Figures 43, 44, and 45 show a sequence of migration results with $W = 0.4, -0.5$, and -0.75 , respectively. We observe that the migration results become worse with each decrease in W .

In this model, the large step in velocity is introduced. Since this large velocity step violates the rule of linearly increasing velocity with depth used to calculate the value for W (Diet, 1979), the variable velocity scheme with this value of W did not quite give us an acceptable result.

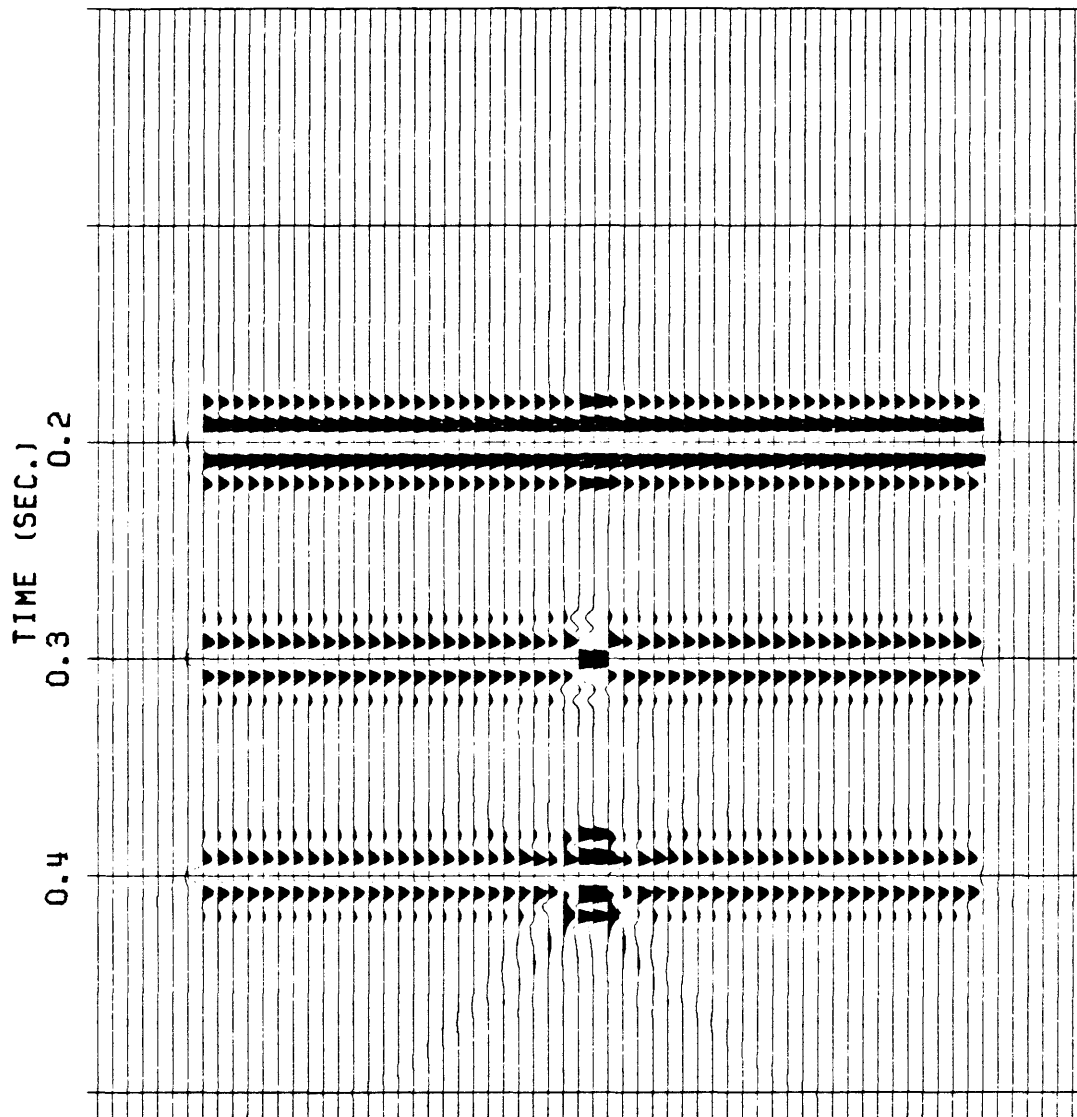


Figure 41: The variable velocity migration of model 3 with $W = 0.6$.

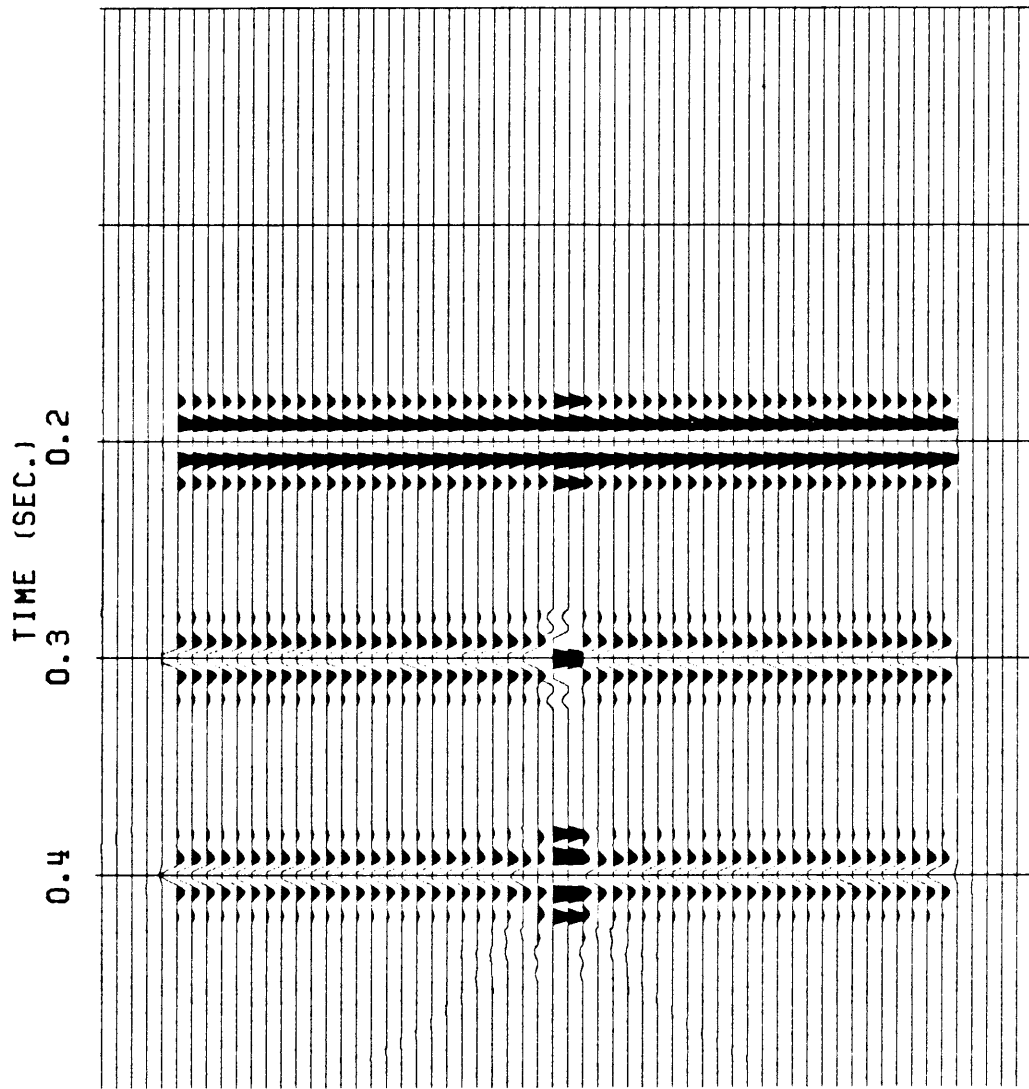


Figure 42: The incremental migration of model 3.

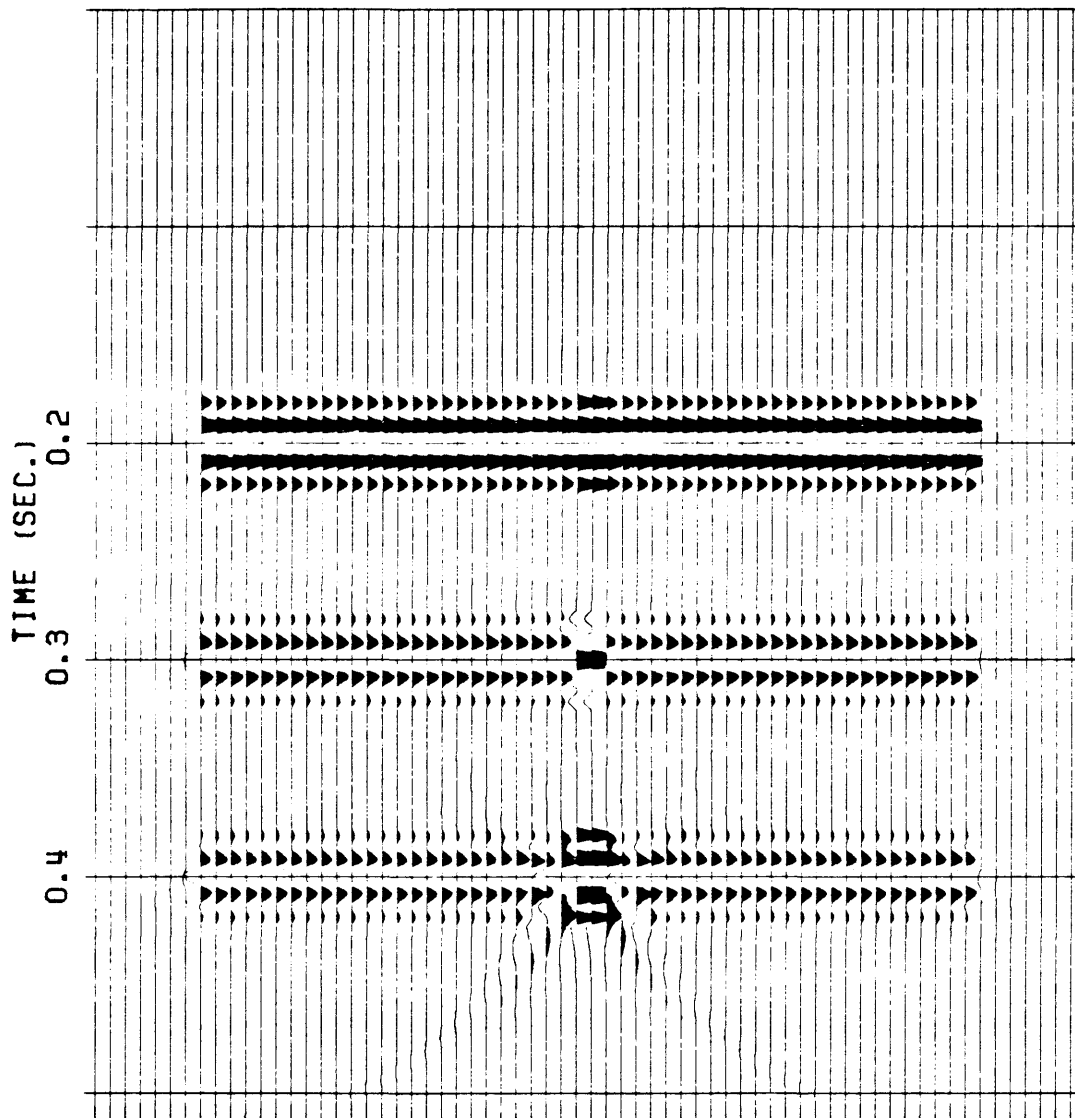


Figure 43: The variable velocity migration of model 3 with $W = 0.4$.

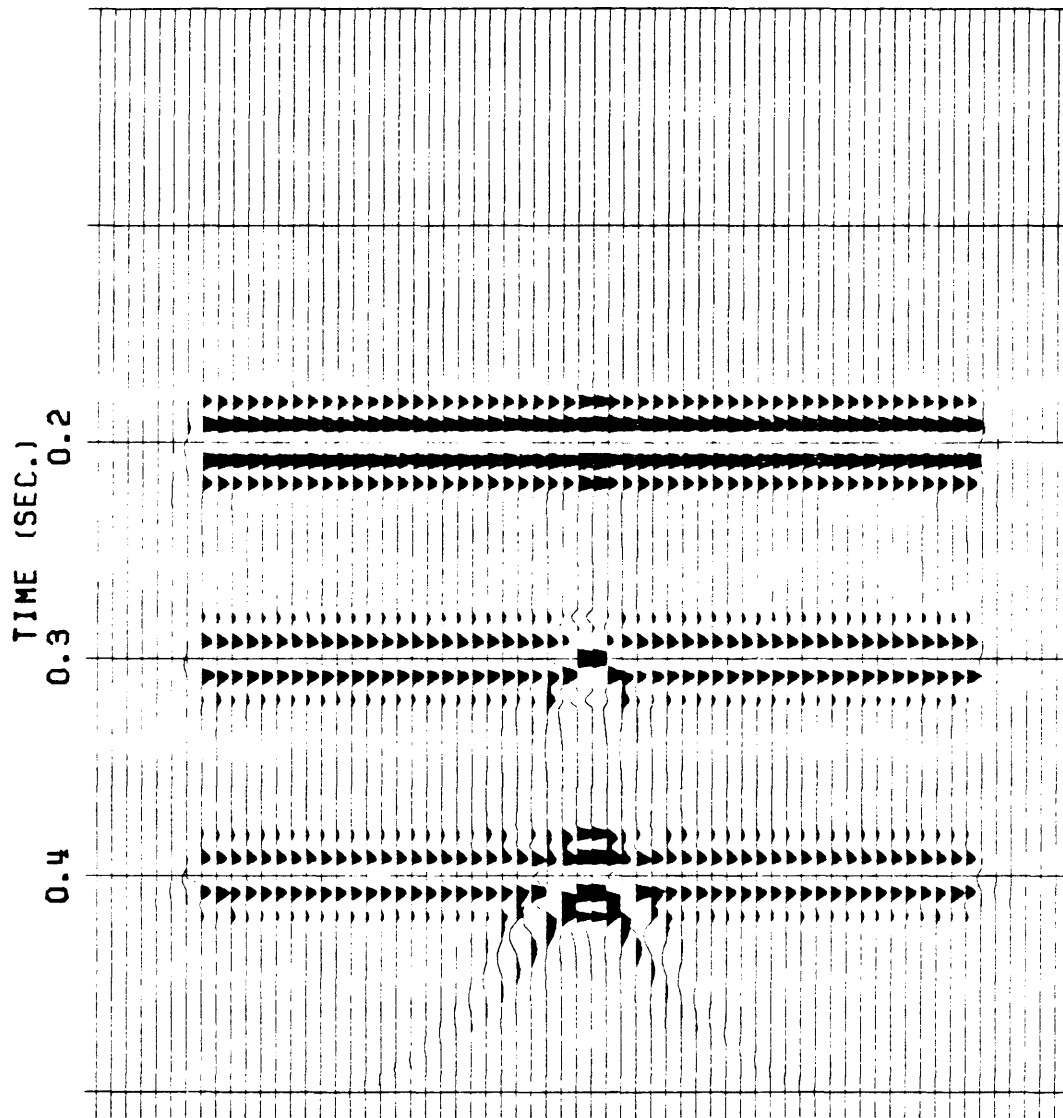


Figure 44: The variable velocity migration of model 3 with $W = -0.5$.

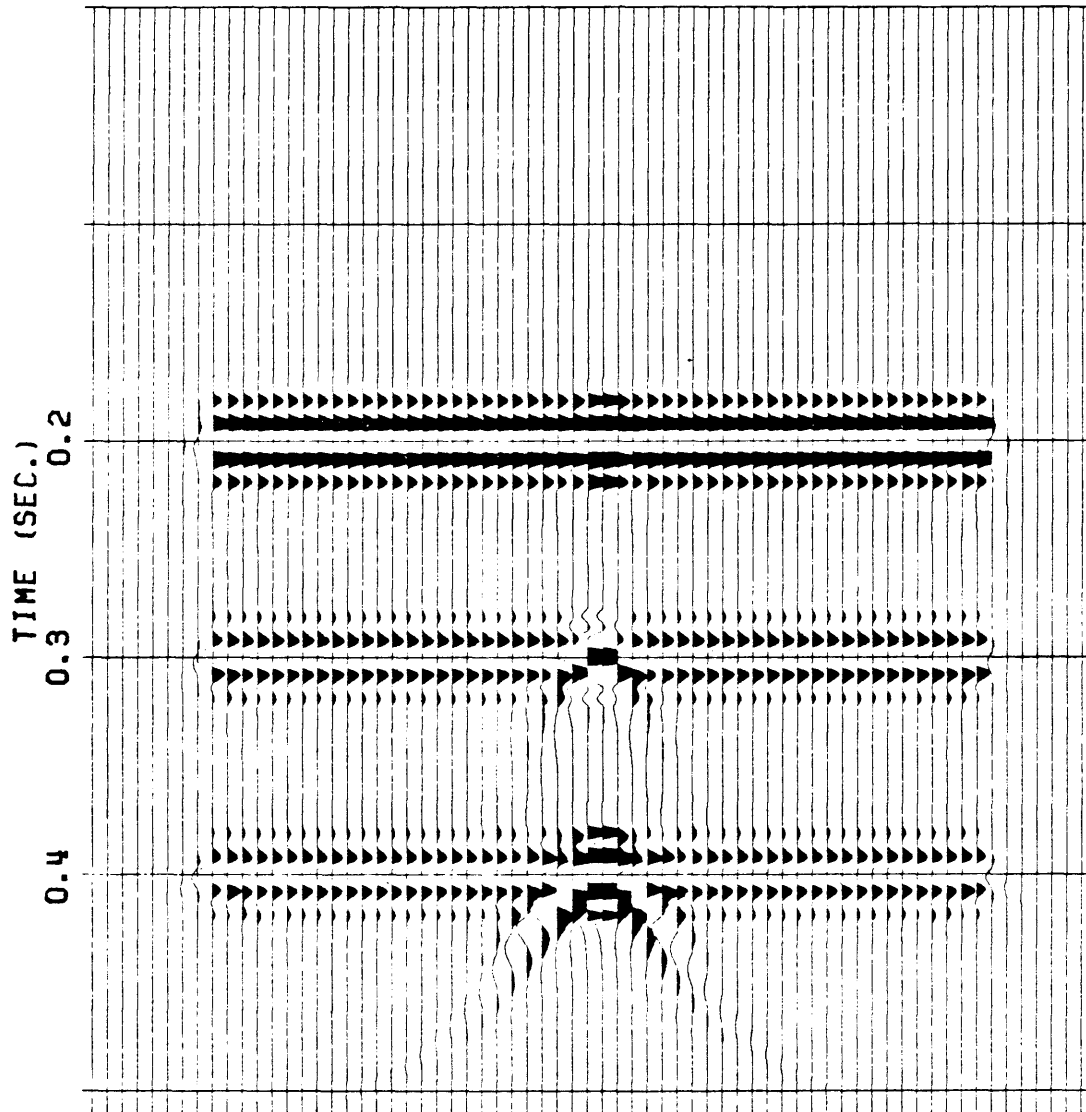


Figure 45: The variable velocity migration of model 3 with $W = -0.75$.

POSSIBLE EXTENSION OF THE INCREMENTAL METHOD IN THE
PRESENCE OF LATERAL VELOCITY VARIATIONS

From the investigation carried out for vertical velocity gradients, it is obvious that the incremental method is superior to the variable velocity method.

Naturally, the next thing we try is to consider the applicability of the incremental method in the presence of both vertical and lateral velocity variations.

In order for this scheme to be properly applied, velocity inhomogeneities must be in the z -direction only. In this scheme for vertical velocity variations, we assumed constant interval velocities within discretized layers. Therefore we really do not have any analytical expressions for lateral velocity variations. But there is a possible detour around this difficulty.

If a velocity function of x and t ; that is, $V(x,t)$ may be approximated by a new velocity function of t , $V(t)$, then the incremental method can be used to migrate sections.

For the variable velocity method, we understand that the minor lateral velocity variation is taken care of by the pseudo-depth conversion. The idea we use here is similar to the pseudo-depth conversion.

Let $\bar{V}(t)$ be a mean average velocity function for an entire section, then a depth function, $\bar{D}(t)$, associated with $\bar{V}(t)$ can be obtained by

$$\bar{D}(t) = \frac{\bar{V}(t) \cdot t}{2} \quad (40)$$

There is a velocity function associated with each CDP, so a depth function at a CDP is described by

$$D_j(x,t) = \frac{V_j(x,t) \cdot t}{2} \quad (41)$$

where j is the index for CDP.

Then the next step is to find new times t 's on the average depth scale ($\bar{D}(t)$) for depths at each CDP. Figures 46 and 47 illustrate the ways to find new time t 's, and to interpolate traces.

Then the migration procedure is modified as follows:

- 1) Interpolation of traces ($t - t'$)
- 2) Migration with $\bar{V}(t)$
- 3) Interpolation of traces back to original time ($t' - t$).

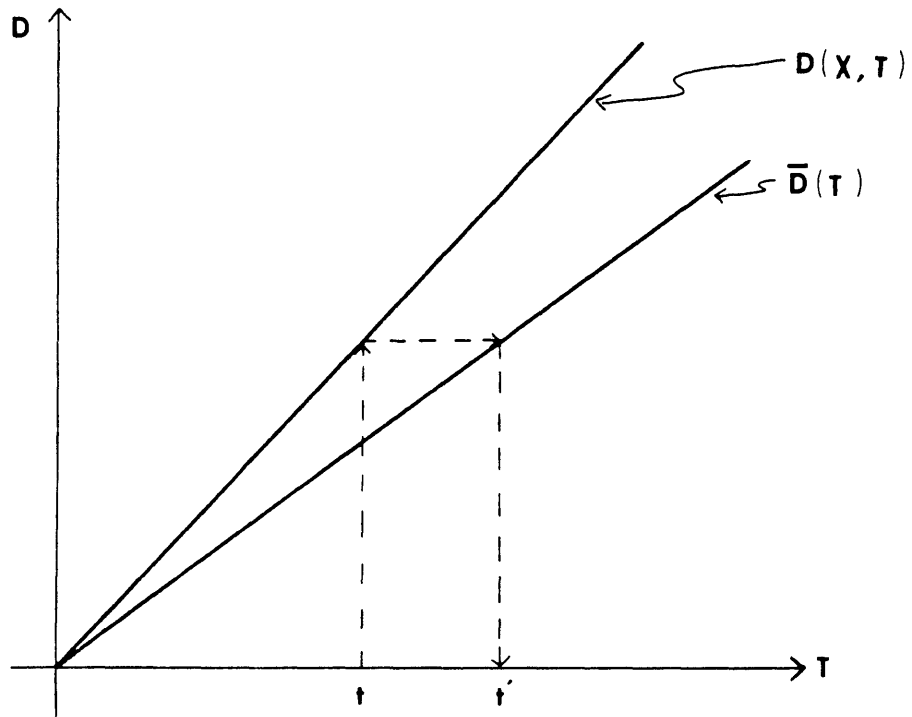


Figure 46: The simplified diagram showing how to obtain new time t' .

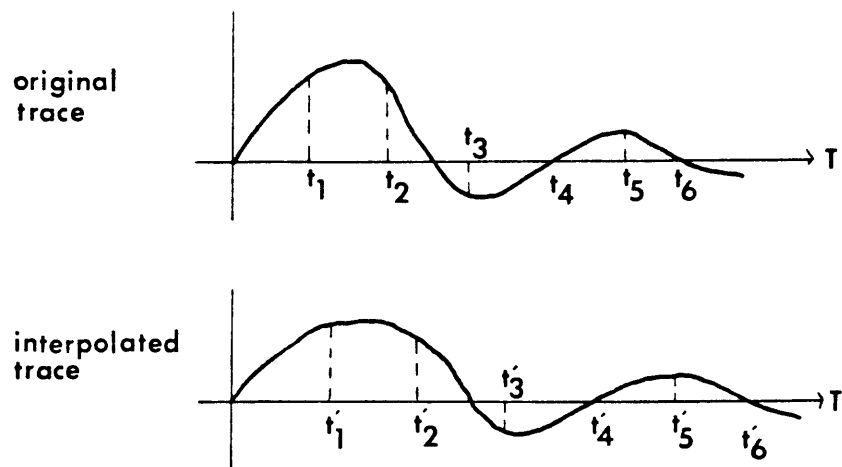


Figure 47: Schematic of trace interpolation.

Dipping layer with diffractor. (Model 4)

This model tests the applicability of the incremental method on a simple example of a lateral velocity variation. Figure 48 shows the physical parameters of model 4. This is intended to simulate a water bottom reflection with a dip of about 14° . A diffractor is added beneath the dipping water bottom. It might be noted that the large velocity contrast is used here in order to have sufficient lateral shift of a diffraction apex discussed below. Figure 49 is the synthetic seismic section with CDP spacing of 50 feet generated by a ray - tracing program. A spike section was convolved with a zero - phase symmetrical Ricker wavelet with a pseudo period of 36 Hz. to produce Figure 49.

Note that in Figure 49 the true apex position, shown by the arrow, of the diffraction has shifted to the left. Note also the asymmetric shape of the diffraction. The lateral shift of the apex is about 450 feet and this is caused by presence of the dipping bottom layer as is shown in Figure 50.

Migration of this section with $W=1.0$, standard F - K migration, is shown in Figure 51. Velocity functions were input at both edges of the section and the program is supposed to interpolate to obtain velocity functions for CDPs between them. The apex has shifted back closer to

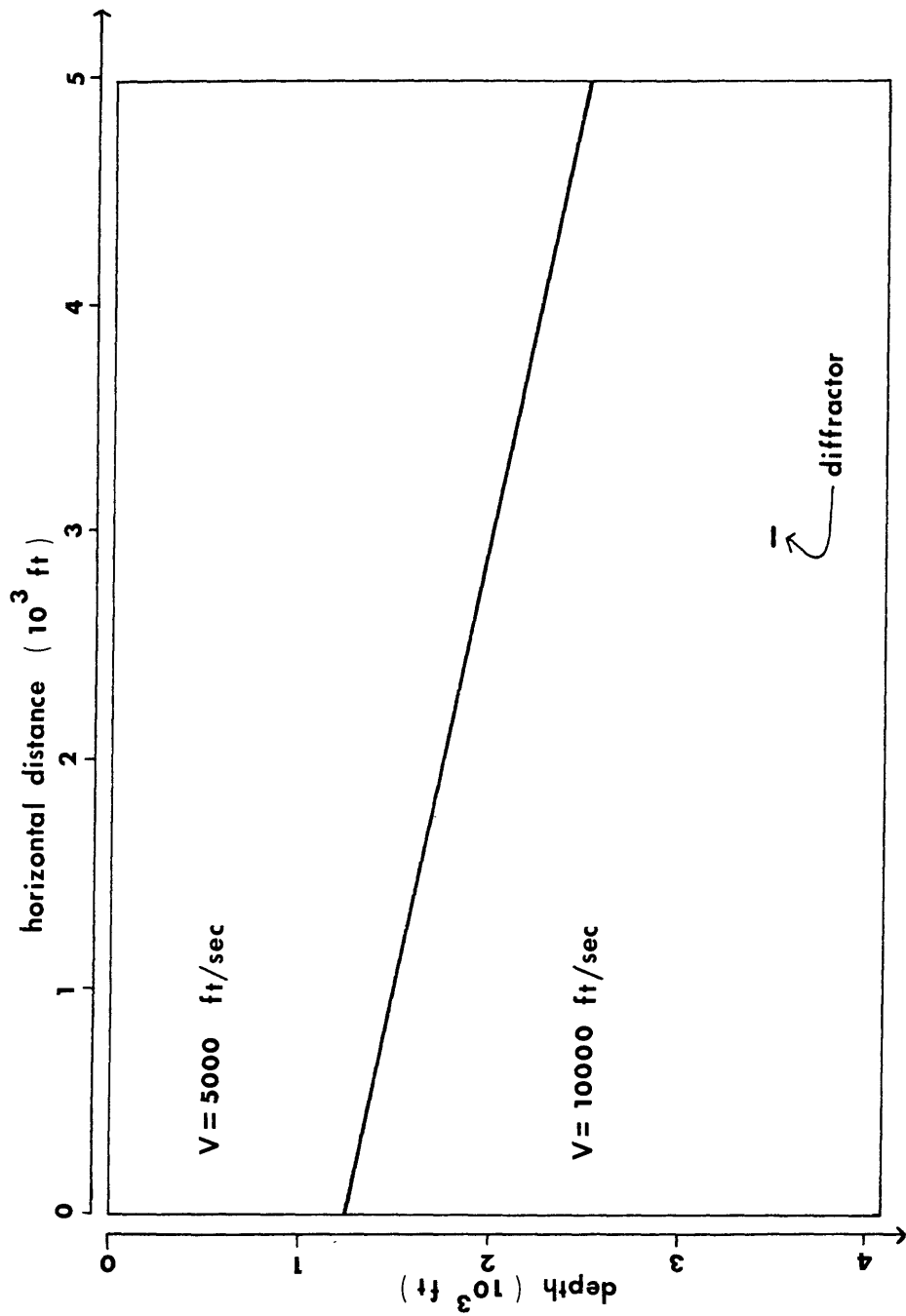


Figure 48: Physical parameters of model 4.

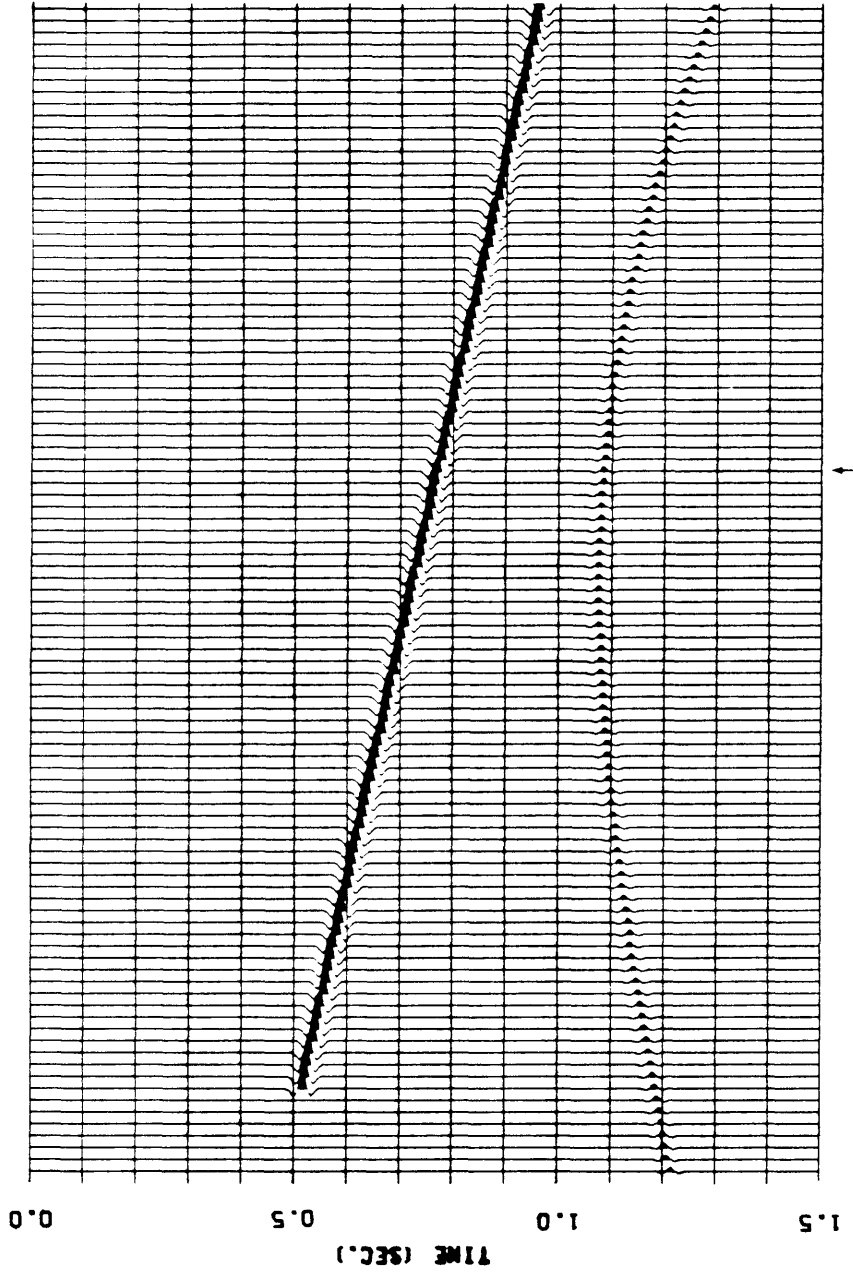


Figure 49: Synthetic time section of model 4. The arrow shows the correct position of the diffractor apex.

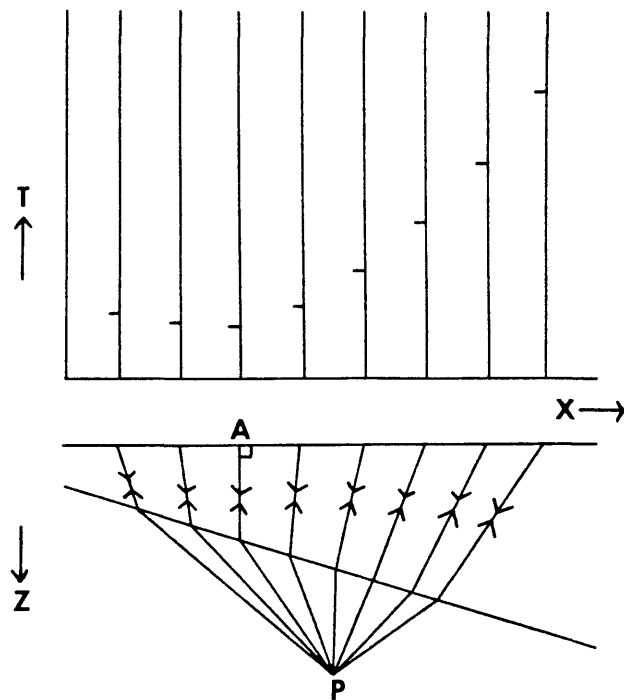


Figure 50: Bottom: raypaths from a scatterer below a dipping interface. The interface separates a low-velocity layer above from a high-velocity layer below. Top: resulting diffraction curve on a time section. (After Larner et al., 1981).

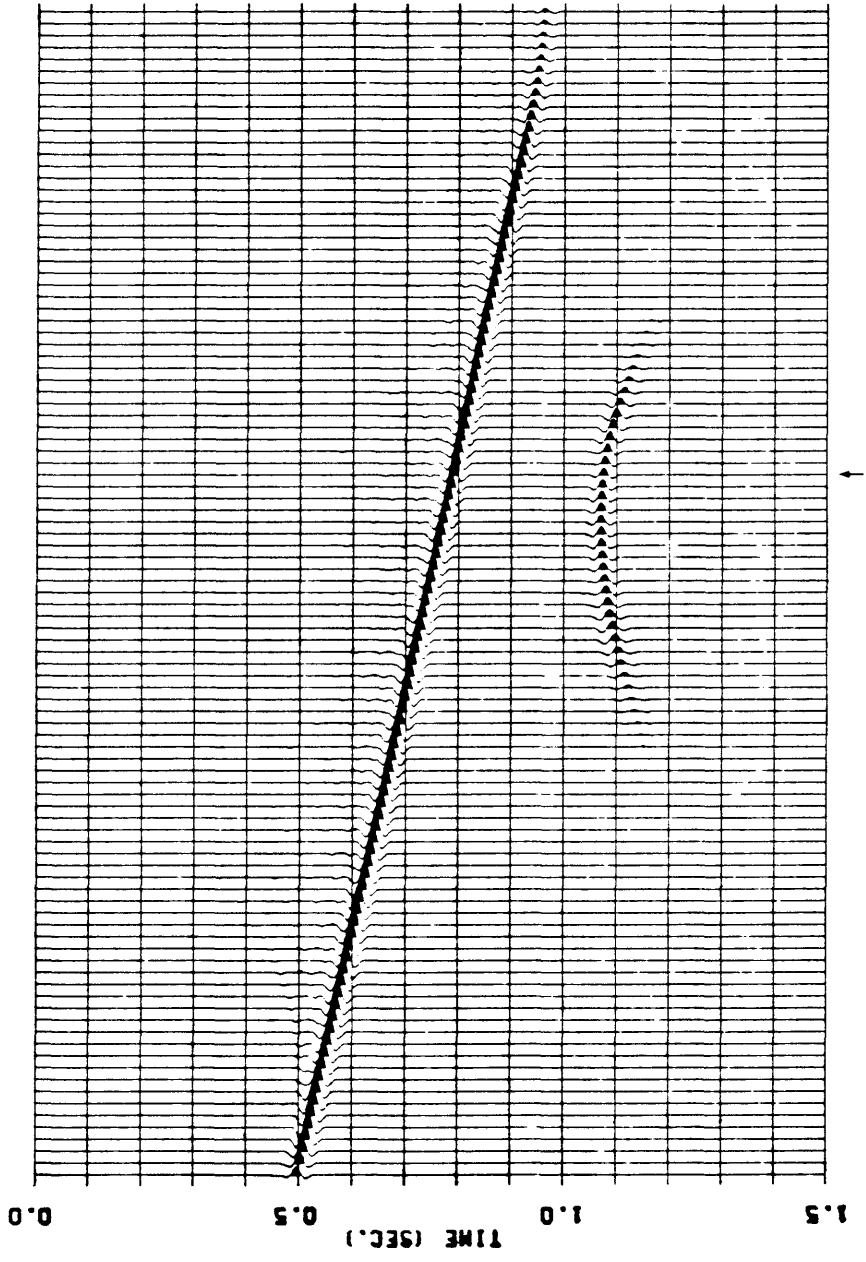


Figure 51: The variable velocity migration of model 4 with $W = 1.0$.
The arrow shows the correct position of the apex.

the true position, denoted by the arrow, but the diffraction has not been collapsed completely. This indicates that the migration velocity used is too slow.

Figures 52, 53, 54, and 55 show variable velocity migration results with $W = -0.43, -0.2, +0.2, \text{ and } +0.43$, respectively. There are not prominent changes among the results. This probably is due to the introduction of a lateral velocity variation, which consequently caused the ineffectiveness of W , the shaping parameter.

Since W has no effects on the results, and the velocity seems too slow, the input velocity was increased to observe changes in the migration results. Figures 56, 57, 58, 59, and 60 correspond to migration results with velocity increases of +10%, +15%, +20%, +25%, and +30%, respectively. As we notice here, the diffraction becomes better focused with the increases of velocity. But also notice that these increases in velocity caused the over-migration of the dipping layer. The optimum migration result is obtained with 25% increase in velocity. Even though the apex is moved very close to the true position, it is a very large adjustment of velocity to have to make.

A detailed study of the diffraction may be done in order to understand the asymmetric diffraction pattern. The plots of T^2 vs. X^2 have been produced for the original synthetic section of Figure 49. Figure 61 is for traces

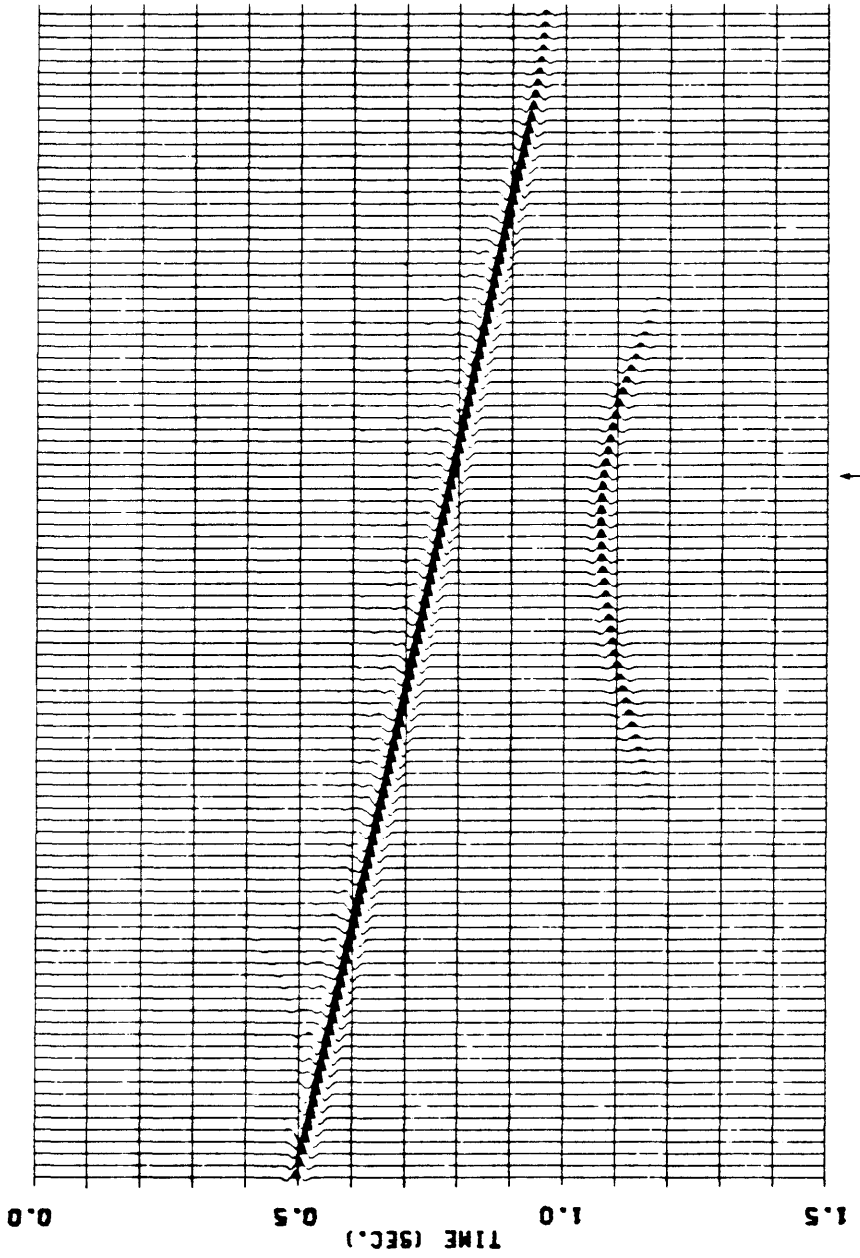


Figure 52: The variable velocity migration of model 4 with $W = -0.43$.
The arrow shows the correct position of the apex.

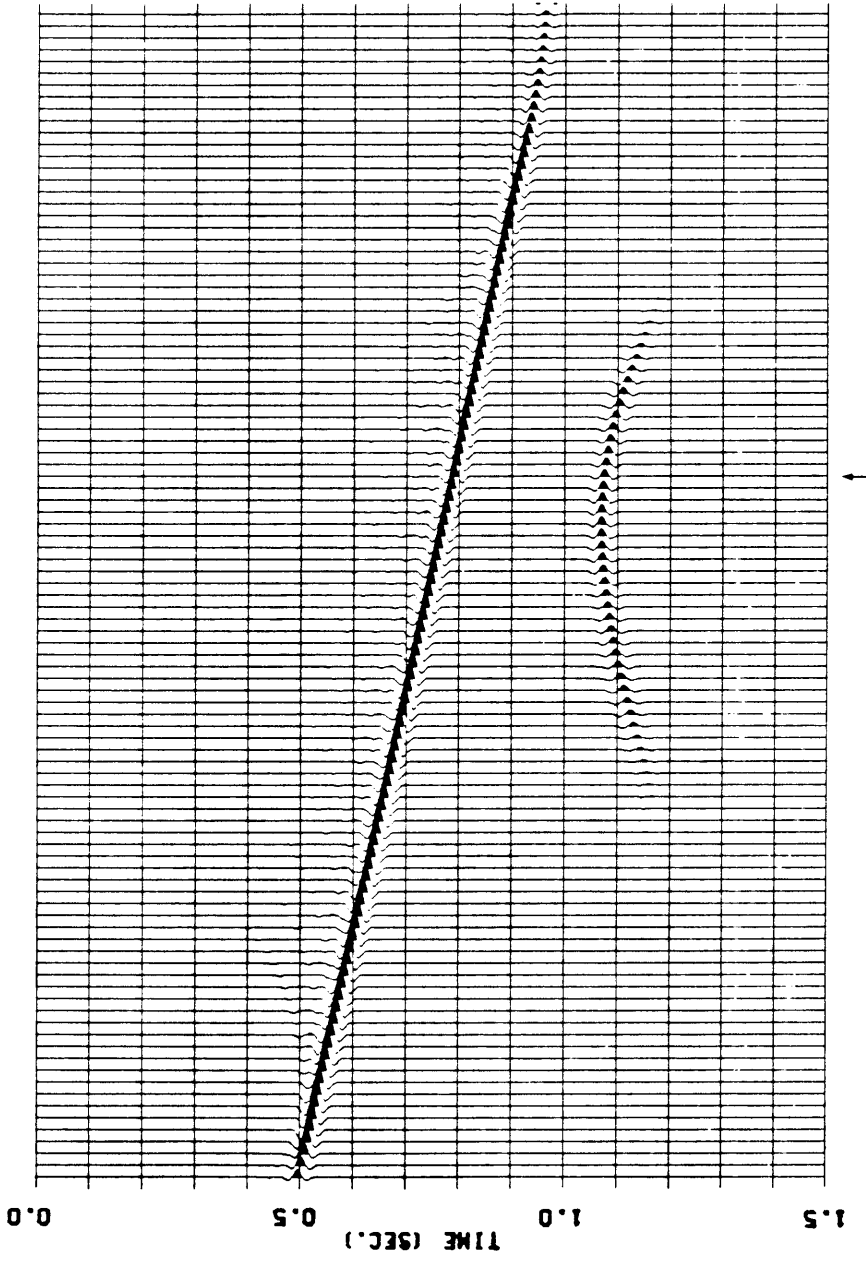


Figure 53: The variable velocity migration of model 4 with $W = -0.2$,
The arrow shows the correct position of the apex.

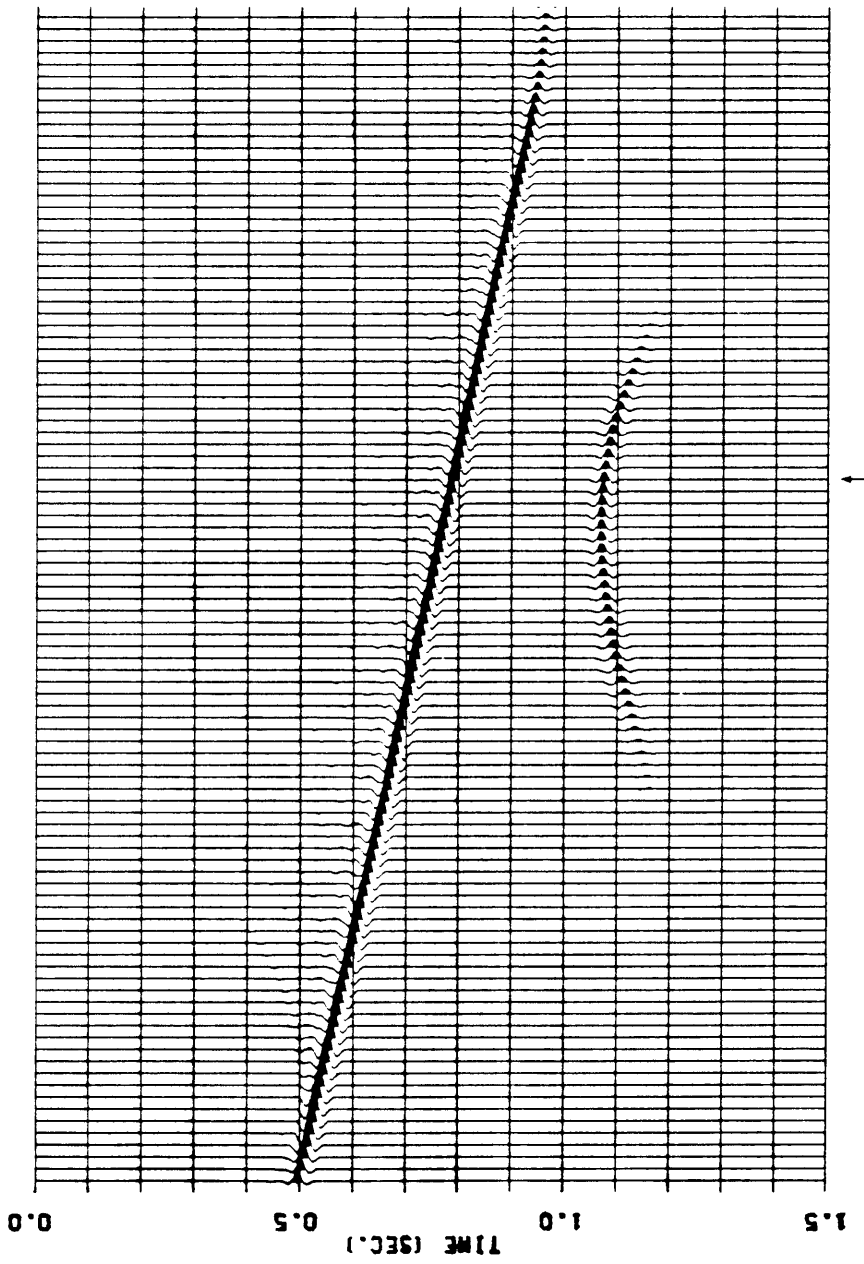


Figure 54: The variable velocity migration of model 4 with $W = 0.2$,
The arrow shows the correct position of the apex.

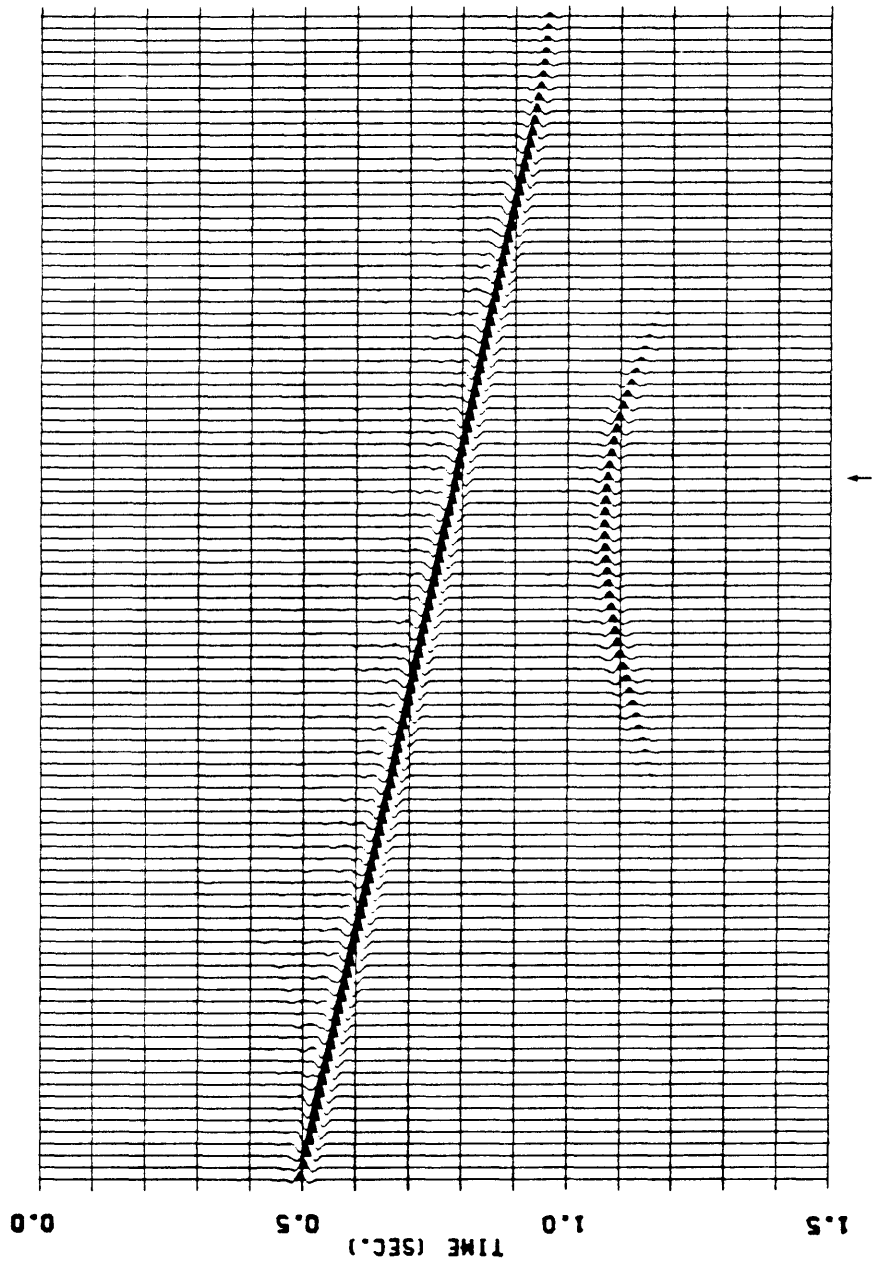


Figure 55: The variable velocity migration of model 4 with $W = 0.43$,
The arrow shows the correct position of the apex.

TABLE III

Velocity	Interval velocity Layer 1	Interval velocity Layer 2	Corresponding figure
+ 0 %	5000.0	10000.0	Figure 55
+ 10 %	5500.0	11000.0	Figure 56
+ 15 %	5750.0	11500.0	Figure 57
+ 20 %	6000.0	12000.0	Figure 58
+ 25 %	6250.0	12500.0	Figure 59
+ 30 %	6500.0	13000.0	Figure 60

Table III: Table of velocity increase used in the variable velocity migration.

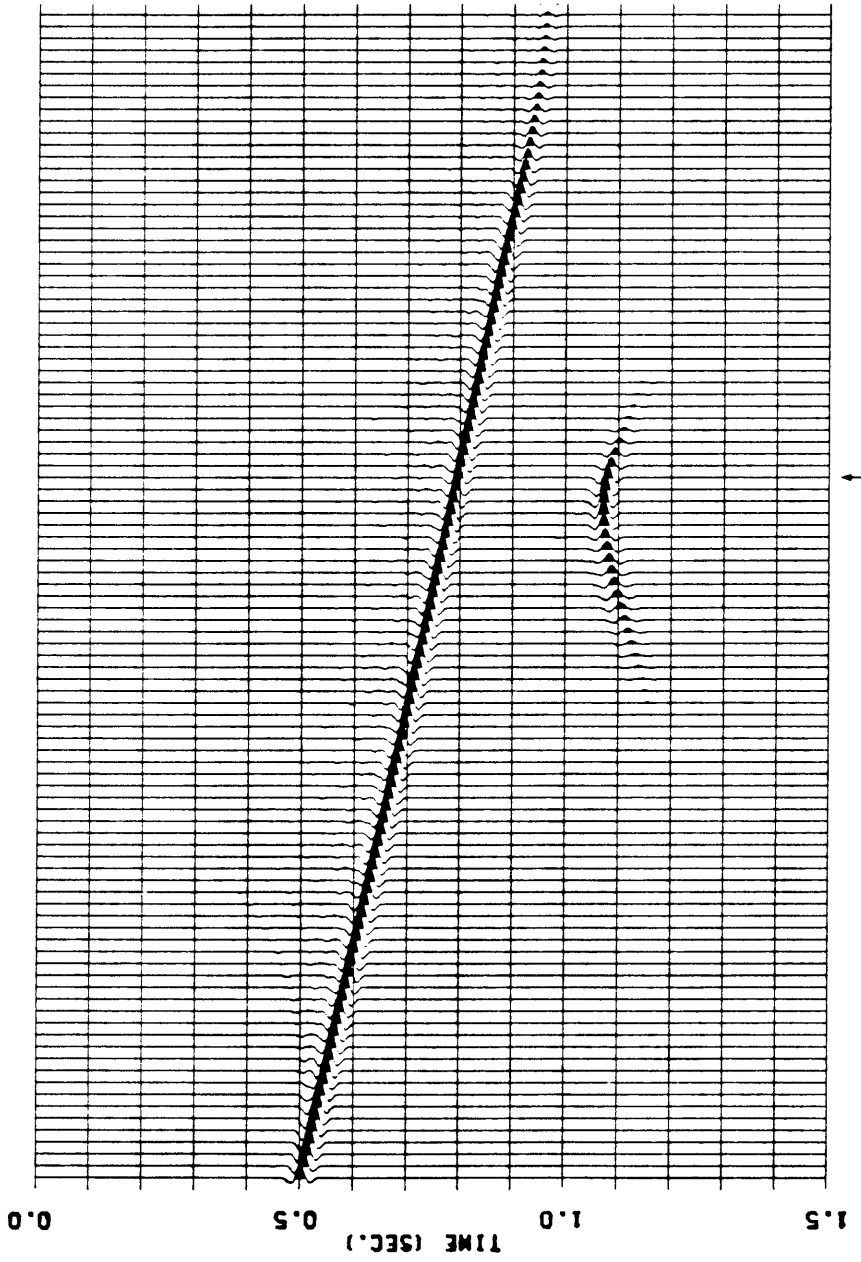


Figure 56: The variable velocity migration of model 4 with $W = 0.43$, and velocity increase by 10%. The arrow shows the correct position of the apex.

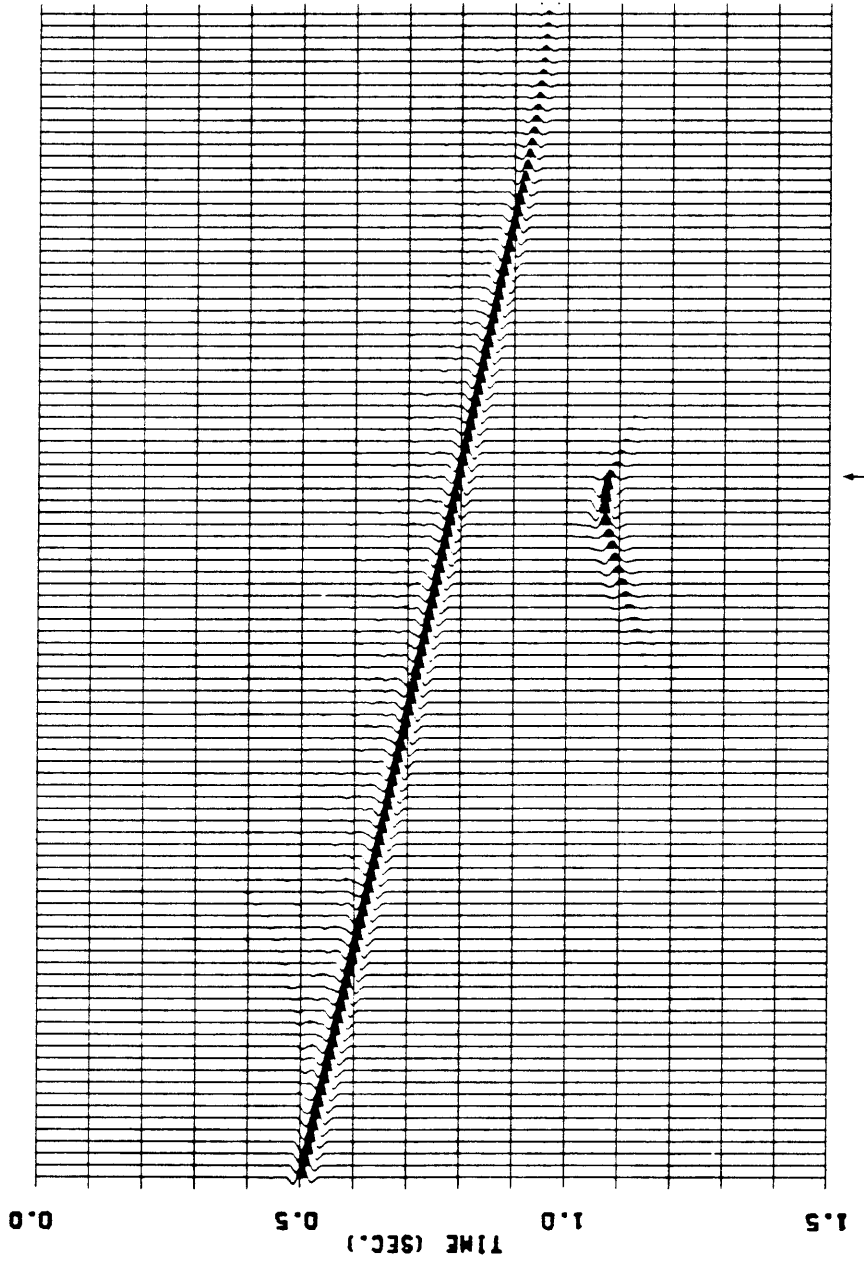


Figure 57: The variable velocity migration of model 4 with $W = 0.43$, and velocity increase by 15%. The arrow shows the correct position of the apex.

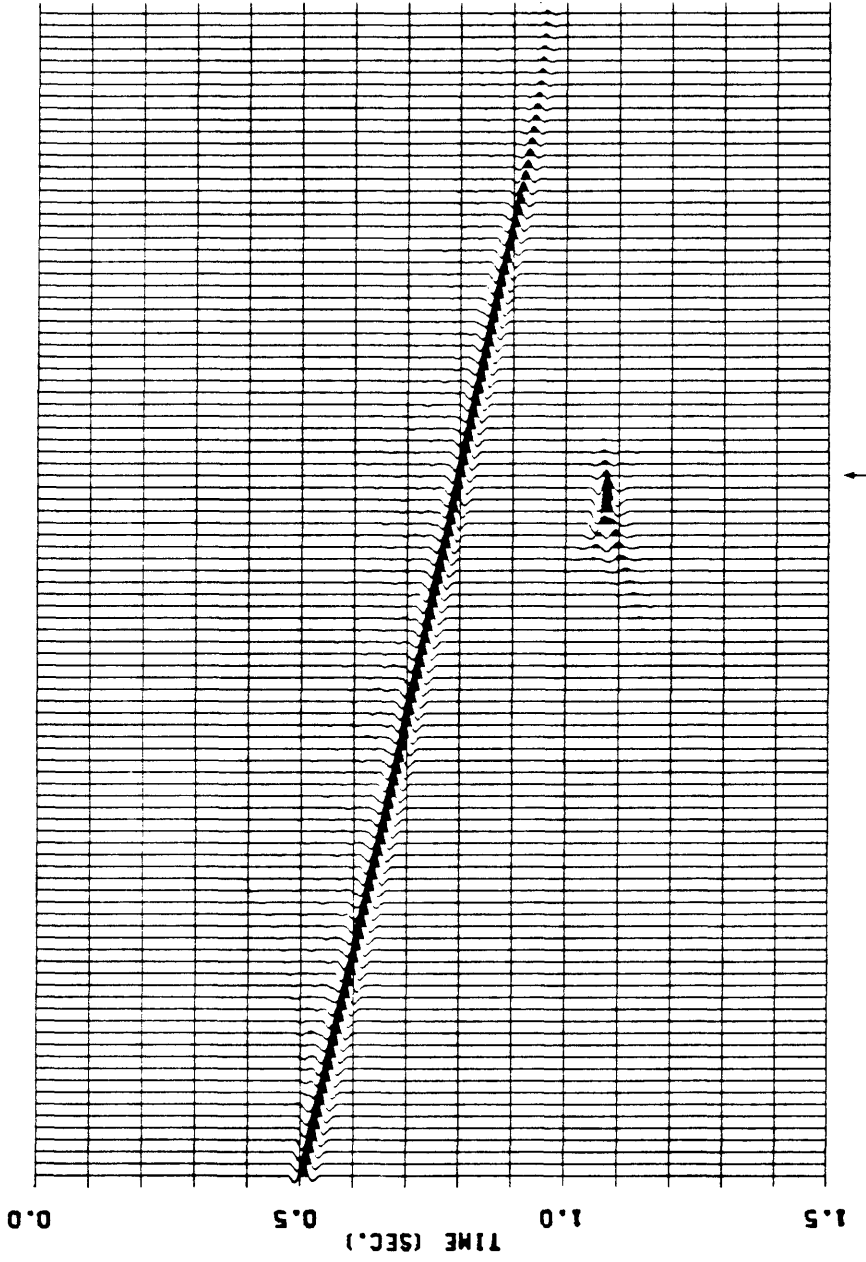


Figure 58: The variable velocity migration of model 4 with $W = 0.43$, and velocity increase by 20%. The arrow shows the correct position of the apex.

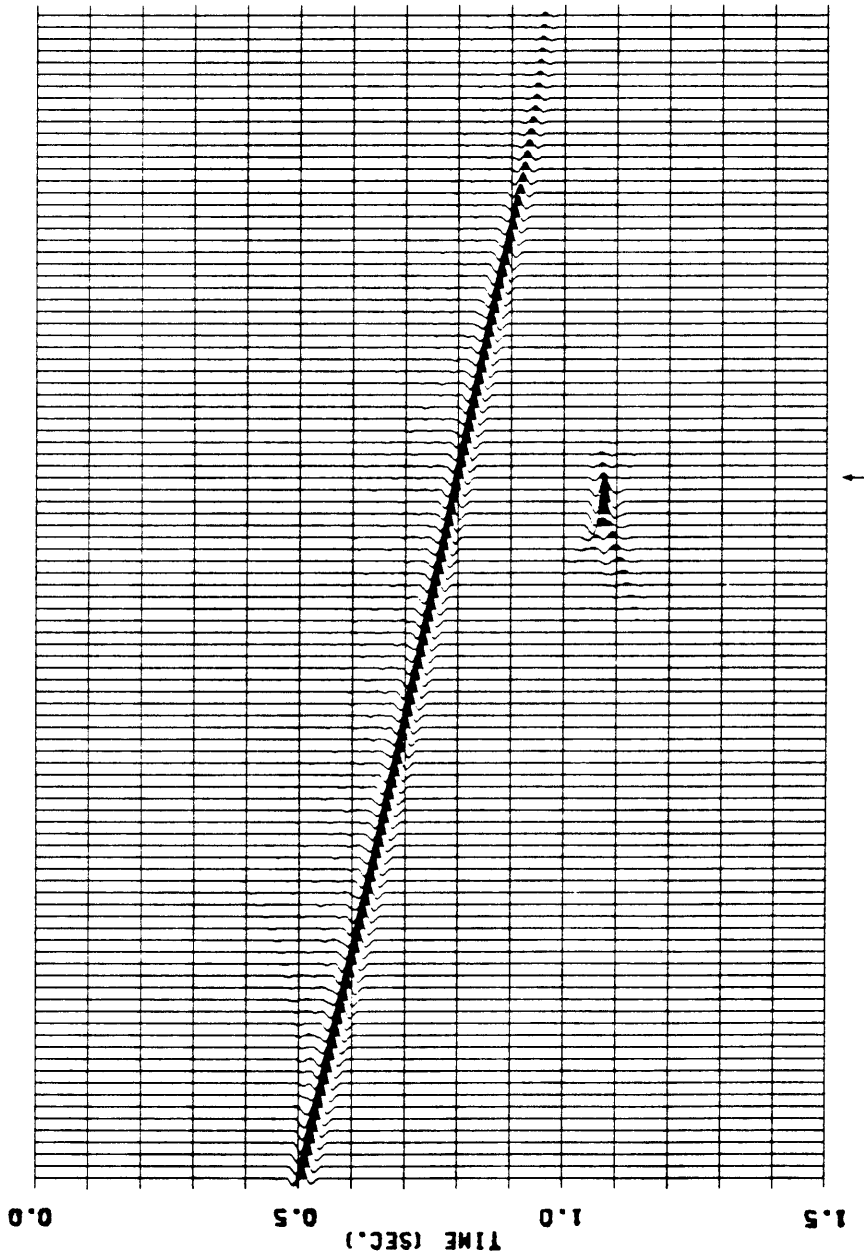


Figure 59: The variable velocity migration of model 4 with $W = 0.43$, and velocity increase by 25%. The arrow shows the correct position of the apex.

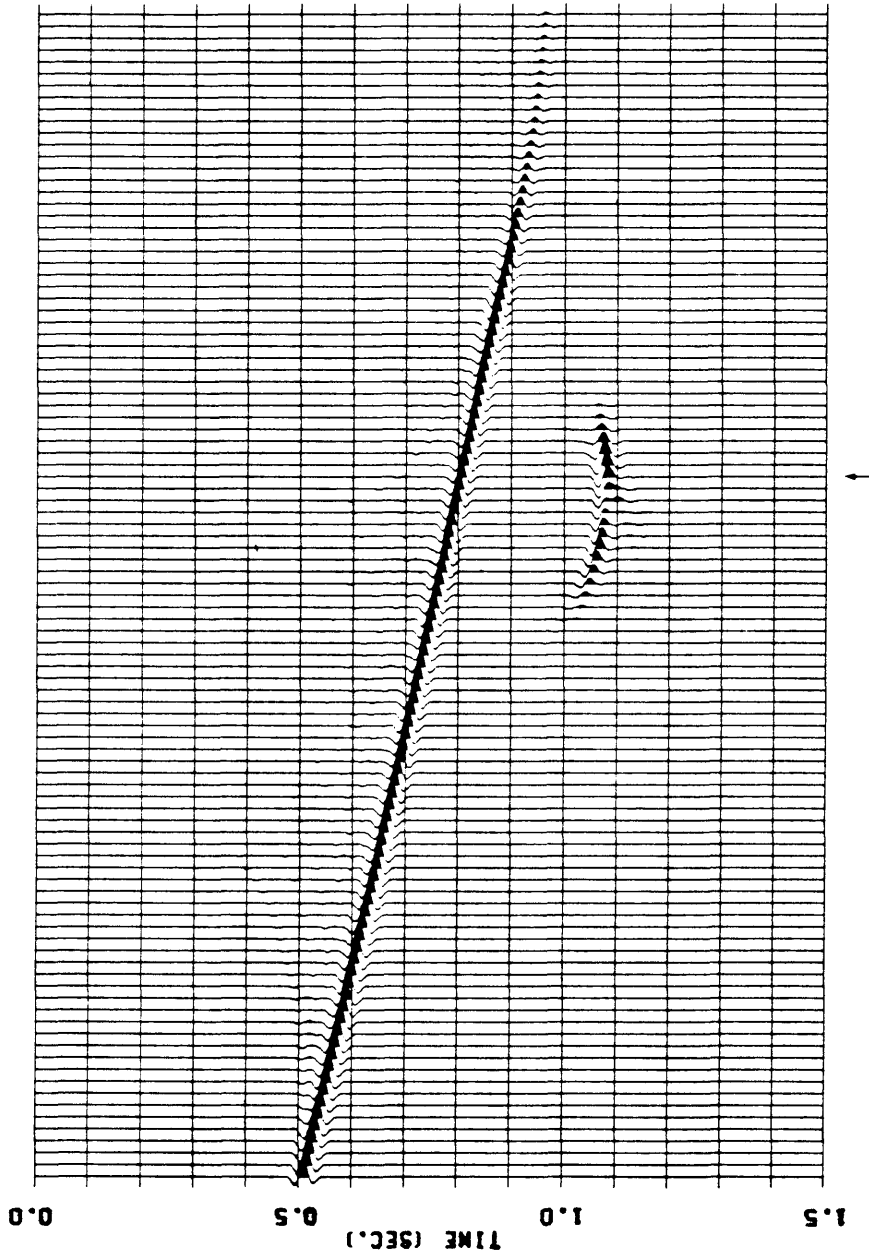


Figure 60: The variable velocity migration of model 4 with $W = 0.43$, and velocity increase by 30%. The arrow shows the correct position of the apex.

1 through 50 and RMS velocity came out to be about 8118 ft/sec., and Figure 62 is for traces 50 through 100 and RMS velocity is about 5641 ft/sec. This is reflected in the migration result in Figure 59; the diffraction on the right side of the apex has been collapsed but on the left side it is still undermigrated.

Now let us turn our attentions to the incremental method. As it was mentioned, a mean average velocity, $\bar{V}(t)$, has to be approximated from $V(x,t)$. For our simple test case, let $\bar{V}(t)$, shown in Figure 63, be a mean average velocity. It can be seen in Figure 63 that we have a transition zone from 0.5 sec. to 1.0 sec. The velocity is increased linearly from 5000 ft/sec. to 10000 ft/sec. in the transition zone. There are no justifications for using this velocity function, it is strictly the test case. The lower plot in Figure 63 shows corresponding depth functions at CDP 1, CDP 100, and $\bar{D}(t)$.

The incremental migration of the section without interpolation before and after migration is shown in Figure 64. The apex stayed at the original recorded position, which is at CDP 50, and there is some unmigrated energy present. This result is reasonable because the algorithm tries to focus the diffracted energy at the apex on the observed time section.

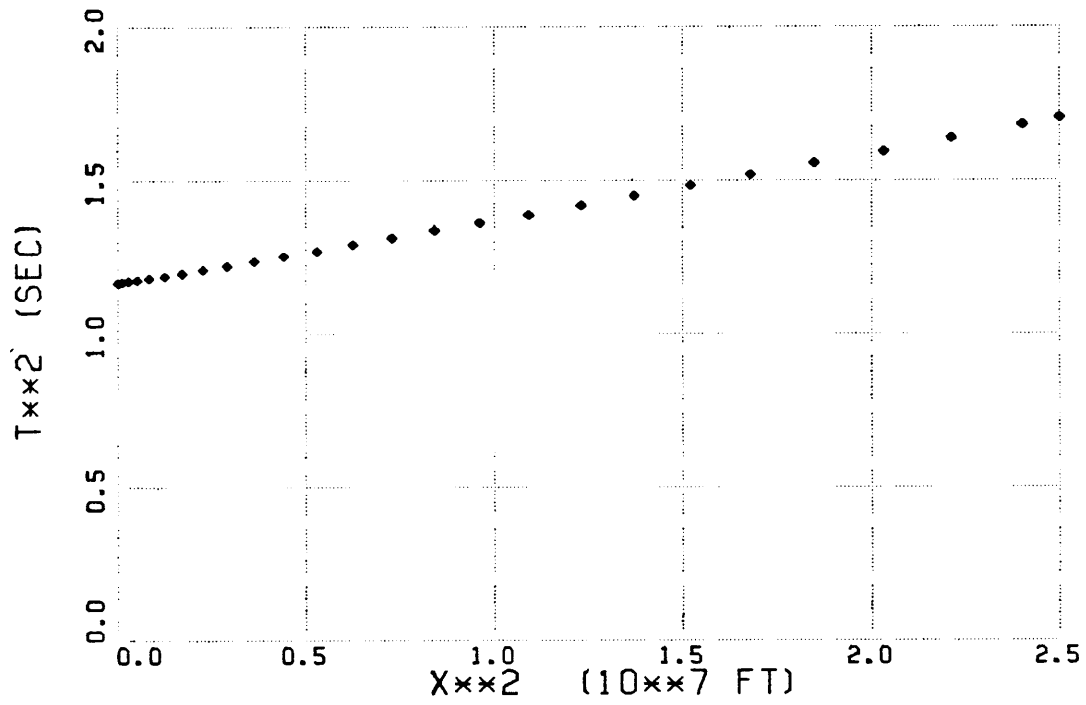


Figure 61: The plot of T^2 vs. X^2 of original synthetic section (Fig. 49) for traces 1 through 50. RMS velocity is about 8118 ft/sec..

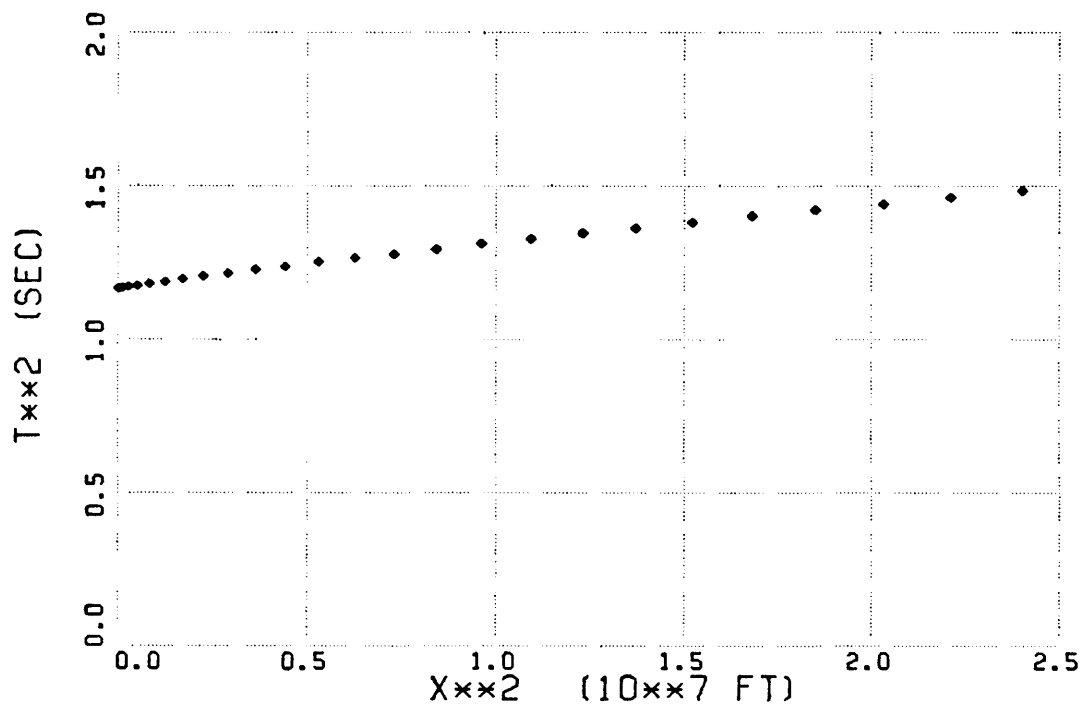


Figure 62: The plot of T^2 vs. X^2 of original synthetic section (Fig. 49) for traces 50 through 100. RMS velocity is about 5641 ft/sec. .

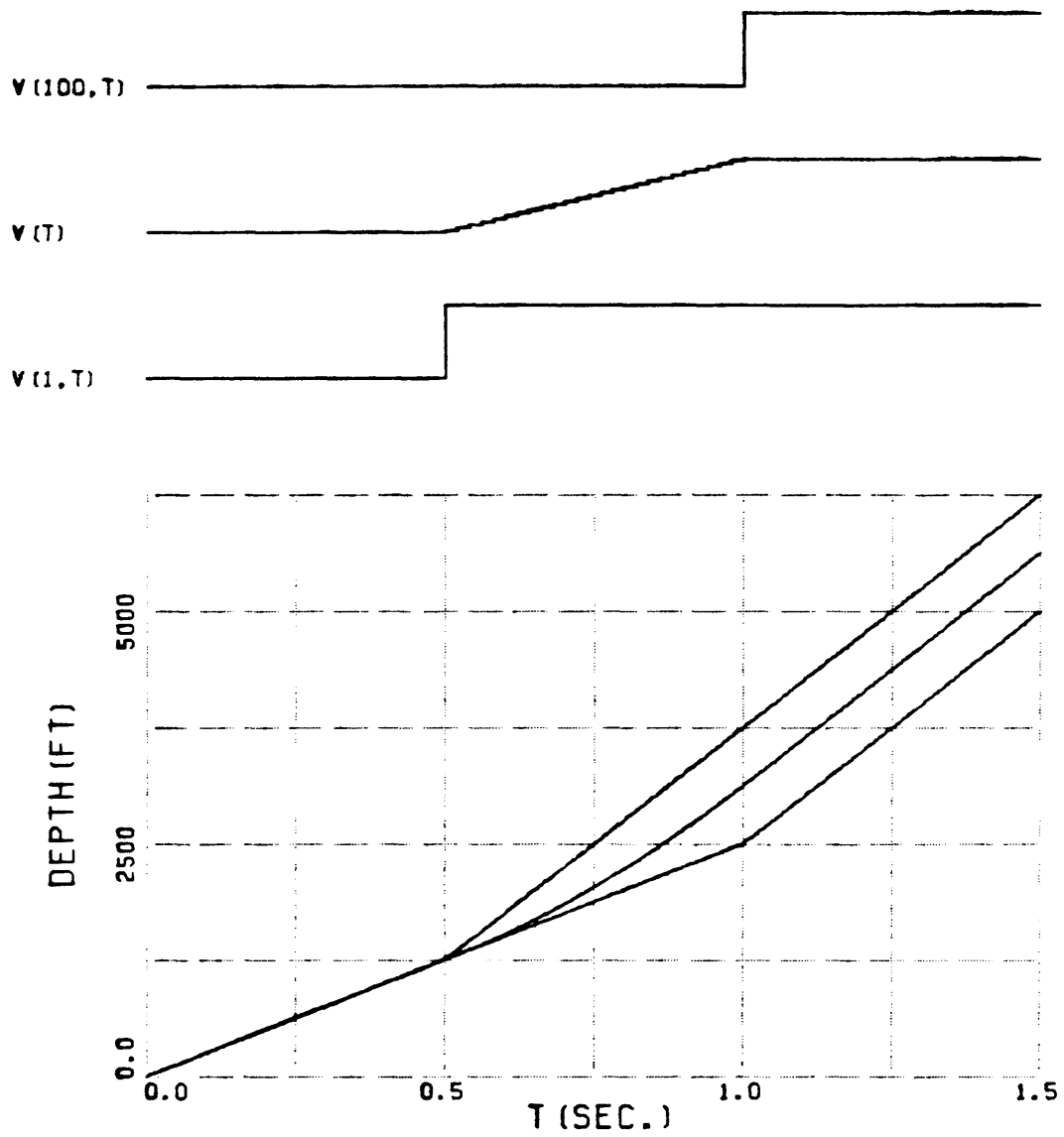


Figure 63: Top: mean velocity used for the incremental migration. Bottom: corresponding depth function.

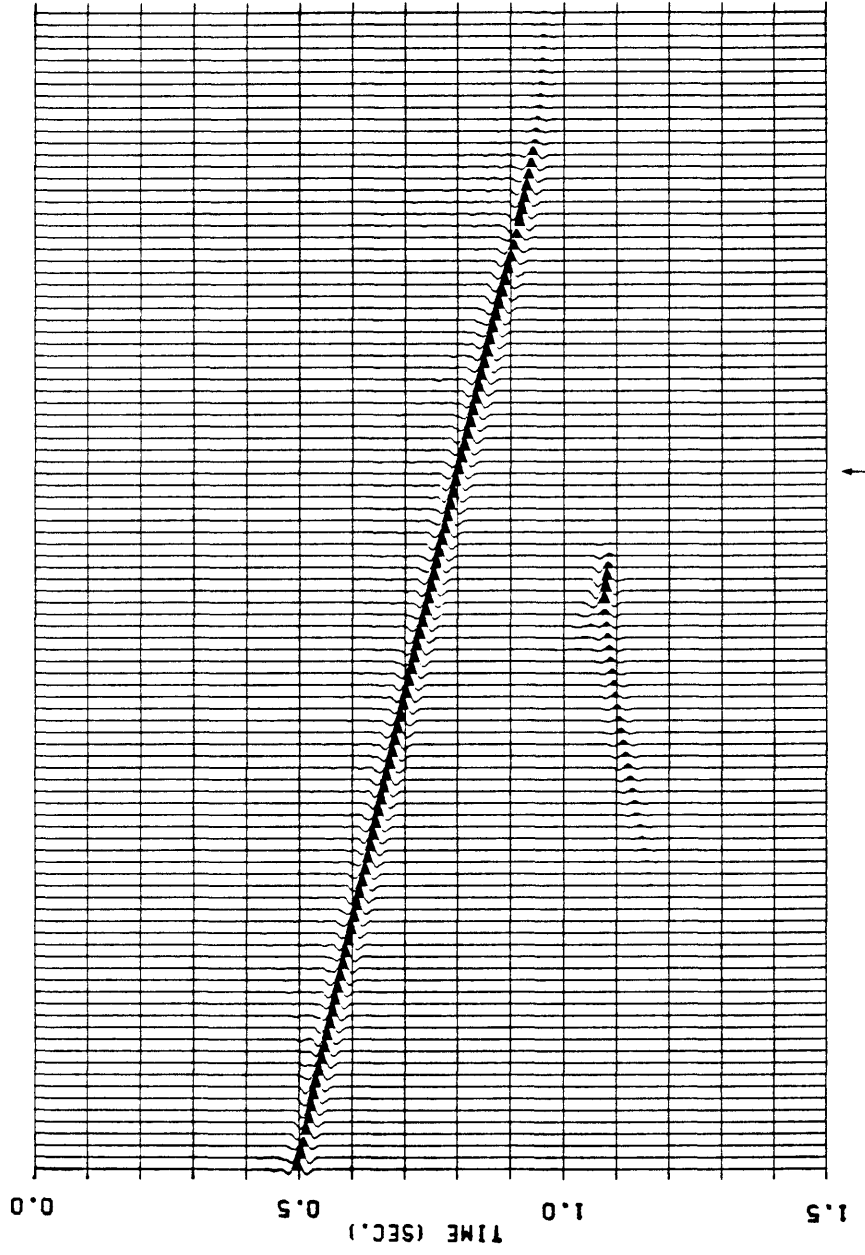


Figure 64: The incremental migration of model 4 without interpolation of trace before and after the migration. The arrow shows the correct position of the apex.

Now we go back to an idea we proposed earlier; the interpolation of traces before and after migration. Figure 65 is an interpolated section before migration. The diffraction looks symmetrical but the apex of the diffraction has been shifted to around CDP 64, about 4 traces too far. This may mean that $\bar{V}(t)$ used here is not the correct mean velocity. But let us proceed to migrate the section. Figure 66 shows the migrated section with this mean velocity. The diffraction has not been collapsed completely and close examination shows that the apex is shifted down about 5 msec. The dipping layer is now shifted a little upward. These errors were caused by the interpolation of traces. Figure 67 shows the migration result with velocity increased by 10%. As we see here, the diffraction is fairly well collapsed but the same phenomenon occurs here; the shift in time of the apex. Also the frequency content of the dipping events become higher. We feel that this probably is caused during the process of interpolation, also.

Here the possibility of extending the incremental method in the laterally inhomogeneous media was investigated in a rather experimental manner. A more analytical study of the process will help in understanding the difficulties encountered here.

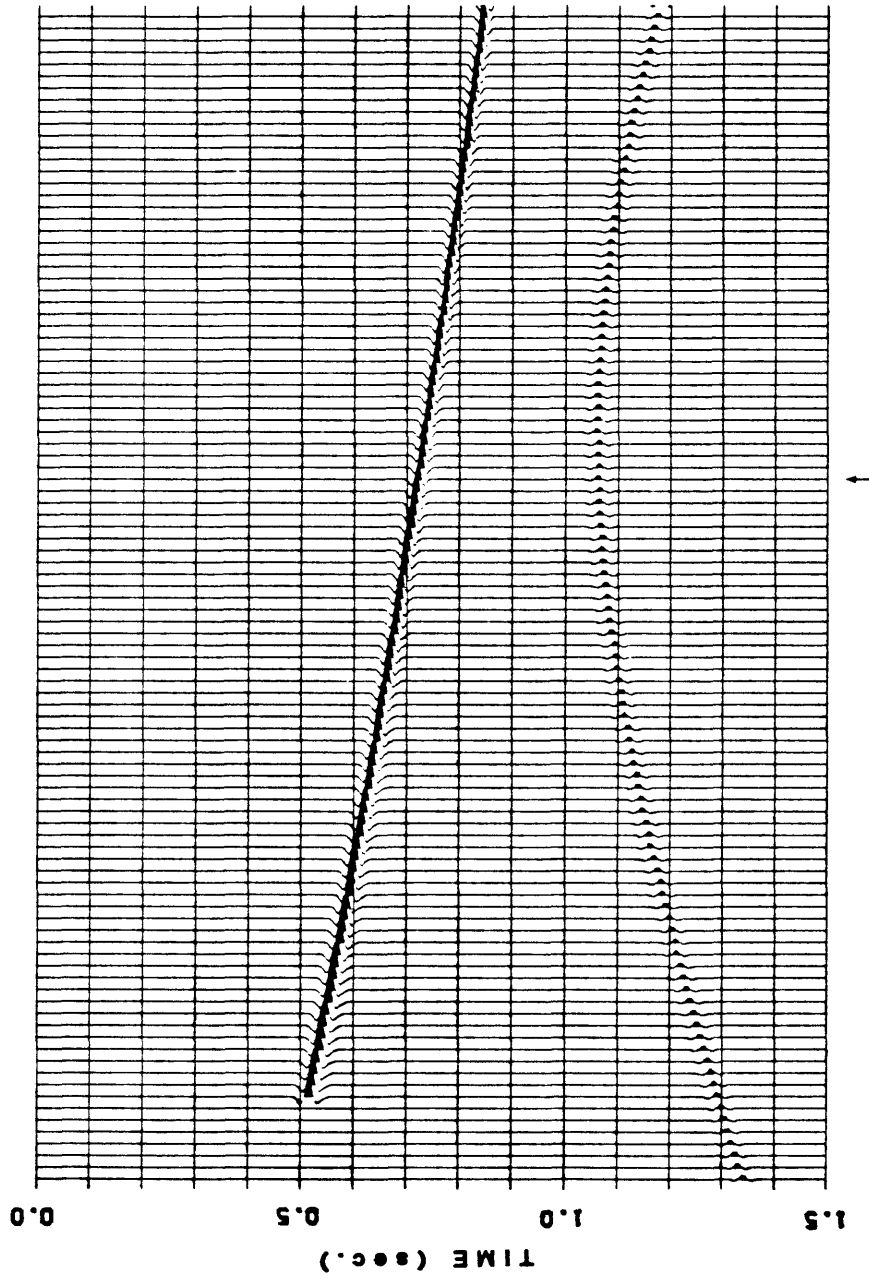


Figure 65: The interpolated section before migration using the mean velocity of figure 61. The arrow shows the correct position of the apex.

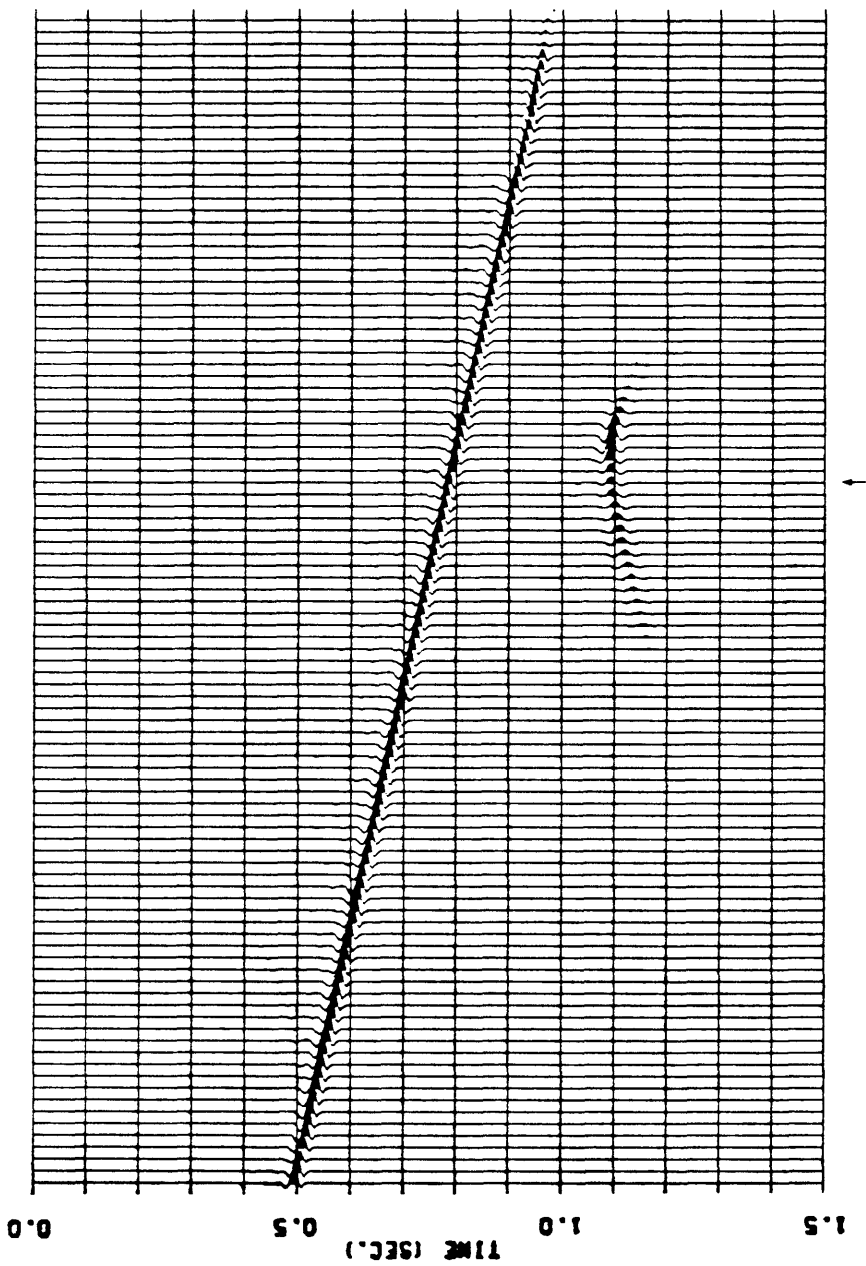


Figure 66: The incremental migration of model 4 using the mean velocity of figure 61. The arrow shows the correct position of the apex.

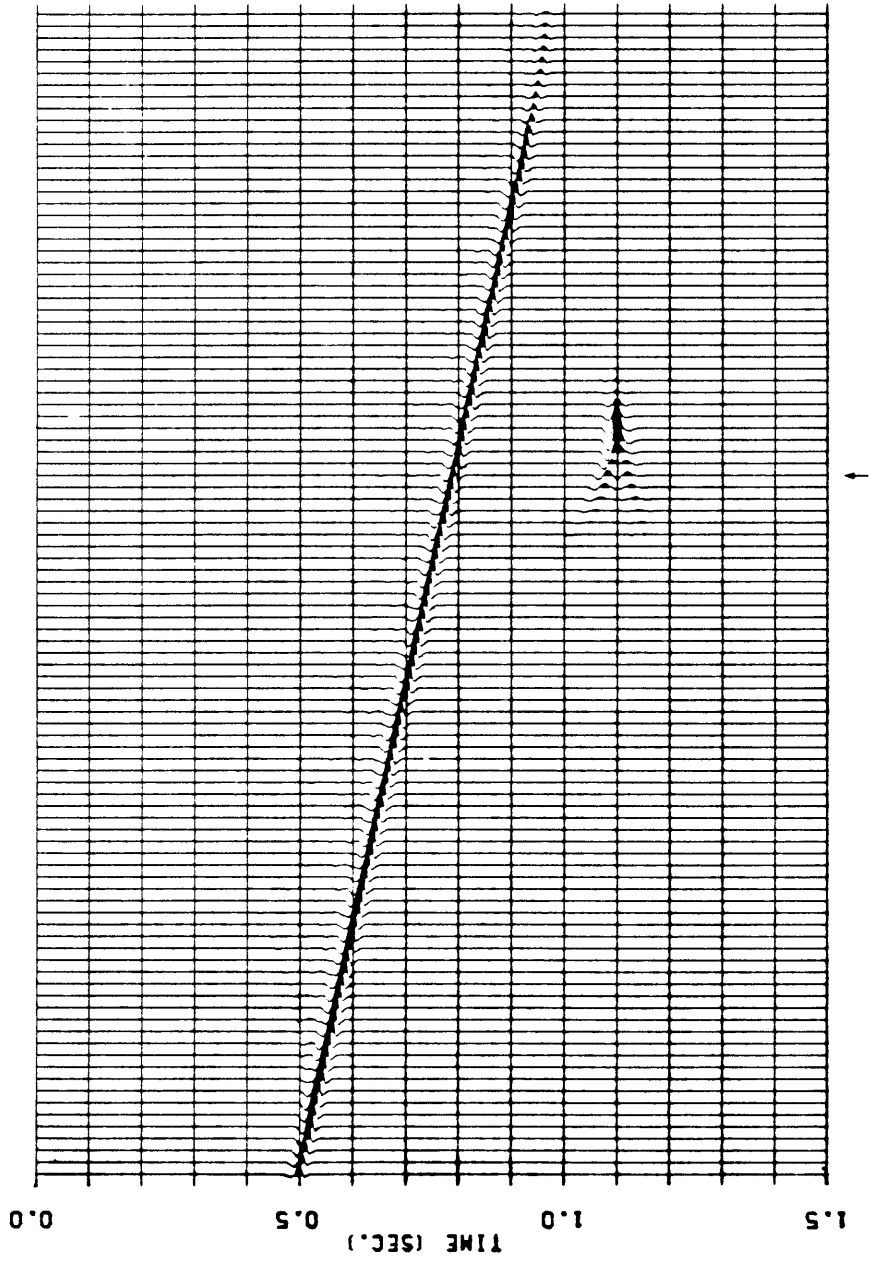


Figure 67: The incremental migration of model 4 using the mean velocity increased by 10 %. The arrow shows the correct position of the apex.

SUMMARY AND CONCLUSIONS

The incremental approach to frequency wavenumber domain migration was developed in this paper. This is a recursive scheme in the $F-K$ domain as opposed to the variable velocity method which is a straight mapping scheme.

Several examples have been presented illustrating the comparisons of the two methods in the presence of vertical velocity gradients. Also, the effort was extended to account for a minor lateral velocity gradient.

From the study carried out here, several conclusions can be drawn,

- 1) Determination of a correct value of shaping parameter, W , is essential to the success of the variable velocity method.
- 2) The incremental method gives better results in the presence of vertical velocity gradients.
- 3) Ineffectiveness of shaping parameter, W , is observed in the presence of lateral velocity gradients. And finally,

- 4) With more rigorous analytical study, the incremental method may be applied in the presence of both lateral and vertical velocity gradients.

BIBLIOGRAPHY

- Berkhout, A. J., and Van Wuefften Palthe, D. W., 1979, Migration in terms of spatial deconvolution: Geophysical Prospecting, V. 27, pp. 261-291.
- _____, 1980, Seismic migration: Elsevier Scientific Publishing Company.
- Bolondi, G., Rocca, F., and Savelli, S., 1978, A frequency domain approach to two-dimensional migration: Geophysical Prospecting, V. 26, pp. 750-772.
- Brigham, E. O., 1974, The fast fourier transform: Prentice-Hall, Inc.
- Chun, J. H., and Jacewitz, C. A., 1981, Fundamental of frequency domain migration: Geophysics, V. 46, No. 5, pp. 714-733.
- Claerbout, J. F., and Doherty, S. M., 1972, Downward continuation of moveout corrected seismograms: Geophysics, V. 37, No. 5, pp. 741-768.
- Diet, J. P., 1979, Determination of the shape parameter W in Stolt's frequency domain migration scheme: reprint of paper S. 19 SEG 1979.
- Gazdag, J., 1978, Wave equation migration with the phase shift method: Geophysics, V. 43, No. 7, pp. 1342.
- Hatton, L., Larner, K. L., and Gibson, B. S., 1981, Migration of seismic data from inhomogeneous media: Geophysics, V. 46, No. 5, pp. 751-767.
- Hood, P., 1978, Finite difference and wave number migration: Geophysical Prospecting, V. 24, pp. 773-789.
- Johnson, J. D., 1979, Comparisons of finite difference, f-k, and kirchhoff approaches to wave equation migration:
- Larner, K. L., Hatton, L., Gibson, B. S., and Hsu, I-C., 1981, Depth migration of imaged time sections: Geophysics, V. 46, No. 5, pp. 734-750.

- Lowenthal, D., Lu, L., Roberson, R., and Sherwood, J.,
1976, The wave equation applied to migration:
Geophysical Prospecting, V. 24, pp. 380-399.
- Neale, G. H., Stone, D. G., and Atherton, J. L., 1978,
Migration in the frequency domain: Geophysical
Society of Houston (Seminar).
- Papoulis, A., 1962, The fourier integral and its applications:
McGraw-Hill Book Company, Inc.
- Schneider, W. A., 1971, Developments in seismic data
processing and analysis (1968-1970):
Geophysics, V. 36, No. 6, pp. 1043-1073.
- _____, 1978, Integral formation for migration
in two and three dimensions: Geophysics, V. 43,
No. 1, pp. 49-76.
- Sheriff, R. E., 1978, History and overview of seismic
migration methods: Geophysical Society of Houston
(Seminar).
- Stolt, R. H., 1978, Migration by fourier transform:
Geophysics, V. 43, No. 1, pp. 23-48.

APPENDIX A

DESCRIPTION OF THE COMPUTER PROGRAM

COMPUTER PROGRAM

In order to test the incremental scheme, computer program has been developed. First the program was written in a regular Fortran program format to undergo tests. Later it was converted to CGG module format because of the following advantages:

- 1) easy access to synthetic data generated by the CGG modelling program, and also output to the CGG plotting routine.
- 2) easy to make use of special routines and MAP 3 array processor calls already existing within the CGG library.

General structure of the program is borrowed from FKMIIG (CGG software) and necessary changes were made by the author.

INPUT

The module, YOMIG, takes the same format as other modules in the CGG package.

CONTROL CARD

<u>Column</u>	<u>Field</u>	<u>Content</u>
1	Identification	*
3 - 7	Name	YOMIG
9 - 10	Primary option	Not used
12 - 13	Secondary option	Not used
15 - 16	Input Buffer	Disk Buffer
23 - 24	Output Buffer	Disk Buffer, must be different from input buffer
31 - 80	DATA (all the numbers are integer)	
NTa	a = number of traces to process, maximum 350.	
SIi	i = sampling interval in milliseconds.	
Ec	c = distance between CDP.	
RLd	d = length of the trace to process in milliseconds.	
RLMe	d = maximum time to migrate. (default, RLM=RL)	

ECSf f = limitation of ECs requirements;
 when necessary, mentioning ECSf in
 the data field will reduce the
 requirements to f words.
 (default, f = 60000)

MNPADg g = number of traces to be padded in
 x-direction before FFT. NX + MNPAD
 had to be less than 512.

FMAXh h = maximum frequency to migrate.

LEVCj j = number of bit shift to apply, if
 necessary, for output.

NOMAP YOMIG normally uses the MAP 3. Coding
 NOMAP forces the program to execute the
 calculations outside the MAP 3.

ZYKMV YOMIG normally goes through the execution
 without any pause. Coding ZYKMV forces
 the program to stop after the overlay
 ZYKMV and print out the necessary
 parameters for migration.

MV=TkVil, TmVIn, , VFo
 input format of migration velocity.
 k = time in miliseconds.
 l = interval velocity up to time k.
 and same format for m, n.
 o = final interval velocity

total of 30 pairs plus 1 final velocity can
 be input.

FILES

1) IHEDR

- It is created by the overlay ZYKRT, initialized with zeros.
- It stores input traces, managed by FICH package.
- It consists of one group and as many sub-groups as input traces.

2) MUXR

- It is created by the overlay ZYFKA.
- It stores all the (F - K) information with different structures according to the computation phase.
- It is managed by XED package for fast DISK - ECS direct transfer.

OVERLAY NAME		Routine used in addition to common SOS routine	
YOMIG	YOMIG1	PCLRW	
ZYINI	ZYINI1		
ZYKRT	ZYKRT1		
ZYKMV	ZYKMV1	ZYKMV2	
ZYFKA	ZKMIA21	FFTINF NPFMAX BMUX1 RFFT	PCLRW SINE, PCLRW, FOUR1, FFOUR1
ZYFKB	ZKMIB21	KTRANS1	SINE, PCLRW, FOUR1, CALSPEC, FREQSUM, FFOUR1
ZYKFC	ZKMIC21	RIFFT BDMUX	SINE, FOUR1, FFOUR1 LOWER

```

/JOB
YD,T1500.
USER,M749019,KATA.
CHARGE,I,WA*SCHNEIDER.
CPT(1234567,1234,A,1234A,1234)
ATTACH,SQSIN=MODEL3.
PURGE,MODEL3M/NA.
DEFINE,SQS001=MODEL3M.
ECSFILE,TABSOS.
SOS.
GOTO,1.
EXIT.
1,DAYFILE.
REPLACE,OUTPUT=DAYYOM.
/EOB
** EXAMPLE-YDMIG
**345678901234567890123456789012345678901234567890
* DEFIN 1 1000 EA,DA(4*24),DB(4*24)
* LIBRI TR B1009,F1=(R1T1-R1T71,I1,G1)
* LIBRI BD UNITC1=B9999(Rw)
* LIBRI HB 1 2 YDMIG
3 MODEL 3
* BOUCL 1
* INPTR EA DA RL500
* TRANS EA DA
* FINBO
* BOUCL 2
* YGMIG DA DB NT71,SI1,E50,RL500,FMAX100,
ECS6000,MNPAD40,LEVC3,
MV=T100VI5000,T200VI6000,
T300VI7000,T400VI8000,VF9000
* FINBO
* BOUCL 3 EA
* TRANS DB EA ECH750,G35,PAS50,LSG,GD,NEX1,
* RAGOU EA AG LH81,CT100,AG
* OUTBD EA 500 UNIT01
* FINBO
* PRGCS 71(B1)+82+71(83)
/EOB
/EOF

```

OVERLAY YOMIG

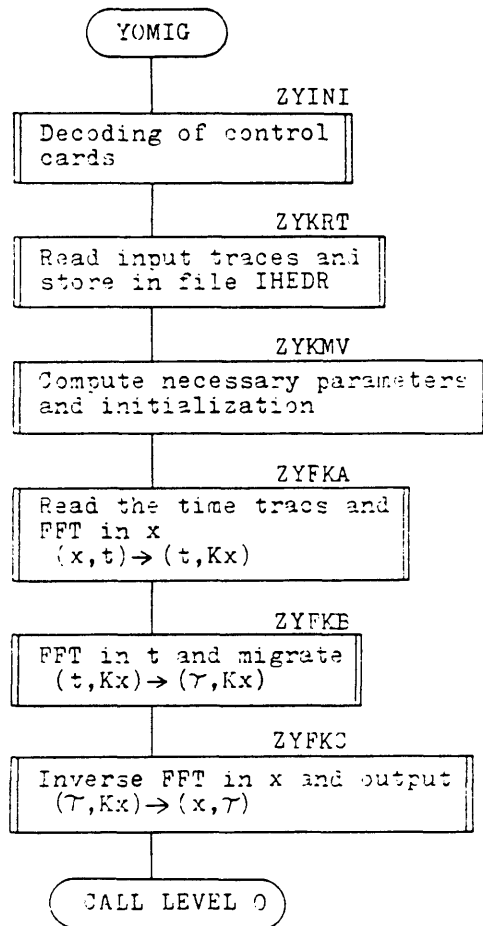


Figure A - 1 : Flow diagram of overlay YOMIG(1,0).

OVERLAY ZYFKA

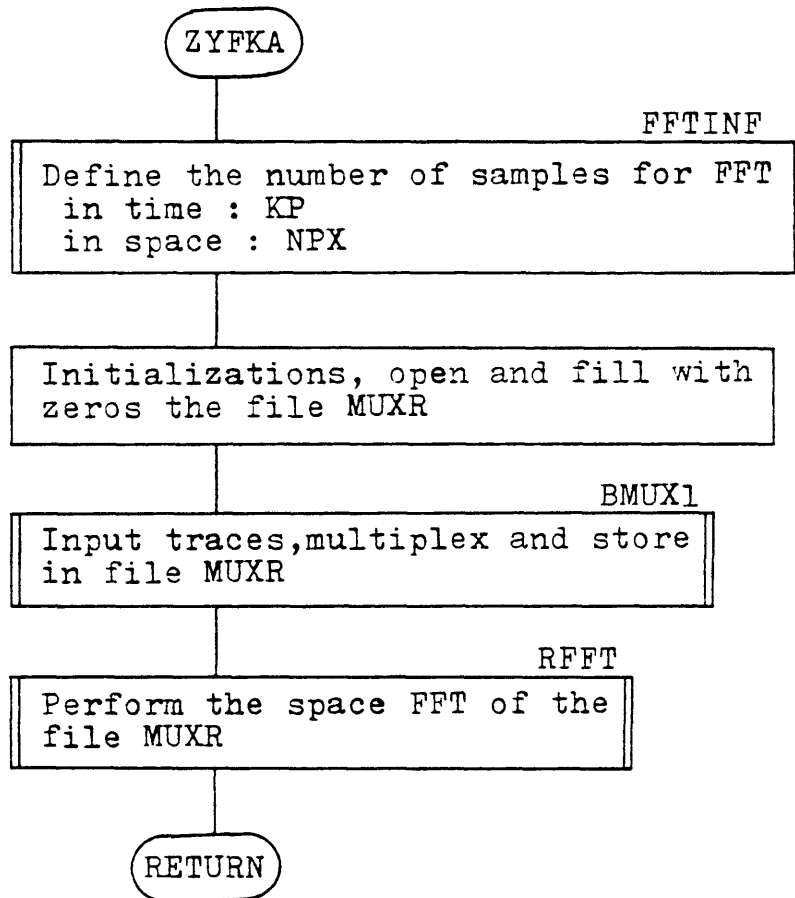


Figure A - 2 : Flow diagram of overlay ZYFKA(1,1).

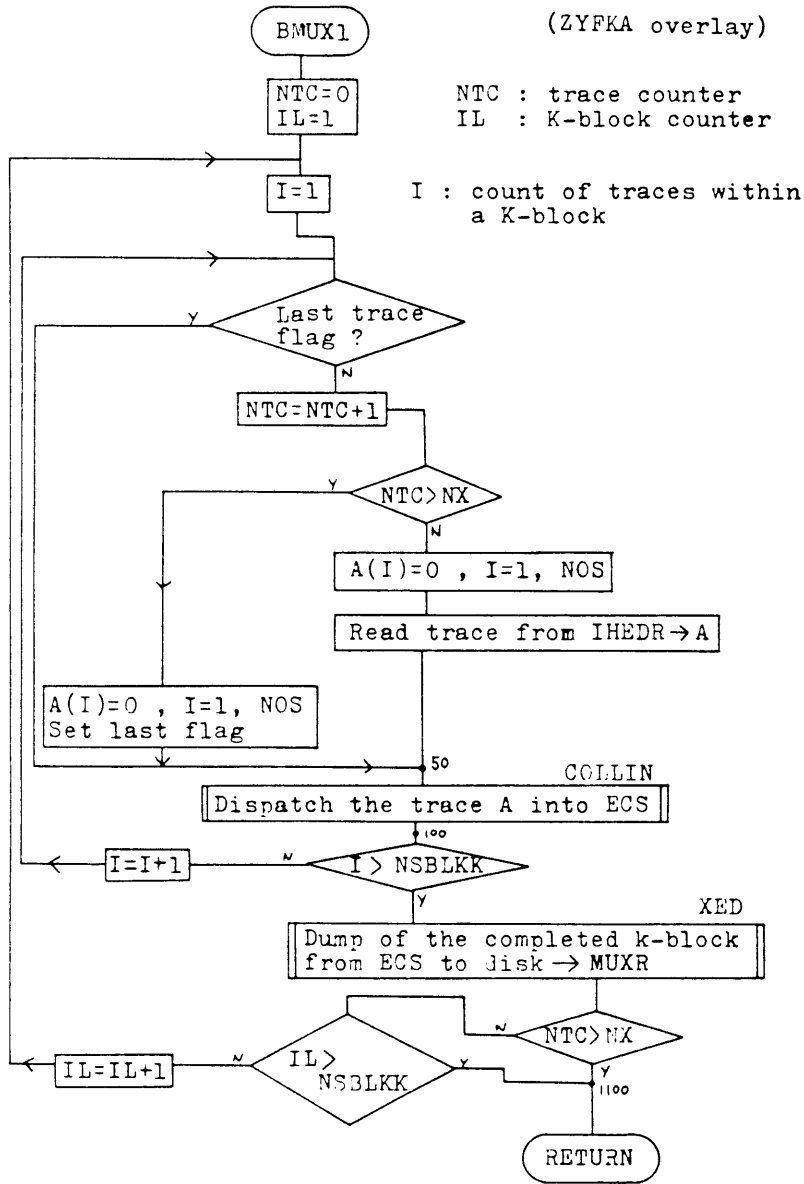


Figure A - 3 : Flow diagram of subroutine BMUX1 in overlay ZYFKA.

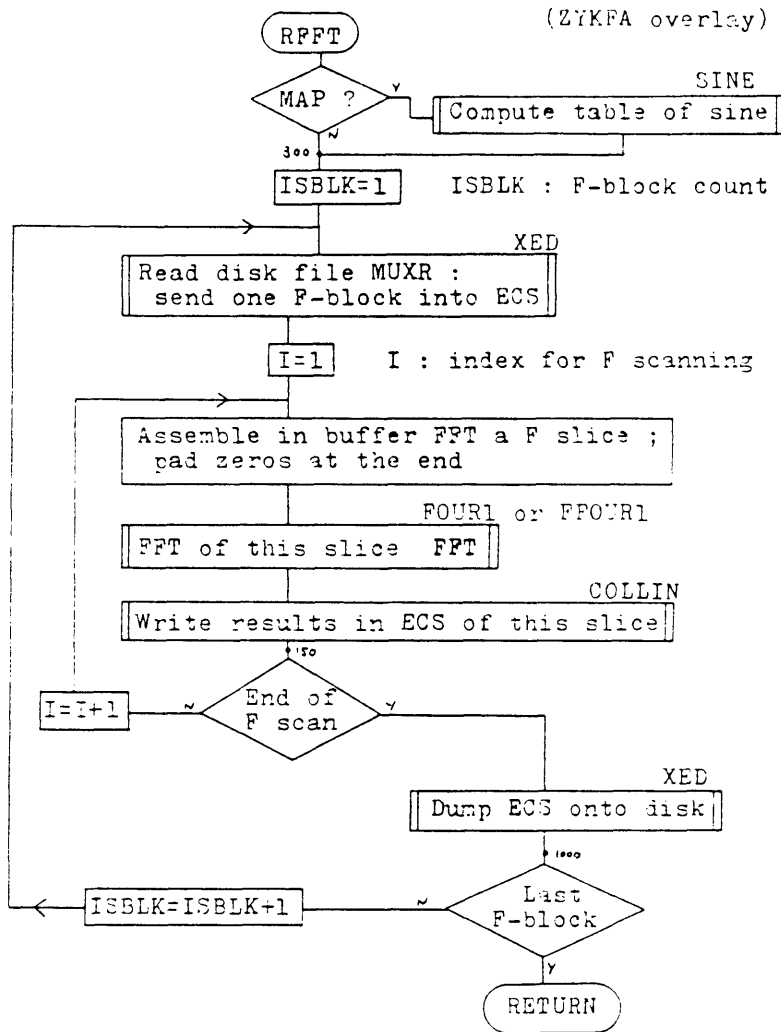


Figure A - 4 : Flow diagram of subroutine RFFT in overlay ZYFKA.

OVERLAY ZYFKB

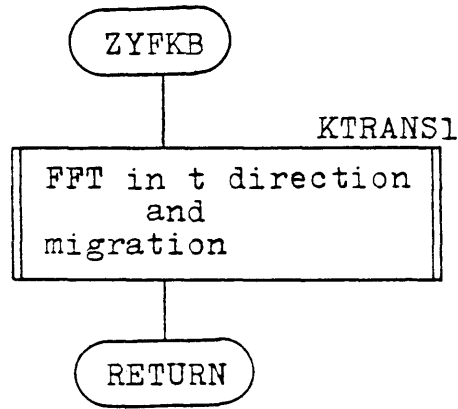


Figure A - 5 : Flow diagram of overlay ZYFKB(1,1).

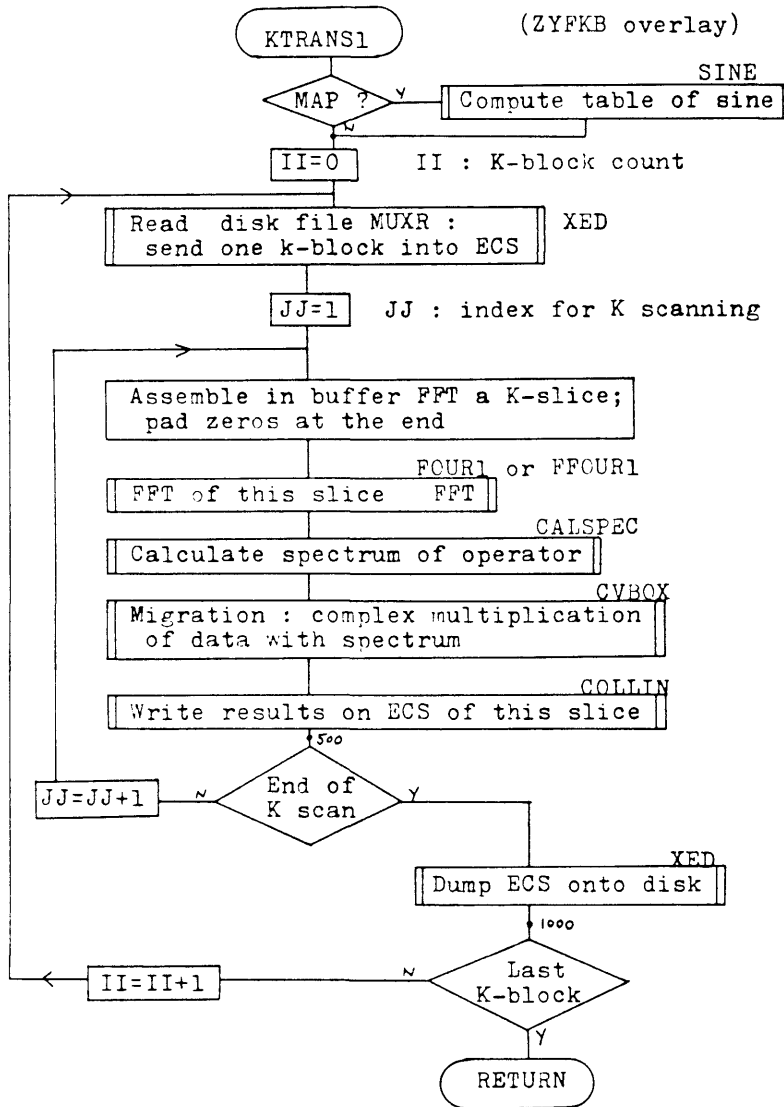


Figure A - 6 : Flow diagram of subroutine KTRANS1 in overlay ZYFKB.

OVERLAY ZYFKC

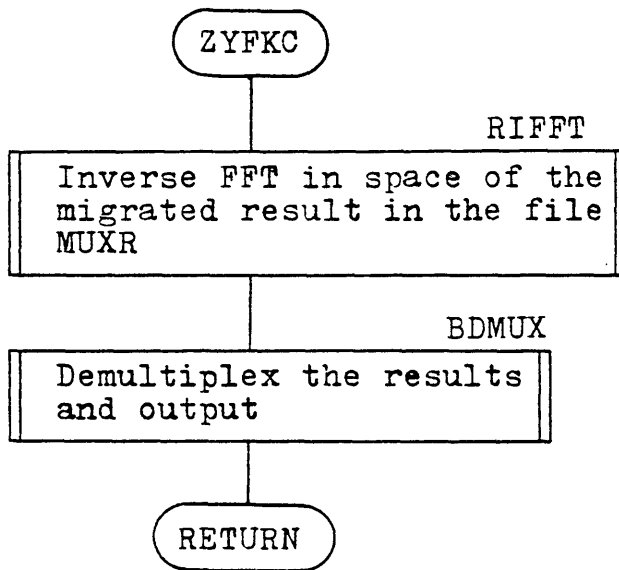


Figure A - 7 : Flow diagram of overlay ZYFKC(1,1).

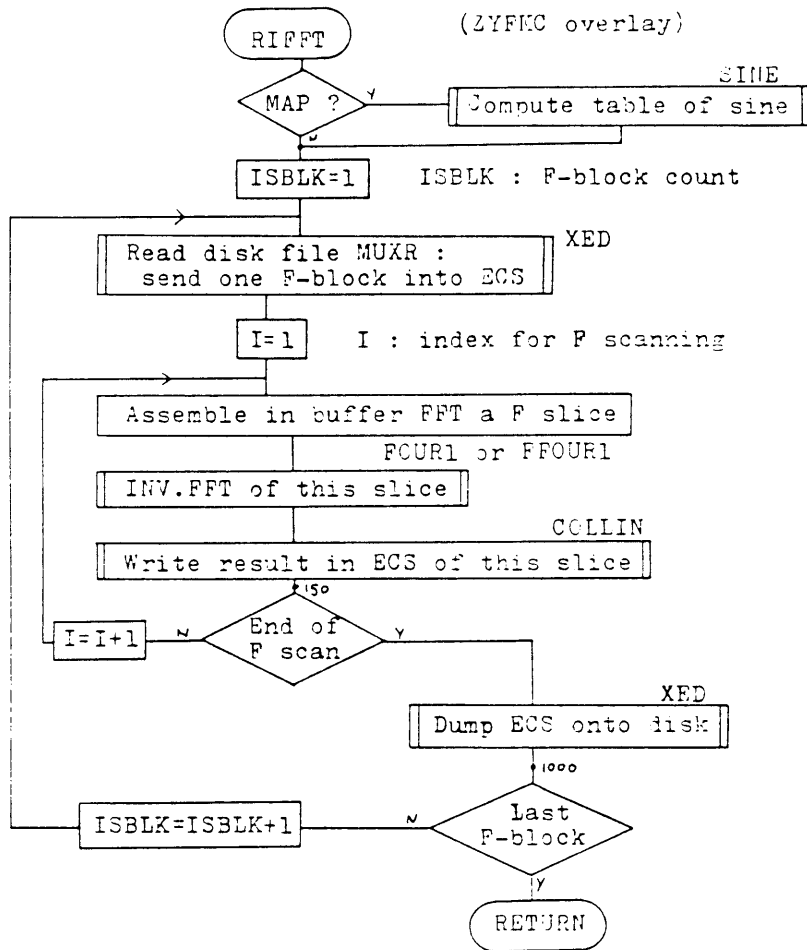


Figure A - 8 : Flow diagram of subroutine RIFFT in overlay ZYFKC.

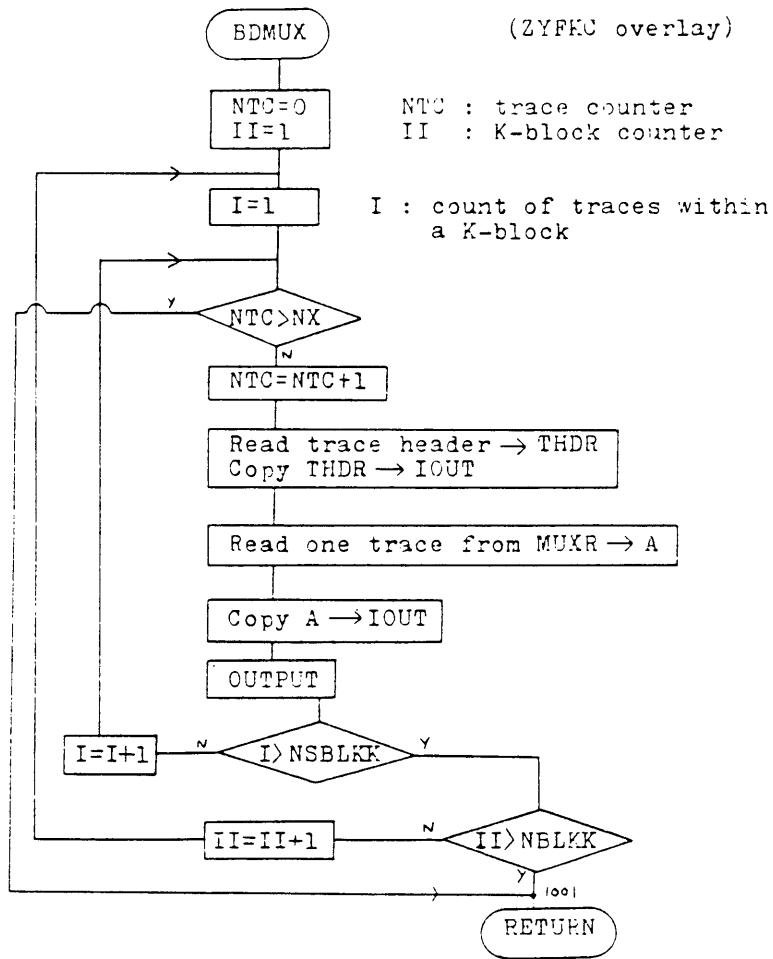


Figure A - 9 : Flow diagram of subroutine BDMUX in overlay ZYFKC.

APPENDIX B

LIST OF THE COMPUTER PROGRAM


```

C      SUBROUTINE YOMIG1(NCO,NDA,LDA,NIN,LIN,NOU,LOU,
*      *A,LAA,IOUT,LOUT,ICM,LCM,ICMN,LCMN,IECS,LECS,
*      *KSCS,LSCS,KSS,LSS)
C
C      DIMENSION NCO(1),NDA(1),NOU(1),A(1),IOUT(1),ICM(1)
C      DIMENSION ICMN(1),NIN(1)
C
C      COMMON/COMM/ISZCOM,NOS,NSI,NX,NGI,IHEDR,MUXR,FMAX,
*      *NTN,NSBLKF,NBLKF,NSBLKK,NBLKK,NPX,KP,MNPAD,ISTFLAG,
*      *NOTIME,NMTIME,NOSMIG,THICK(31),DELZ(31),LEVC,
*      *DTIME(31),NITER(31),VI(31),NOL
C
C      -----
C
C      IMV=20008
C
C      DO 1000 I=1,LCM
1000  ICM(I)=0
C
C      DO 1001 I=1,LCMN
1001  ICMN(I)=0
C
C      DO 1002 I=1,2000
1002  A(I)=0
      CALL WRITEC(A,IECS,2000)
C
C      INITIALIZE AND DECORING OF CARD
C      CALL CHARGOV(5LZYINI,IMV,0)
C
C      READ TRACES
C      CALL CHARGOV(5LZYKRT,IMV,0)
C
C      CALL CHARGOV(5LZYKRV,IMV,0)
C      IF(ISTFLAG.EQ.1) GO TO 2000
C
C      CALL CHARGOV(5LZYFKA,IMV,0)
C
C      CALL CHARGOV(5LZYFKB,IMV,0)
C
C      CALL CHARGOV(5LZYFKC,IMV,0)
C
C
C      2000 RETURN
      END

```

```
C
C *****
C
C      SUBROUTINE PCLR(C,IC,N,FLAG)
C
C      ZERO AN ARRAY
C
C      C - INPUT ARRAY TO BE ZEROED.
C      IC - INCREMENT OF ARRAY * 2
C      N - NUMBER OF POINTS IN C
C      FLAG - UNUSED.
C
C      DIMENSION C(N)
150  CONTINUE
      J=IC/2
      JJ=1
      DO 120 L=1,N
      C(JJ)=C.
      JJ=JJ+J
120  CONTINUE
      RETURN
      ENTRY PCLRW
      GO TO 150
      ENTRY PAAIT
      RETURN
      END
C
C
```



```

      SUBROUTINE FFTINF(NSAMPS,NSR,NPAIRS,DF)
C
C   OBTAIN INFORMATION CONCERNING FFT
C
C   INPUT
C     NSAMPS - NUMBER OF POINTS TO BE FFT.
              (DCES NOT HAS TO BE MULTIPLE OF 2,
              ROUTINE AUTOMATICALLY FINDS NPAIRS WHICH
              IS MULTIPLE OF 2)
C     NSR - SAMPLING INTERVAL IN MSEC.
C   OUTPUT
C     NPAIRS - NUMBER OF PAIRS FOR FFT/2
C     DF - INCREMENT IN FREQUENCY DOMAIN.
C
      N=NSAMPS
      DO 1 I=1,15
      N=N/2
      IF(N.LE.1) GO TO 2
1     CONTINUE
2     NP=2**I
      IF(NP.LT.NSAMPS) I=I+1
      NPAIRS=(2**I)/2
C
      P=FLOAT(NPAIRS)
      SR=FLOAT(NSR)/1000.
      DF=0.5/(SR*P)
      RETURN
      END

```

```

C
C
C      SUBROUTINE LOWER(KSC,NOS,LEVC)
C
C      BIT SHIFT
C      SET MAX. BETWEEN 2**24 AND 2**23
C      KSC CONTAINS NOS + 64 HEADER WORD FOR EACH TRACE.
C      ROUTINE PUTS BIT SHIFT IN 13TH WORD ,AND
C      MAXIMUM NUMBER IN 14TH WORD OF KSC.
C
C      KSC - INPUT AND OUTPUT ARRAY.
C      NOS - NUMBER OF DATA POINTS.
C      LEVC - NUMBER OF BIT SHIFT TO BE APPLIED.
C
C      DIMENSION KSC(1)
C      LT=NOS+64
C      BIG=FLOAT(KSC(14))
C      RMAX=2.**24
C      RMIN=2.**23
C      LL=0
1     CONTINUE
      IF(BIG.LT.RMAX) GO TO 3
      LL=LL+1
      BIG=BIG/2.
      GO TO 1
3     CONTINUE
      IF(BIG.GT.RMIN) GO TO 5
      LL=LL-1
      BIG=BIG*2.
      GO TO 3
5     CONTINUE
      KSC(13)=KSC(13)+LL+LEVC
      KSC(14)=INT(FLOAT(KSC(14))/(2.**LL))
      DO 10 KK=65,LT
      KSC(KK)=INT(FLOAT(KSC(KK))/(2.**LL))
10    CONTINUE
      RETURN
      END

```

C
C
COVERLAY(ZYINI,1,1,C2000)
PROGRAM ZYINI
EXTERNAL ZYINI1C
C
C
C
C

OVERLAY ZYINI

DECODING OF CONTROL CARD.

CALL START (ZYINI1)
CALL LEVEL1
END

```

C      SUBROUTINE ZYINI1(NCO,NOA,LDA,NIN,LIN,NOU,LOU,A,LAA,
C      *IGOUT,LOUT,ICM,LCM,ICMN,LCMN,IECS,LECS,KSCS,LSCS,
C      *KSS,LSS)
C
C      DIMENSION NCO(1),NDA(1),NOU(1),A(1),IGOUT(1),ICM(1)
C      DIMENSION NIN(1),ICMN(1)
C
C      DIMENSION TABLE(17)
C
C      EQUIVALENCE(NUM,FNUM)
C
C      COMMON/COMM/ISZCOM,NOS,NSI,NX,NGI,IHEDR,MUXR,FMAX,
C      *NTN,NSBLKF,NBLKF,NSBLKK,NBLKK,NPX,KP,MNPAG,ISTFLAG,
C      *NOTIME,NMTIME,NOSMIG,THICK(31),DELZ(31),LEVC,
C      *DIME(31),NITER(31),VI(31),NOL
C
C      DATA(TABLE(I),I=1,17)/3RNT1,3RSI1,2RE1,3RRL1,
C      *4RRLM1,4RECS1,2RB1,5RMV=T1,3RVI1,1R,,2RT1,3RVF1,
C      *6RMNPAD1,5RFMAX1,5RLEVC1,5RZYKMV,5RNQMAP/
C
C      ICM(15)=KSCS+100
C      ICM(1)=118000
C      ICM(32)=0
C      KODE=0
C      NBS=17
C      NC=31
C      IV=50
C      ITM=80
C      INPS=C
C      ISTFLAG=0
C
C      DECODE CONTROL CARD
C
C      2000 CALL CARDIN(TABLE,NBS,NOA,LDA,NC,NUM,KODE)
C      GO TO (1,2,3,4,5,6,7,8,9,2000,11,12,13,14,
C      *15,16,17,2001,9888) ,KODE
C
C      NT
C      1      NX=NUM
C      ICM(13)=NUM
C      GO TO 2000
C
C      SI
C      2      NSI=NUM
C      ICM(2)=NUM
C      GO TO 2000
C
C      E
C      3      NGI=NUM*100
C      ICM(8)=NUM
C      GO TO 2000
C
C      RL
C      4      NOTIME=NUM
C      GO TO 2000
C

```

```
C   RLM
C
C   5     NMTIME=NUM
        GO TO 2000
C
C   ECS
C
C   6     ICM(1)=NUM
        IF(ICM(1).LT.45000) ICM(1)=45000
        GO TO 2000
C
C   POST LOOP B
C
C   7     ICM(50)=NUM
        GO TO 2000
C
C   MV=T
C
C   8     INPS=INPS+1
        ITM=ITM+1
        ICM(48)=INPS
        ICM(ITM)=NUM
        KT=1
        GO TO 2000
C
C   VI
C
C   9     IV=IV+1
        ICM(IV)=NUM*100
        KT=KT-1
        GO TO 2000
C
C   T
C
C  11     INPS=INPS+1
        IF(KT.EQ.1) GO TO 1007
        KT=1
        IF(INPS.GT.30) GO TO 1008
        ITM=ITM+1
        ICM(48)=INPS
        ICM(ITM)=NUM
        IF(ICM(ITM).LE.ICM(ITM-1)) GO TO 1009
        GO TO 2000
        ICM(ITM)=NUM
        GO TO 2000
C
C   VF
C
C  12     ICM(111)=NUM*100
        GO TO 2000
C
C   MNPAD
C
C  13     MNPAD=NUM
        GO TO 2000
C
C   FMAX
C
C  14     FMAX=FLOAT(NUM)
        GO TO 2000
C
C   LEVC
C
C  15     LEVC=NUM
```

```

      GO TO 2000
C
C   ZYKMY
C
16   ISTFLAG=1
      GO TO 2000
C
C   NOMAP
C
17   ICM(32)=3
      GO TO 2000
C
C
2001 CONTINUE
      IF(LLECS.GE.ICM(1)) GO TO 3000
      LLECS=ICM(1)
      CALL MODIF(1,7,LLECS,1)
3000 CONTINUE
C
C
      IF(MNPAD.EQ.0) GO TO 4000
      IF(NX.EQ.0) GO TO 1004
      IF(FMAX.EQ.0.0) GO TO 1005
      IF(NX.GT.350) GO TO 1010
      IF(NX+MNPAD.GT.512) GO TO 1011
C
C   IF(NGI.EQ.0) GO TO 1002
      IF(NOTIME.EQ.0) GO TO 1003
      IF(NSI.EQ.0) GO TO 2002
      NOS=NOTIME/NSI
      NOSMIG=NOS
      IF(NMTIME.EQ.0) GO TO 1500
      NOSMIG=NMTIME/NSI
      GO TO 1501
1500 NMTIME=NOTIME
1501 CONTINUE
      FNY=1000./(2.*FLOAT(NSI))
      IF(FMAX.GT.FNY) GO TO 1006
2002 CONTINUE
C
C
C
      GO TO 9999
C
4000 CALL REMARK(16H** YOMIG ERR. **)
      CALL REMARK(29H = MNPAD MUST BE SPECIFIED =)
      GO TO 9889
1001 CALL REMARK(16H** YOMIG ERR. **)
      CALL REMARK(27H = NSI MUST BE SPECIFIED =)
      GO TO 9889
1002 CALL REMARK(16H** YOMIG ERR. **)
      CALL REMARK(27H = NGI MUST BE SPECIFIED =)
      GO TO 9889
1003 CALL REMARK(16H** YOMIG ERR. **)
      CALL REMARK(26H = RL MUST BE SPECIFIED =)
      GO TO 9889
1004 CALL REMARK(16H** YOMIG ERR. **)
      CALL REMARK(26H = NT MUST BE SPECIFIED =)
      GO TO 9889
1005 CALL REMARK(16H** YOMIG ERR. **)
      CALL REMARK(23H = FMAX MUST BE SPECIFIED =)
      GO TO 9889
1006 CALL REMARK(16H** YOMIG ERR. **)

```

```
CALL REMARK(20H = FMAX .GT. FNYG =)
GO TO 9889
1007 CALL REMARK(16H** YOMIG ERR. **)
CALL REMARK(22H = VI MUST FOLLOW T =)
GO TO 9889
1008 CALL REMARK(16H** YOMIG ERR. **)
CALL REMARK(21H = NO. PAIRS GT 10 =)
GO TO 9889
1009 CALL REMARK(16H** YOMIG ERR. **)
CALL REMARK(26H = T MUST BE INCREASING =)
GO TO 9889
1010 CALL REMARK(16H** YOMIG ERR. **)
CALL REMARK(17H = NX .GT. 350 =)
GO TO 9889
1011 CALL REMARK(16H** YOMIG ERR. **)
CALL REMARK(23H = NX+MNPAD .GT. 512 =)
GO TO 9889
9990 CALL REMARK(16H** YOMIG ERR. **)
CALL REMARK(23H** VI MUST BE SPECIFIED)
GO TO 9889
C
9888 CONTINUE
CALL REMARK(28H** YOMIG ERR. = ILLIGAL CARD)
9889 NCO(1)=NCO(1).DR.1L5
CALL LEVLO
9999 CONTINUE
C
C
RETURN
END
```

```
C
C      OVERLAY(ZYKRT,1,1,C2000)
      PROGRAM ZYKRT
      EXTERNAL ZYKRT1
C
C      OVERLAY ZYKRT
C
C      READ INPUT TRACES INTO FILE IHEDR
C
      CALL START (ZYKRT1)
      CALL LEVEL 1
      END
```



```

C
* SUBROUTINE ZYKRT1(NCO,NDA,LDA,NIN,LIN,NOU,LOU,
*   A,LAA,IOUT,LOUT,
*   ICM,LCM,ICMN,LCMN,
*   IECS,LECS,KSCS,LSCS,
*   KSS,LSS)
C
* DIMENSION NCO(1),NDA(1),NIN(1),NOU(1),
*   A(1),IOUT(1),ICM(1),ICMN(1)
C
COMMON/CCMM/ISZCOM,NOS,NSI,NX,NGI,IHEOR,MUXR,FMAX,
*NTN,NSBLKF,NBLKF,NSBLKK,NBLKK,NPX,KP,MNPAD,ISTFLAG,
*NOTIME,NMTIME,NOSMIG,THICK(31),DELZ(31),LEVC,
*DTIME(31),NITER(31),VI(31),NOL
C
C INITIALIZE DISK FILR IHEOR
C READ TRACES FROM DISK BUFFER AND
C STORE IN IHEOR
C
IF(NOTIME.EQ.0.OR.NSI.EQ.0.OR.NGI.EQ.0) GO TO 90
JIPUT=1
GO TO 100
C
90 CONTINUE
JIPUT=2
CALL RTRACE(1,1,IOUT)
CALL PRETE(1,1)
C
IF(NSI.EQ.0) NSI=IOUT(9)
IF(NGI.EQ.0) NGI=(IOUT(15).AND.000000000000001777778)
* *50
IF(NOTIME.EQ.0) NOTIME=IOUT(10)
NOS=NOTIME/NSI
NOSMIG=NOS
IF(NMTIME.EQ.0) GO TO 210
NOSMIG=NMTIME/NSI
GO TO 110
210 NMTIME=NOTIME
110 CONTINUE
FNY=1000./(2.*FLOAT(NSI))
IF(FMAX.GT.FNY) GO TO 1006
GO TO 100
1006 CALL REMARK(16H** YDMIG ERR. **)
CALL REMARK(20H = FMAX .GT. FNYQ =)
NCO(1)=NCO(1).OR.1L5
CALL LEVELO
100 CONTINUE
C
LONG=NOS+64
INOM=5LIHEOR
DO 1700 I=1, LONG
A(I)=0.
1700 CONTINUE
C
L=1
LL=16
NG=1
NSGR=NX
NSG=NSGR+1
KED=ICM(15)
ICM(15)=ICM(15)+NSG
CALL CREFICH(INOM,ICMN(L),LL,KED,NSG,1,NSGR)
CALL CREGR(INOM,1, LONG)

```

```

DO 1701 I=1,NSGR
CALL WRFICH(INOM,1,I,A,LONG,0)
CALL ATTEENTE(INOM)
1701 CONTINUE
C
C IF(JIPUT.EQ.1) GO TO 300
C
NAL=IOUT(13)
DO 1801 J=1,64
A(J)=FLOAT(IOUT(J))
1801 CONTINUE
IF(IOUT(11).EQ.7) GO TO 1850
MOTON=IOUT(11)
IOUT(11)=7
IOUT(13)=0
NAL=IOUT(13)
DO 1851 J=1,NOS
IOUT(64+J)=0
1851 CONTINUE
DO 1849 J=1,64
A(J)=FLOAT(IOUT(J))
1849 CONTINUE
IOUT(11)=0
C
1850 CONTINUE
DO 1852 J=1,NOS
A(64+J)=IOUT(64+J)*(2.**NAL)
1852 CONTINUE
CALL SUPRSGR(INOM,1,1)
CALL WRFICH(INOM,1,1,A,LONG,0)
CALL ATTEENTE(INOM)
C
300 CONTINUE
DO 1900 I=JIPUT,NX
CALL RTRACE(1,I,IOUT)
CALL PRETE(1,I)
NAL=IOUT(13)
DO 1901 J=1,64
A(J)=FLOAT(IOUT(J))
1901 CONTINUE
IF(IOUT(11).EQ.7) GO TO 1950
MOTON=IOUT(11)
IOUT(11)=7
IOUT(13)=0
NAL=IOUT(13)
DO 1951 J=1,NOS
IOUT(64+J)=0
1951 CONTINUE
DO 1949 J=1,64
A(J)=FLOAT(IOUT(J))
1949 CONTINUE
IOUT(11)=0
C
1950 CONTINUE
DO 1952 J=1,NOS
A(64+J)=IOUT(64+J)*(2.**NAL)
1952 CONTINUE
CALL SUPRSGR(INOM,1,I)
CALL WRFICH(INOM,1,I,A,LONG,0)
CALL ATTEENTE(INOM)
1900 CONTINUE
RETURN
END

```

```
C
C      OVERLAY(ZYKMOV,1,1,C2C00)
      PROGRAM ZYKMOV
      EXTERNAL ZYKMIV1
C
C      OVERLAY ZYKMOV
C
C      INITIALIZATION AND CALCULATION
C      OF NECESSARY PARAMETERS.
C
      CALL START 1 (ZYKMIV1)
      CALL LEVEL 1
      END
```

```
C      SUBROUTINE ZYKMIV1(NCO,NDA,LDA,NIN,LIN,NOU,LOU,  
*      A,LAA,IOUT,LOUT,  
*      ICM,LCM,ICMN,LCMN,  
*      IECS,LECS,KSCS,LSCS,  
*      KSS,LSS,NSCA,NSCB)  
*      DIMENSION NCO(1),NDA(1),NOU(1),A(1),NIN(1),  
*      IOUT(1),ICM(1),ICMN(1)  
C  
C      DIMENSION NSCA(1)  
C  
C      KA=13000  
C      CALL RFLCM(KA)  
C      CALL ZYKMV2(NSCA(1),NSCA(101),A,IECS,ICM,ICMN,NCO)  
C      CALL REDUCE(2)  
C      RETURN  
C      END
```

```

C
C
C      SUBROUTINE ZYKMOV2(A,B,C,IECS,ICM,ICMN,NCO)
C
C      THIS SUBROUTINE INITIALIZE PARAMETERS
C      FIND DELZ,OTIME,NITER, ETC ...
C
C      DIMENSION NCO(1),A(1),B(1),C(1),ICM(1),ICMN(1)
C
C      COMMON/COMM/ISZCOM,NOS,NSI,NX,NGI,IHEDR,MUXR,FMAX,
C      *NTN,NSBLKF,NBLKF,NSBLKK,NBLKK,NPX,KP,MNPAD,ISTFLAG,
C      *NOTIME,NMTIME,NOSMIG,THICK(31),DELZ(31),LEVC,
C      *DTIME(31),NITER(31),VI(31),NOL
C
C      FOR COMMON /COMM/
C
C      ISZCOM      SIZE OF THIS COMMON
C      NOS        NUMBER OF SAMPLES
C      NSI        SAMPLING INTERVAL(MSEC)
C      NX         NO. OF TRACES TO PROCESS
C      NGI        CDP INTERVAL *100
C      IHEDR      LOGICAL NO. FOR FILE IHEDR
C      MUXR       LOGICAL NO. FOR FILE MUXR
C      FMAX       MAX. FREQ. TO MIGRATE
C      NTN        NO. OF PTS IN F UP TO FMAX
C      NSBLKF     NO. OF PTS IN ONE F BLOCK
C      NBLKF     NO. OF BLOCKS IN F
C      NSBLKK    NO. OF PTS IN ONE K BLOCK
C      NBLKK     NO. OF BLOCKS IN K
C      NPX        NO. OF PTS IN K FOR FFT /2
C      KP         NO. OF PTS IN F FOR FFT
C      MNPAD     NO. OF ZERO TRACSE TO PAD FOR FFT
C      ISTFLAG   FLAG FOR ZYKMOV , 1 FOR STOP
C                0 FOR NO-STOP
C
C      NOTIME    INPUT RECORD LENGTH
C      NMTIME    MAX. TIME TO MIGRATE
C      NOSMIG    NO. OF PTS FOR NMTIME
C      THICK     THICKNESS FOR EACH LAYER
C      DELZ      Z INCREMENTS FOR EACH LAYER
C      LEVC      NO. OF BIT SHIFT WHICH CAN
C                INCREASED OR DECREASED
C      OTIME     DEL TIME FOR EACH LAYER
C      NITER     NO. OF ITERATION WITHIN LAYER
C      VI        INTERVAL VEL. FOR EACH LAYER
C      NOL       NO. OF LAYER
C
C
C      IHEDR=5
C      MUXR=1
C      NPAIR=ICM(48)
C      IV=50
C      ITM=80
C      VI(1)=FLOAT(ICM(51))/100
C      THICK(1)=(FLOAT(ICM(81)*ICM(51))/100000)/2
C      IF(NPAIR.EQ.1) GO TO 6
C
C      DO 5 I=2,NPAIR
C      VI(I)=FLOAT(ICM(IV+I))/100
C      THICK(I)=(FLOAT((ICM(IV+I)*(ICM(ITM+I)-ICM(ITM+I-1)
C      *))))/100000)/2
C
C      5 CONTINUE
C      6 CONTINUE

```

```

VI(NPAIR+1)=FLOAT(ICM(111))/100
KTIME=NMTIME-ICM(ITM+NPAIR)
THICK(NPAIR+1)=(FLOAT(KTIME*ICM(111))/100000)/2
C
C
NOL=NPAIR+1
SIM=FLOAT(NSI)/1000
C
C SET UP NUMBER OF ITERATION AT DESIRED
C SAMPLING INTERVAL
C
DO 10 I=1,NOL
TTEST=THICK(I)/VI(I)
IF(TTEST.LT.SIM/2) GO TO 500
CONTINUE
GO TO 12
10
C
500 CALL REMARK(16H** YOMIG ERR. **)
CALL REMARK(17H* DELZ .LT. SIM *)
NCO(1)=NCO(1).CR.1L5
CALL LEVELO
C
12 CONTINUE
DDTIME=C.
DO 15 I=1,NOL
TIMEINT=THICK(I)/VI(I)-DDTIME
DELZ(I)=SIM*VI(I)/2
NITER(I)=INT(TIMEINT*2/SIM)+2
17 DDT=SIM*NITER(I)/2
ADDT=ABS(DDT-TIMEINT)
IF(ADDT.LE.SIM/100) GO TO 20
IF(DDT.LT.TIMEINT) GO TO 22
NITER(I)=NITER(I)-1
GO TO 17
22 DF1=TIMEINT-DDT
IF(DF1.GF.SIM/2) GO TO 24
DTIME(I)=DF1
DDTIME=SIM/2-DF1
GO TO 15
24 NITER(I)=NITER(I)+1
GO TO 17
20 DDTIME=C.0
DTIME(I)=0.0
15 CONTINUE
C
CALL LOCK
PRINT 1070,FMAX
1070 FORMAT(/,2X,*MAX. FREQ. TO MIGRATE =*,F10.2,/)
PRINT 1071
1071 FORMAT(/,4X,*THICK*,5X,*VI*,4X,*NITER*,4X,*DELZ*,
*4X,*DDTIME*,/)
DO 7 I=1,NOL
PRINT 1072, THICK(I),VI(I),NITER(I),DELZ(I),DTIME(I)
1072 FORMAT(3X,F7.2,2X,F7.0,3X,I3,4X,F5.2,3X,F8.6)
7 CONTINUE
CALL DELCK
C
C
CALL RELEASE
RETURN
END

```

```
C
C      OVERLAY (ZYFKA,1,1,C2000)
      PROGRAM ZYFKA
      EXTERNAL ZKMIA21
C
C      OVERLAY ZYFKA
C
C      BMUX1 - MULTIPLEX OF DATA TO FILE MUXR
C      RFFT - FFT IN X - DIRECTION
C
      CALL START (ZKMIA21)
      CALL LEVEL1
      END
```



```

C      IF(NSBLKF.GT.KPP) NSBLKF=KPP
C      IF(NSBLKK.GT.NPXX) NSBLKK=NPXX
C      GET NO BLOCKS IN F --- NBLKF
15     CONTINUE
C      NBLKF=KPP/NSBLKF
C      IF(NBLKF*NSBLKF.LT.KPP) NBLKF=NBLKF+1
C      MAKE NSBLKK EVEN FOR FMIG3
C      NSBLKK=NSBLKK/2*2
C      GET NO BLOCKS IN K --- NBLKK
20     CONTINUE
C      NBLKK=NPXX/NSBLKK
C      IF(NBLKK*NSBLKK.LT.NPXX) NBLKK=NBLKK+1
C
C      IC=NBLKK*NSBLKK*NSBLKF
C      IF(IC.LE.ICSIZE) GO TO 30
C      NSBLKF=NSBLKF-8
C      IF(NSBLKF.GT.0) GO TO 15
C      JFLAG=10
C      GO TO 81
C      IF(NSBLKF.LE.0) GO TO 16
C      GO TO 15
16     CALL REMARK (17H** YOMIG ERROR **)
C      CALL REMARK(33H= NO OF SAMPS/BLOCK TOO SMALL =)
C      NCO(1)=NCO(1).OR.1L5
C      CALL LEVELO
30     CONTINUE
C
C      TOTAL NUMBER OF BLOCKS
C      GET LARGER NO SAMPS TOTAL K OR F SLICE
C      IC=NBLKK*NSBLKK*NSBLKF
C      IB=NBLKF*NSBLKK*NSBLKF
C      IF(IC.GT.IB) IB=IC
C
C      FIND NO 16 BIT WORD PER DISK DUMP
C
C      NSPDMP=NSBLKK*NSBLKF
C      Z=NBLKF
C      ZZ=NBLKK+2
C      ZZ=Z*ZZ
C
C      CHECK CORE
C      NCCORE=IA+IB
C      IF(NCCORE.LE.ICOR) GO TO 40
C      NSBLKK=NSBLKK-2
C      GO TO 20
40     CONTINUE
C
C      INITIALIZE DISK FILE
C
C      DO 2000 I=1,LAA
2000    A(I)=0.
C
C      MUXR FILE
C
C      KKLmux=NSPDMP+100
C      CALL RFLCM(KKLmux)
C      DO 2005 I=1,NSPDMP
2005    NSCA(I)=0
C      INCM=4LMUXR

```

```

LL=69
ICMN(LL-1)=LOCF(ICMN)
L=16
NSGR=ZZ
NSG=ZZ+1
KEDS=ICM(15)
LONG=NSPOMP
CALL WRITEC(NSCA,IECS+2000,LONG)
CALL REDUCE(2)
CALL XEDOPEN(INOM,LONG,ICMN(105),KSS,ISTAT)

DO 2001 I=1,NSGR
CALL XEDWRIT(ICMN(105),IECS+2000,I,I,G,ISTAT)
CALL XEDWAIT(ICMN(105),ISTAT)
2001 CONTINUE
C
C      COMPUTE ARRAY INDEXES
C
LTC=1
C
ITHDR=1+LTC+NX
C
IXD=ITHDR+64
C
IDEP=IXD+NOS+22
C
IWORK=IDEP
C
C      MUX - DMUX ARRAY
C
MPX=IWORK+NOS+65
C
C
C      START OF F SLICE FFT ARRAY
C
IFFT=1
C      MUX ARRAY WHEN DOING F SLICE FFT
MPX2=IFFT+NPXX+NPXX+1
C
C
C      DO BIG MULTIPLEX
C
KA=MPX+500
IF(KA.LT.(MPX2+500)) KA=MPX2+500
CALL RFLCM(KA)
CALL BMUX1(NSCA(ITHDR),NSCA(IXD),NSCA(MPX),A,
*NSCA(LTC),ICM,IOUT,LOUT,IECS,ICMN,KSCS)
C
C      DO F SLICE FFT,S
C
CALL RELEASE
CALL RFFT(NSCA(IFFT),NSCA(MPX2),NSBLKF,NBLKF,
*NSBLKK,NBLKK,NPX,NX,NOS,IECS,NSCA,ICMN,ICM)
CALL REDUCE(2)
C
CALL RELEASE
RETURN
END

```



```
C
C      NBLKF TOTAL BLOCK F
      INQM=4LMUXR
      IADSS=IADS+MXJ
      CALL COLLIN(1,A(MX),NSBLKF,IADS+MXJ,NSBFK,NBLKF,
+NSBLKF)
      GO TO 100
C      END OF INPUTS,COME HERE
5000  CONTINUE
      CALL PCLR*(A,2,NOS,15)
      ILAST=1
      GO TO 50

C
C 100  CONTINUE
C
C      CORE FULL  NOW DUMP TO DISK
C
      MXX=1
      NMB2=NMB+NBLKF-1
      CALL XEDWRIT(ICMN(105),IADS+MXX,NMB,NMB2,0,ISTAT)
      CALL XEDWAIT(ICMN(105),ISTAT)
      NMB=NMB+NBLKF

C
C      IF(NTC.GT.NX) GO TO 1100
C
C 1000 CONTINUE
1100  CONTINUE
      RETURN
      END
```

```
C
C
C      FUNCTION NPFMAX(FMAX,NSI,KP)
C      FIND NO OF POINT FOR FMAX
C      FMAX - MAXIMUM FREQUENCY OF INTEREST.
C      NSI - SAMPLING INTERVAL IN MSEC.
C      KP - NUMBER OF POINTS IN FREQUENCY DOMAIN.
C
C      DF=1000./((FLOAT(NSI)*FLOAT(KP))
C      IPOINT=0
C      DDF=0.
C      DO 100 I=1,10000
C      IF(DDF.GT.FMAX) GO TO 200
C      DDF=DDF+DF
C      IPOINT=IPOINT+1
100  CONTINUE
200  CONTINUE
      NPFMAX=IPOINT+1
      RETURN
      END
```

```

C
C
C *****
C
C
C $TITLE -RFFT
C $NAME -RFFT
C $ABSTRACT -TO PERFORM FIRST PART OF THE
C $ -TWO DIMENSIONAL TRANSFORM
C $SAMPLE CALL -CALL RFFT(FFT,A,NSBLKF,NBLKF,
C $ -NSBLKK,NBLKK,NPX,NX,NOS)
C $CALLING PARAMETER
C $ -FFT -FFT ARRAY
C $ -A -ARRAY TO HOLD MPLX. DATA
C $ -NSBLKF -SAMPLES/BLOCK F
C $ -NBLKF -BLOCKS OF F
C $ -NSBLKK -SAMPLES/BLOCK K
C $ -NBLKK -BLOCKS OF K
C $ -NPX -(NO. OF PAIRS IN F SLICE FFT)/2
C $ -NX -NO. TRACES
C $ -NOS -NO. SAMPLES PER TRACE
C $
C SUBROUTINE RFFT(FFT,A,NSBLKF,NBLKF,NSBLKK,
C *NBLKK,NPX,NX,NOS,IECS,NSCA,ICMN,ICM)
C
C DIMENSION IADSS(2)
C DIMENSION FFT(1),A(1)
C DIMENSION ICMN(1)
C DIMENSION NSCA(1)
C DIMENSION ICM(1)
C
C IADS=IECS+2000
C
C IADSS(1)=((IECS+ICM(1)-(NPX*4+500))/8)*8
C IADSS(2)=IADSS(1)+NPX*2+708
C JOB=1478
C
C IARG=ICM(32)
C
C INOM=4LMUXR
C NSBF2=NSBLKF*2
C N=2*NX+1
C L=4*NPX
C L=L-N
C NPX4=NPX*4
C NSINC=NSBLKK*NSBLKF
C LONG=NSINC
C
C NBLKF NO. BLOCKS/TRACE
C
C IF(IARG.EQ.3) GO TO 300
C NNN=NPX*2
C CALL SINE(FFT,IADSS,NNN)
C NB=NNN
300 CONTINUE
C DO 1000 ISBLK=1,NBLKF
C
C READ UP DATA FOR F SLICE FFT
C MX=1
C IBLK=ISBLK
C DO 10 II=1,NBLKK
C DCNT DO MORE THAN NEEDED
C IB=(II-1)*NSBLKK

```

```

IF(IB.GT.NX) GO TO 20
CALL XEDREAD(ICMN(105),IADS+MX,IBLK,IBLK,0,ISTAT)
CALL XEDWAIT(ICMN(105),ISTAT)
IBLK=IBLK+NBLKF
MX=MX+NSINC
CONTINUE
10
C
C      DO NSBLKF F SLICE FFTS
C      SET LOOP COUNTER SO NOT
C      TO DO MORE THAN NEEDED
20
CONTINUE
NSBF=NSBLKF
IC=NSBLKF*ISBLK
IF(IC.GT.NOS) NSBF=NSBF-(IC-NOS)
C
DO 150 I=1,NSBF
C      GET F SLICE TO FFT
MX=I
CALL COLLIN(2,FFT(1),2,IADS+MX,NSBLKF,NX,1)
C      CLEAR THE TAIL
CALL PCLRW(FFT(2),4,NX,15)
CALL PCLRW(FFT(N),2,L,15)
C      FFT THE TRACE
S=1.0
NNN=NPX*2
IF(IARG.NE.3) GO TO 310
CALL FOUR1(FFT,NNN,1)
GO TO 320
310
320
CALL FFJOUR1(FFT,IADSS,NB,JOB,1)
CONTINUE
C
C      MOVE FFTED F SLICE BACK TO MPLX. ARRAY
CALL COLLIN(1,FFT,1,IADS+MX,NSBLKF,NPX4,1)
C
150
CONTINUE
C
C      WRITE FFTED BLOCKS BACK TO DISK
C      NBLKK NO. BLOCKS TO HOLD F SLICE FFTS
C
C
C      IBLK=ISBLK
C      MX=1
C      DO 200 II=1,NBLKK
C      CALL XEDWRIT(ICMN(105),IADS+MX,IBLK,IBLK,0,ISTAT)
C      CALL XEDWAIT(ICMN(105),ISTAT)
C      IBLK=IBLK+NBLKF
C      MX=MX+NSINC
200
CONTINUE
C
C
1000
CONTINUE
RETURN
END

```

C
C
COVERLAY (ZYFKB,1,1,C2000)
PROGRAM ZYFKB
EXTERNAL ZKMIB21C
C
C
C

OVERLAY ZYFKB

FFT IN T - DIRECTION AND MIGRATE

CALL START (ZKMIB21)
CALL LEVEL1
END


```

C*****
SUBROUTINE ZKMIBZ1(NCO,NDA,LDA,NIN,LIN,NOU,LOU,
*           A,LAA,
*           IOUT,LOUT,
*           ICM,LCM,ICMN,LCMN,
*           IECS,LECS,KSCS,LSCS,
*           KSS,LSS,NSCA,NSCB)
  DIMENSION NCO(1),NDA(1),NOU(1),NIN(1),
*           A(1),
*           IOUT(1),
*           ICM(1),ICMN(1)
  DIMENSION NSCA(1)
  COMMON/COMM/ISZCOM,NOS,NSI,NX,NGI,IHEOR,MUXR,FMAX,
*NTN,NSBLKF,NBLKF,NSBLKK,NBLKK,NPX,KP,MNPAD,ISTFLAG,
*NOTIME,NMTIME,NOSMIG,THICK(31),DELZ(31),LEVCI,
*DTIME(31),NITER(31),VI(31),NOL
* $
* $ ABSTRACT          -TO DO LAST PART OF TRANSFORM
* $                  -AND MIGRATE
* $
C
C                   SET ARRAY INDEXES
  IFFT=1
  IWORK=IFFT+NBLKF*NSBLKF*2+5
  IWORK1=IWORK+NOSMIG*2+4
  IB=IWORK1+66
C
C                   CHECK FOR ENOUGH CORE
  IC=ICM(1)-17000
  MPLX=IB
  NWS=0
  IF(IB.GT.MPLX)NWS=IB-MPLX+4
510 CONTINUE
C
C                   GO MIGRATE DATA
  KA=IB+500
  CALL RFLCM(KA)
  CALL KTRANS1(NSCA,NSCA(MPLX),NSCA(IFFT),
*NSCA(IWORK),A,NWS,IECS,ICMN,ICM)
  CALL REDUCE(2)
C
  CALL RELEASE
  RETURN
  END

```

```

C
C
*$TITLE           -KTRANS1
*$NAME           -KTRANS1
*$ABSTRACT       -TO DO THE LAST PART OF
*$              -THE TRANSFORM AND MIGRATE
*$              -THE DATA
*$
*$
*$SAMPLE CALL     -CALL KTRANS1(NSCA,A,FFT,FFT1,WORK,
*$              NWRIT)
*$CALLING PARAMETER
*$              -A           -ARRAY FOR MPLX DATA
*$              -FFT        -ARRAY FOR UNMIGRATED SPECTRUM
*$              -WORK       -ARRAY FOR DOWNWARD CONTINUATION
*$                      SPECTRUM
*$              -FFT1       -ARRAY FOR MIGRATED SPECTRUM
*$              -NWRIT      -NO OF 12 WORDS TO WRITE TO DISC
*$

```

```

SUBROUTINE KTRANS1(NSCA,A,FFT,FFT1,WORK,NWRIT,IECS,
*ICMN,ICM)
EXTERNAL PREMP91

```

```

C
DIMENSION ICMN(1)
DIMENSION ICM(1)
DIMENSION FFT(1),WORK(1),FFT1(1)
DIMENSION NSCA(1)
DIMENSION IADSS(2)
DIMENSION A(1)
INTEGER VVO(5),VV1(5),VV2(5),ISTM(2)

```

```

C
COMMON/COMM/ISZCOM,NCS,NSI,NX,NGI,IHEDR,MUXX,FMAX,
*NTN,NSBLKF,NBLKF,NSBLKK,NBLKK,NPX,KP,MNPAD,ISTFLAG,
*NOTIME,NMTIME,NOSMIG,THICK(31),DELZ(31),LEVC,
*DTIME(31),NITER(31),VI(31),NOL

```

```

C
C
C
C
C
C
INITIALIZATION FOR MAP CMULT

```

```

VVO(1)=LOCDF(PREMP91)
VVO(2)=91
VVO(3)=NTN
VVO(4)=0
VVO(5)=0
VV1(1)=2LFF
VV1(2)=1
VV1(3)=NTN*2
VV1(4)=0
VV1(5)=1478
VV2(1)=2LFF
VV2(2)=2
VV2(3)=NTN*2
VV2(4)=1
VV2(5)=1478

```

```

C
C
COMPUTE CONSTANT
IADS=IECS+1000
DELTAK=100./((FLOAT(NGI)*FLOAT(NPX)*2.)
DELTAJ=1000./((FLOAT(NSI)*FLOAT(KP))
KP2=KP*2
IADSS(1)=((IECS+ICM(1)-(KP2+500))/8)*8
IADSS(2)=IADSS(1)+KP+70B

```

```

        JOB=1478
        IARG=ICM(32)
        IF(IARG.EQ.3) GO TO 600
        NNN=KP
        CALL SINE(FFT,IADSS,NNN)
        NB=NNN
600    CONTINUE
C----- IDSK IS DISC BLK COUNT
C
        KQ=KP
        NSBFK=NSBLKF*NSBLKK
        NSBF2=NSBLKF*2
        NS2=NOS*2
        L=KP2-NS2
        N=NS2+1
        ICNT=0
        IB=1
C
        SIM=FLOAT(NSI)/1000
C
        DO 1000 II=1,NBLKK
C          READ UP NSBLKK/2 K SLICES
C
        MX=1
        IBLK=IB
        IBLK2=IBLK+NBLKF-1
        CALL XEDREAD(ICMN(105),IADS+MX,IBLK,IBLK2,0,ISTAT)
        CALL XEDWAIT(ICMN(105),ISTAT)
C
        NSBLKD=NSBLKK/2
        DO 500 JJ=1,NSBLKD
C          MI=(JJ-1)*NSBF2+1
C          GET K SLICE
        ICNT=ICNT+1
        IF(ICNT.GT.2*NPX) GO TO 500
        MX=MI
        MJ=1
        DO 100 J=1,NBLKF
        CALL COLLIN(2,FFT(MJ),2,IADS+MX,1,NSBLKF,1)
        CALL COLLIN(2,FFT(MJ+1),2,IADS+MX+NSBLKF,1,NSBLKF,1)
        MX=MX+NSBFK
        MJ=MJ+NSBF2
100    CONTINUE
C
        CLEAR TAIL
        CALL PCLR*(FFT(N),2,L,15)
C
        COMPLEX FFT THE K SLICE
        S=1.0
        NNN=KP
        IF(IARG.NE.3) GO TO 610
621    CONTINUE
        CALL FOUR1(FFT,NNN,1)
        GO TO 620
610    IF(NNN.GE.4096) GO TO 621
        CALL FFOUR1(FFT,IADSS,NB,JOB,1)
620    CONTINUE
C
C
C    MIGRATION
C
        IJCNT=ICNT

```

```

C      IF(ICNT.GT.NPX+1) IJCNT=NPX*2-ICNT+2
C      CALL FREQSUM(FFT,NTN,DELTA F,PRI,PII)
      FFT1(1)=PRI
      FFT1(2)=PII
C
      NOSM=2
      DO 700 KI=1,NOL
      VEL2=VI(KI)*VI(KI)
      CALL CALSPEC(IJCNT,DELTAK,DELTA F,NTN,VEL2,DELZ(KI),
*WORK)
      INITER=NITER(KI)
      DO 710 IK=1,INITER
C
      ISTM(1)=1
      CALL CVBOX(VVO,ISTM,2,FFT,VV1,WORK,VV2)
C
      CALL FREQSUM(FFT,NTN,DELTA F,PRI,PII)
      FFT1(NOSM*2-1)=PRI
      FFT1(NOSM*2)=PII
C
      NOSM=NOSM+1
      IF(NOSM.GT.NOSMIG) GO TO 800
710    CONTINUE
C
C THIS PART TAKES CARE OF INTERFACE
C
      IF(DTIME(KI).EQ.0.0) GO TO 700
      DDEP=DTIME(KI)*VI(KI)
      CALL CALSPEC(IJCNT,DELTAK,DELTA F,NTN,VEL2,DDEP,
*WORK)
      ISTM(1)=1
      CALL CVBOX(VVO,ISTM,2,FFT,VV1,WORK,VV2)
      IF(KI.EQ.NOL) GO TO 755
      VEL2=VI(KI+1)*VI(KI+1)
      GO TO 760
755    VEL2=VI(KI)*VI(KI)
760    DDTIME=SIM/2-DTIME(KI)
      DDDEP=DDTIME*SQRT(VEL2)
      CALL CALSPEC(IJCNT,DELTAK,DELTA F,NTN,VEL2,DDDEP,
*WORK)
      ISTM(1)=1
      CALL CVBOX(VVO,ISTM,2,FFT,VV1,WORK,VV2)
      CALL FREQSUM(FFT,NTN,DELTA F,PRI,PII)
      FFT1(NOSM*2-1)=PRI
      FFT1(NOSM*2)=PII
      NOSM=NOSM+1
      IF(NOSM.GT.NOSMIG) GO TO 800
C
700    CONTINUE
C
800    CONTINUE
C
C
C      PUT K SLICE BACK
C
      MX=MI
      MJ=1
      DO 200 J=1,NSBLKF
      CALL COLLIN(1,FFT1(MJ),2,IADS+MX,1,NSBLKF,1)
      CALL COLLIN(1,FFT1(MJ+1),2,IADS+MX+NSBLKF,1,NSBLKF,1)
      MX=MX+NSBLKF

```

```
      MJ=MJ+NSBF2
200  CONTINUE
      490  CONTINUE
      500  CONTINUE
      C
      C      WRITE DOWN DATA IN DISC
      C
      MX=1
      IBLK=IB
      IBLK2=IBLK+NBLKF-1
      CALL XEDWRIT(ICMN(105),IADS+MX,IBLK,IBLK2,0,ISTAT)
      CALL XEDWAIT(ICMN(105),ISTAT)
      C
      IB=IB+NBLKF
1000 CONTINUE
      C
      RETURN
      END
```

```

C
C
* $\$$       -CALSPEC(JX,DKX,DF,III,VEL2,THICK,SPECT)
* $\$$       -CALCULATE COMPLEX SPECTRUM OF MIGRATION
* $\$$       OPERATOR
* $\$$ 
* $\$$           -JX          INDEX IN KX DIRECTION
* $\$$           -DKX        DELTA INCREMENT IN KX
* $\$$           -DF         DELTA INCREMENT IN F
* $\$$           -III        NUMBER OF PAIRS IN F-DIRECTION
* $\$$           -VEL2       VEL**2
* $\$$           -THICK      THICKNESS OF LAYER
* $\$$ 
* $\$$           -SPECT      OUTPUT SPECTRUM
* $\$$ 
SUBROUTINE CALSPEC(JX,DKX,DF,NTN,VEL2,THICK,SPECT)
DIMENSION SPECT(1)
DATA PAI2/6.2831852/
C
AKX=(JX-1)*DKX
AKX2=AKX*AKX
C
JJJ=1
DO 10 JZ=1,NTN
AF=(JZ-1)*DF
AF2=AF*AF
DIS=(4.0*AF2/VEL2-AKX2)
IF(DIS.LT.0.0) GO TO 20
D=SQRT(DIS)
CC=-PAI2*D*THICK
SPECT(JJJ)=COS(CC)
SPECT(JJJ+1)=SIN(CC)
GO TO 30
20 SPECT(JJJ)=0.0
SPECT(JJJ+1)=0.0
30 JJJ=JJJ+2
10 CONTINUE
RETURN
END

```

```
C *****
C
C SUBROUTINE FREQSUM(COMP,NTN,DF,PRI,PII)
C SUM ALONG FREQUENCY
C COMP - INPUT ARRAY.
C NTN - NUMBER OF PAIRS IN COMP.
C DF - UNUSED.
C PRI - SUMMED REAL PART.
C PII - SUMMED IMAGINARY PART.
C
C DIMENSION COMP(1)
C PRI=0.
C PII=0.
C IJ1=1
C IJ2=2
C
C DO 10 JZ=1,NTN
C PRI=PRI+COMP(IJ1)
C PII=PII+COMP(IJ2)
C IJ1=IJ1+2
C IJ2=IJ2+2
10 CONTINUE
C RETURN
C END
```

```
C
C      OVERLAY (ZYFKC,1,1,C2000)
      PROGRAM ZYFKC
      EXTERNAL ZKMIC21
C
C      OVERLAY ZYFKC
C
C      INVERSE FFT IN X - DIRECTION AND OUTPUT
C
      CALL START (ZKMIC21)
      CALL LEVEL1
      END
```



```

C
  SUBROUTINE ZKMICZ1(NCO,NDA,LDA,NIN,LIN,NOU,LOU,
*                   A,LAA,
*                   IOUT,LOUT,
*                   ICM,LCM,ICMN,LCMN,
*                   IECS,LECS,KSCS,LSCS,
*                   KSS,LSS,NSCA,NSCB)
  DIMENSION NCO(1),NDA(1),NOU(1),NIN(1),
*           A(1),
*           IOUT(1),
*           ICM(1),ICMN(1)
  DIMENSION NSCA(1)
C
  COMMON/COMM/ISZCOM,NOS,NSI,NX,NGI,IHDR,MUXR,FMAX,
*NTN,NSBLKF,NBLKF,NSBLKK,NBLKK,NPX,KP,MNPAD,ISTFLAG,
*NOTIME,NMTIME,NOSMIG,THICK(31),DELZ(31),LEVC,
*DTIME(31),NITER(31),VI(31),NOL
C
C-----
C
C      COMPUTE ARRAY INDEXES
C      START OF F SLICE IFFT ARRAY
C      IFFT=1
C      TRACE HEADER
C      ITHDR=1
C      TRACE DATA
C      IXD=ITHDR+64
C      VELOCITY TABLE
C      IXV=IXD
C      IWORK=IXD
C      WORK ARRAY NOSMIG LONG
C      IDEP=IXD+NOSMIG+65
C
C      MUX - DMUX ARRAY
C      MPX=IDEP+NOSMIG+2
C      DMUX ARRAY WHILE DOING F SLICE IFFT
C      MPX2=IFFT+NPX*4+1
C
C      DO F SLICE IFFT
C
C      KA=MPX+500
C      IF(KA.LT.(MPX2+500)) KA=MPX2+500
C      CALL RFLCM(KA)
C      CALL RIFFT(NSCA,NSCA,A,NSBLKF,NBLKF,NSBLKK,
*NSBLKK,NPX,NX,NOSMIG,MUXR,IECS,KP,ICMN,ICM)
C
C      DO DMUX AND OUTPUT
C
C      CALL 3DMUX(NSCA(ITHDR),NSCA(IXD),A,IECS,KSCS,
* A,ICM,IOUT,LOUT,ICMN)
C      CALL REDUCE(2)
C
C      CALL XEDCLOS(ICMN(105),KSS,ISTAT)
C      CALL RELEASE
C      RETURN
C      END

```

```

C
C
*$TITLE -RIFFT
*$NAME -RIFFT
*$ABSTRACT -TO DO F SLICE IFFT, ON THE
*$ -MULTIPLY DATA
*$SAMPLE CALL -CALL RIFFT(MSCA,FFT,A,NSBLKF,NBLKF,
*$ -NSBLKK,NBLKK,NPX,NX,NOSMIG,MUXR)
*$CALLING PARAMETER
*$ -FFT -FFT ARRAY
*$ -A -ARRAY TO HOLD MPLX. DATA
*$ -NSBLKF -SAMPLE/BLOCK F
*$ -NBLKF -BLOCKS OF F
*$ -NSBLKK -SAMPLES/BLOCK K
*$ -NBLKK -BLOCKS OF K
*$ -NPX -(NO. OF PAIRS IN F SLICE FFT)/2
*$ -NX -NO. OF TRACES
*$ -NOSMIG -NO. MIGRATED SAMPLES PER TRACE
*$ -MUXR -LOGICAL FILE OF MPLX. DATA
*$ -KP -NO. OF PAIRS IN K SLICE FFT
*$

```

```

SUBROUTINE RIFFT(MSCA,FFT,A,NSBLKF,NBLKF,NSBLKK,
*NBLKK,NPX,NX,NOSMIG,MUXR,IECS,KP,ICMN,ICM)

```

```

C
C
DIMENSION A(1)
DIMENSION ICM(1)
DIMENSION ICMN(1)
DIMENSION MSCA(1)
DIMENSION IADSS(2)
DIMENSION FFT(1)
IADS=IECS+2000

```

```

C
C -----
C
IADSS(1)=((IECS+ICM(1)-(NPX*4+500))/8)*8
IADSS(2)=IADSS(1)+NPX*2+708
JOB=1478
IARG=ICM(32)
IF(IARG.EQ.3) GO TO 610
NNN=NPX*2
CALL SINE (FFT,IADSS,NNN)
NB=NNN
610 CONTINUE

```

```

C
C COMPUTE CONSTANTS
C
INOM=4LMUXR
NN=NPX*2+1
NSBF2=NSBLKF*2
NPX4=NPX*4
NSINC=NSBLKK*NSBLKF

```

```

C
C READ UP FFTED F SLICE
C
DO 1000 ISBLK=1,NBLKF
MX=1
IBLK=ISBLK
DO 10 II=1,NBLKK
CALL XEDREAD(ICMN(105),IADS+MX,IBLK,IBLK,0,ISTAT)
CALL XEDWAIT(ICMN(105),ISTAT)
IBLK=IBLK+NBLKF
MX=MX+NSINC

```

```

10  CONTINUE
C
C
NSBF=NSBLKF
IC=NSBLKF*ISBLK
IF(IC.GT.NOSMIG) NSBF=NSBF-(IC-NOSMIG)
DO 150 I=1,NSBF
MX=I
CALL COLLIN(2,FFT,1,IADS+MX,NSBLKF,NPX4,1)
C
C      FOLD BEFORE IFFT
C      IFFT THE F SLICE
C
S=1.0
NNN=NPX*2
IF(IARG.NE.3) GO TO 650
CALL FOUR1(FFT,NNN,-1)
GO TO 660
650  CALL FFOUR1(FFT,IADSS,NB,JOB,-1)
660  CONTINUE
C      COEF=SQRT(2./(NPX*KP*2))
C      IF(IARG.NE.3) GO TO 2001
C      DO 2000 IJJ=1,NX
C      FFT(IJJ)=FFT(IJJ)*COEF
C2000  CONTINUE
C
C2001  CONTINUE
C
C      MOVE F SLICE BACK INTO MPLX ARRAY
C
CALL COLLIN(1,FFT(1),2,IADS+MX,NSBLKF,NX,1)
150  CONTINUE
C
C      WRITE F SLICE DATA BACK TO DISK
C
IBLK=ISBLK
MX=1
DO 200 II=1,NBLKK
IB=(II-1)*NSBLKK
IF(IB.GT.NX) GO TO 999
CALL XEDWRIT(ICMN(105),IADS+MX,IBLK,IBLK,0,ISTAT)
CALL XEDWAIT(ICMN(105),ISTAT)
IBLK=IBLK+NBLKF
MX=MX+NSINC
200  CONTINUE
C
C
999  CONTINUE
1000 CONTINUE
C
RETURN
END

```

```

C
C
C
*$TITLE                -BDMUX
*$NAME                 -BDMUX
*$ABSTRACT              -TO DO DEMULTIPLEX AND OUTPUT
*$SAMPLE CALL          -CALL BDMUX(THDR,A,B,IWORK)
*$CALLING PARAMETER
*$      -THDR           -TRACE HEADER ARRAY
*$      -A              -TIME CONVERTED OUTPUT ARRAY
*$      -B              -SCRATCH ARRAY
*$      -IWORK          -SCRATCH ARRAY
*$
SUBROUTINE BDMUX(THDR,A,B,IECS,KSCS,IWORK,ICM,
*$IOUT,LOUT,ICMN)
C
C      INTEGER Z
C
C      COMMON/CGMM/ISZCOM,NCS,NSI,NX,NGI,IHEDK,MUXR,FMAX,
*$NTN,NSBLKF,NBLKF,NSBLKK,NBLKK,NPX,KP,MNPAD,ISTFLAG,
*$NOTIME,NMTIME,NOSMIG,THICK(31),DELZ(31),LEVC,
*$DTIME(31),NITER(31),VI(31),NOL
C
C      DIMENSION ICM(1)
C
C      DIMENSION IOUT(1),ICMN(1)
C      DIMENSION THDR(1),A(1),IWORK(1),B(1)
C
C
C
C      IADS=IECS+2000
C      IADSS=IECS+ICM(1)-1000
C      INCM=4LMUXR
C      INOM1=5LIHEDR
C
C      JHORI=0
C      NTC=0
C      NSBKF=NSBLKF*NSBLKK
C
C      READ UP NSBLKK SLICES OF K
C      DO 1000 II=1,NBLKK
C      IBLK=NSBLKF
C      Z=II-1
C      IBLK=Z*IBLK+1
C      MXX=1
C      LONG=NSBKF
C      IBLK2=IBLK+NSBLKF-1
C      CALL XEDREAD(ICMN(105),IADS+MXX,IBLK,IBLK2,0,ISTAT)
C      CALL XEDWAIT(ICMN(105),ISTAT)
C
C      DO 500 I=1,NSBLKK
C      MXX=(I-1)*NSBLKF+1
C      MX=1
C      MXJ=MXX
C      NTC=NTC+1
C      IF(NTC.GT.NX) GO TO 1001
C
C
C      CALL COLLIN(2,A(MX),NSBLKF,IADS+MXJ,NSBKF,NBLKF,
*$NSBLKF)
C
C      READ TRACE HEADER
C

```

```
CALL RDFICH(INOM1,1,NTC,THDR,64,0)
CALL ATTENTE(INOM1)
DO 599 KILM=1,64
IOUT(KILM)=INT(THDR(KILM))
599 CONTINUE
DO 601 KILL=1,NOSMIG
IOUT(64+KILL)=A(KILL)/(2.*IOUT(13))
601 CONTINUE
IOUT(1)=NSI*NOSMIG
IOUT(10)=NSI*NOSMIG
CALL MAXR(IOUT(65),NOSMIG,IOUT(14))
CALL LOWER(IOUT,NOSMIG,LEVC)
CALL WTRACE(2,NTC,IOUT)
CALL PRETE(2,NTC)
C
500 CONTINUE
1000 CONTINUE
C
1001 CONTINUE
RETURN
END
```